ENG 334-(EQC 2001/477)

Use of micropiles for remediation of liquefaction prone sites and retrofitting of small structures

Kevin J McManus, University of Canterbury Department of Civil Engineering

Geotechnical Special Publication No. 124: 2004. Drilled Shafts, Micropiling, Deep Mixing Remedial Methods, and Specialty Foundation Systems, Ed. J.P. Turner & P.W. Mayne, ASCE, Reston VA. pp. 134-145.

01/477

EFFECT OF MICROPILES ON SEISMIC SHEAR STRAIN

Kevin J. McManus[1], Guillaume Charton[2], and John P. Turner[3], Member ASCE

ABSTRACT: The use of inclined micropiles as reinforcement to prevent soil liquefaction in level ground has been investigated experimentally. Deposits of loose (D_r = 0.2 to 0.4), dry sand were prepared inside a large (2.0 m deep by 1.8 m long by 0.8 m wide) laminated box and subjected to shaking of different intensities on a one-dimensional shake table. For low intensity shaking (up to 0.12 g) the cyclic shear strains were modest (up to 0.11 percent) and there was a modest settlement (0.31 percent). For higher intensity shaking, (0.16 g) there was a significant transformation in response with much greater cyclic shear strain (0.65 percent) and settlement (3.1 percent).

Other deposits were reinforced by use of Titan 26-14 self-drilling micropiles installed at 30 degrees inclination. Reinforcement by one inclined micropile was found to have little effect on response to shaking but installation of two diagonally opposed, inclined micropiles was found to reduce cyclic shear strain by half and settlement to one fifth that of similar unreinforced deposits.

INTRODUCTION

Soil liquefaction is a significant hazard in earthquake prone regions. The recognized extent of the hazard is growing rapidly in size as regional studies continue to identify large areas of liquefiable soils. There is a growing problem of knowing how to treat sites where small, low cost structures including dwellings are planned. Large projects can more easily absorb the costs of traditional ground improvement techniques such as deep dynamic compaction, stone columns, and vibro-compaction and large structures can economically be founded on piles. But these techniques are seldom found to be economical for smaller projects and they are not applicable to retrofitting numerous existing affected structures.

[1]Senior Lecturer and [2]Graduate Student, Dept. of Civil Engineering, Univ. of Canterbury, Christchurch, New Zealand; k.mcmanus@civil.canterbury.ac.nz
[3]Professor, Dept. of Civil & Arch. Engineering, Univ. of Wyoming, Laramie, WY 82071; turner@uwyo.edu

Traditional ground improvement techniques are highly invasive, require large-size equipment, generate considerable amounts of noise and vibration, make a big mess, and need a large site to operate in. They are unsuited to small or congested sites or where there are near neighbors. By contrast micropiles can be installed with lightweight equipment, quietly, and in confined spaces, even inside of existing buildings.

Horizontal micropiles (usually called "soil nails") have become widely accepted as a means of reinforcing slopes against sliding failures both from static gravity induced forces and earthquakes. This study has investigated the possibility of adapting micropiles to stabilize level ground during earthquakes by installing them as diagonal reinforcement.

Traditional installation techniques for micropiles and soil nails involve drilling, insertion of steel reinforcing, followed by grouting, and are not suited for loose granular soil below the water table without the use of temporary casing. However, self-drilling micropiles (e.g. Ischebeck Titan micropiles) are now available which are ideally suited to installation in loose, liquefiable sands without use of temporary casing.

There is growing understanding that cyclic shear strains rather than cyclic shear stresses determine the onset of soil liquefaction. Soil liquefaction is a result of the tendency of loose sands to densify with shaking, the resulting effort of the soil to expel the excess pore water causing a temporary increase in pore water pressure and loss of effective confining stress. A number of researchers (Silver and Seed, 1971, Youd, 1972) have shown experimentally that the densification of dry sands is controlled by cyclic shear strains and not shear stresses. Further, the existence of a threshold cyclic shear strain has been found below which soil densification does not occur.

Therefore, if the cyclic shear strain in the soil can be kept below this threshold value, then pore pressure should not be generated and liquefaction should not occur. Dobry and Ladd (1980) have found that for different sands, prepared by different methods, and tested at different effective confining pressures the threshold cyclic shear strain for significant pore pressure generation is approximately 0.1 percent.

Dobry et. al. (1982) have proposed a method for estimating the cyclic shear strain amplitude at a point in the ground as:

$$\gamma_{cyc} = 0.65 \frac{a_{\max}}{g} \frac{\sigma_v r_d}{G(\gamma_{cyc})} \tag{1}$$

in which a_{max} = estimated peak ground acceleration at the site and r_d = an empirical reduction factor. The soil shear modulus G is highly non-linear and is a function of the cyclic shear strain. $G_{\max}$, the small strain modulus may be found for the soil profile by use of seismic CPT profiling, for instance. Modulus reduction curves as a function of cyclic shear strain are available (e.g. Vucetic and Dobry, 1991).

From Equation (1), if the shear modulus, G, for the soil mass is enhanced sufficiently by diagonal reinforcement, and the cyclic shear strain maintained below the threshold value of 0.1 percent, then there should be minimal generation of pore water pressure and no liquefaction. Further, by reducing cyclic shear strain the reinforcement should also act to maintain the soil's own initial stiffness which otherwise tends to degrade rapidly.

This study has examined experimentally the effectiveness of inclined micropiles as reinforcement to reduce soil cyclic shear strains during shaking. Full-size prototype micropiles (Titan 26-14) were installed in loose sand in a large (2 m deep x 1.8 m long, x 0.8 m wide) laminated shear box then subjected to different levels of shaking. Results were compared to similar soil deposits without micropile reinforcement.

TESTING PROGRAM

Laminated Sand Tank

Prototype inclined micropiles were tested in a large laminar sand tank on a one degree of freedom shaking table at the University of Canterbury. The purpose of the laminar tank was to simulate free-field shaking response by allowing the soil to deform in simple shear with minimal boundary effects from the tank (e.g. Hushmand et. al., 1988, Iai, 1991, Whitman et. al. 1981). The tank design used for this study follows from that of Hushmand et al., and is shown in Figure 1. The tank has internal dimensions of 1.8 m long by 0.8 m wide by 2.0 m deep.

Laminates were made from 100 mm by 50 mm cold-formed steel channel that was laid on its flat and welded into rectangular frames. Teflon strips of 150 mm long by 10 mm wide by 1 mm thick were glued to both sides of the laminates at six locations to minimize friction. Tests showed that the strips produced a coefficient of friction of 0.07, indicating that at normal stresses equivalent to those at the base of the tank, the load required to shear the laminates was only 2 percent of the load required to shear the soil mass.

Soil was contained within the tank by a flexible membrane liner. Latex rubber sheets, each 1 mm thick, were draped over the inside of the laminates and glued to the top laminate.

The laminates were supported by a steel frame that was constructed from 50 mm by 50 mm rectangular hollow section (RHS), with 10 mm diameter rods acting as cross-bracing members. The frame restricted the laminates to move only in the direction of the shaking table and also supported the stack of laminates when the tank was empty. Both the top-cap and the side members of the supporting frame were coated with Teflon strips to reduce friction during shaking.

Instrumentation

Five potentiometers (Showa type 50LP300) were placed in contact with tank laminates at various heights above the tank base (1.07 m, 1.34 m, 1.55 m, and 1.97 m) and fixed rigidly to the shaking table in order to measure relative lateral displacements of the tank laminates during shaking. An accelerometer (Kyowa AS-5GA) was fixed to one of the tank laminates near to the soil surface (1.77 m above tank base) in order to measure soil acceleration and a similar accelerometer was fixed directly to the shaking table.

Settlement of the soil surface was measured by fixing a vertically oriented potentiometer to the tank support frame and making contact with an aluminium plate resting on the sand surface.

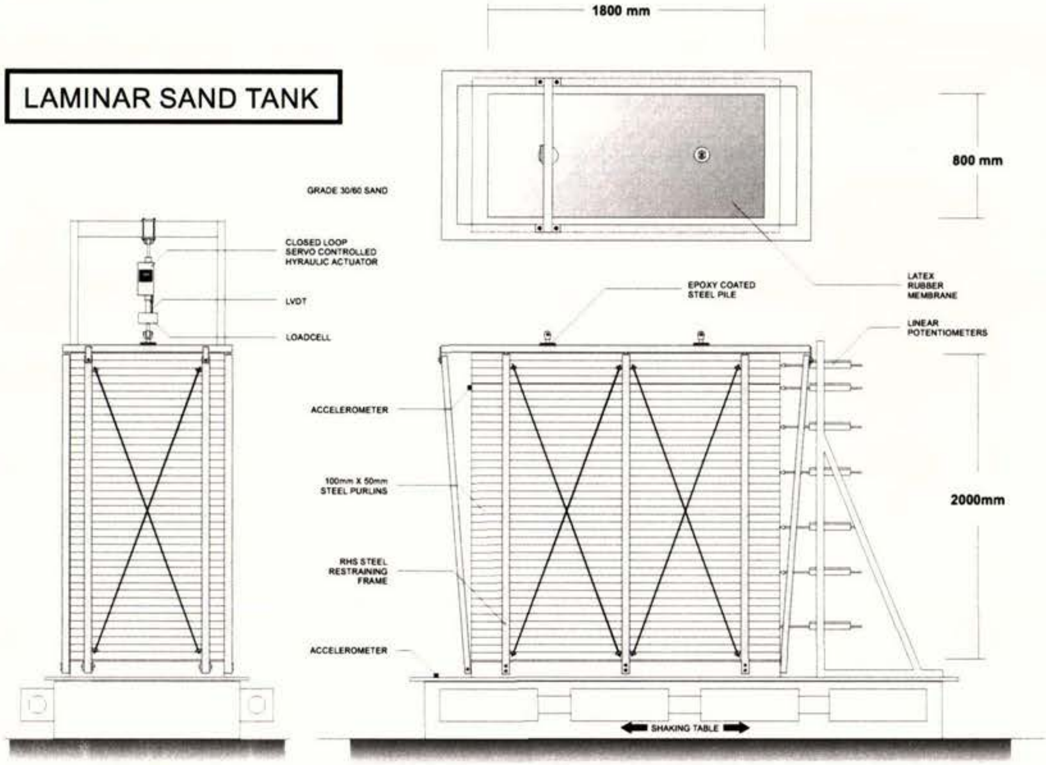

FIG. 1. Laminar sand tank.

Soil Deposits

The soil used was an industrial grade 30/60 silica sand supplied by Commercial Minerals Ltd, Auckland, New Zealand, with properties given in Table 1. This soil was selected because it is suitable for air pluviation and can be re-used without degradation.

Soil deposits were prepared by air pluviation. Sand flowed from a hopper through a gate, was collected in a suspended funnel, then flowed down a 95 mm diameter flexible hose, discharging through a wire mesh diffuser into the laminated tank. The diffuser was made from a 100 mm diameter by 300 mm long section of plastic tube that was packed with wire mesh. By discharging sand from the diffuser directly onto the surface of the deposit, a low initial relative density (six deposits, Dr = 0.17 – 0.26) was achieved. The sand densified somewhat during each episode of shaking enabling some tests to be performed in higher densities (as high as $D_r = 0.4$).

Two cone penetrometer tests (CPT) were performed in one of the deposits. The penetration was found to be consistent throughout the deposit with q_c ranging from 1 MPa to 1.4 MPa.

Shaking Table

Characteristics of the University of Canterbury shaking table are given in Table2. . The table is driven by a closed-loop, servo-controlled hydraulic actuator with an MTS Teststar 2 system controller. Each test was performed under displacement control, with the cyclic table displacements generated by entering the required amplitude, frequency and number of cycles into the controller.

Table 1. Soil Properties

Property	Symbol	Value
Density of Solid Particles	ρ_s	2.65 t/m^3
10% finer	D_{10}	0.30 mm
60% finer	D_{60}	0.45 mm
minimum voids ratio	e_{min}	0.53
maximum voids ratio	e_{max}	0.83
Steady State Friction Angle	ϕ_{ss}	33°

RESULTS

Soil response to shaking

Four deposits were constructed without micropile reinforcement and subjected to shaking to verify behaviour of the laminar tank and to determine baseline soil response. Soil deposits were subjected to individual "earthquakes" consisting of 26 cycles of 1 Hz sine wave shaking at three amplitudes: +/- 20 mm, +/- 30 mm, and +/- 40 mm corresponding to accelerations of 0.08 g, 0.12 g, and 0.16 g.

During shaking, the displacement measurements showed that the soil mass deformed in a linear, simple shear mode from the tank base to a height of 1.6 m, then deformed in a non-linear, irregular mode from 1.6 m to the surface at 2.0 m. The deformation of the surface soil seems to have been affected by surface waves of complex shape that were observed during shaking. Typical displacement measurements are shown in Figure 2.

Cyclic shear strain during shaking is shown in Figure 3 for the three amplitudes of shaking. The peak displacement of each transducer for each cycle of shaking was captured and divided by the height above the tank base then averaged over all of the transducers to give an average peak shear strain for each cycle. Peak strain decreased during each "earthquake" as the initially loose soil densified. For the lower amplitude shaking (0.08 g and 0.12 g) the cyclic shear strains were modest (0.08 percent and 0.11 percent for cycle 13) but for the higher amplitude shaking (0.16 g) the cyclic shear strain was much greater (0.65 percent for cycle 13).

Significant settlements occurred at the surface of each soil deposit during shaking as the initially loose sand densified. The amount of settlement varied significantly depending on the amplitude of shaking, as shown in Figure 4. For the shaking at 0.08 g and 0.12 g the settlement was modest and similar(0.31 percent and 0.35 percent), but, for the higher level shaking at 0.16 g the settlement was much greater (3.1 percent).

Table 2. Characteristics of the University of Canterbury Shaking Table

Property	Value
Plan Dimensions	4.0 m x 2.0 m
Maximum Allowable Load	200 kN
Maximum Horizontal Force	200 kN
Maximum acceleration with a mass of 5 tonne	2.7 g
Maximum Velocity	1.0 m/s
Maximum Displacement	0.30 m

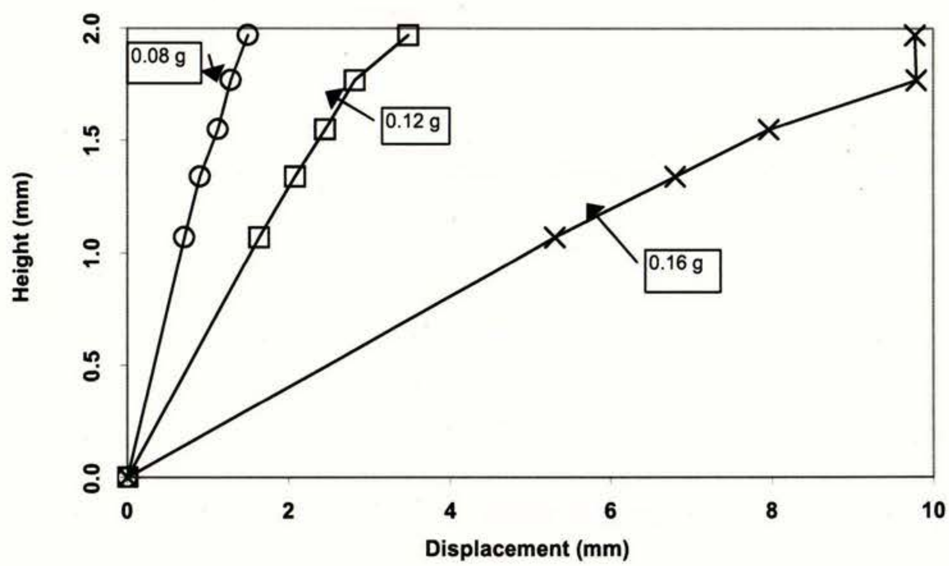

FIG. 2. Displacement profiles for unreinforced soil deposits.

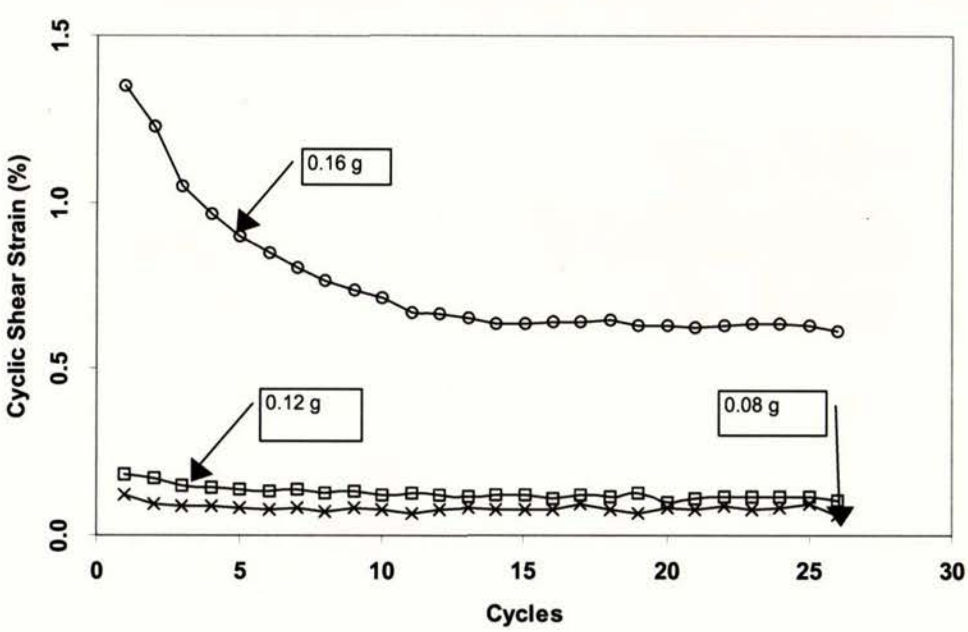

FIG. 3. Average peak cyclic shear strain for unreinforced soil deposits (D_r = 0.2)

Clearly, a significant transformation in response occurred between the shaking at 0.12 g and the shaking at 0.16 g, with settlement jumping from 0.35 percent to 3.1 percent. The shaking at 0.12 g caused a cyclic shear strain of 0.11 percent which is very close to the threshold value for liquefaction of 0.1 percent suggested by Dobry and Ladd (1980). Increasing the shaking intensity further to 0.16 g may have triggered some "collapse" of the soil fabric with a large reduction in shear stiffness and increase in settlement. This "collapse" may be equivalent to liquefaction occurring in a saturated sand deposit.

Micropile Installation

Two soil deposits were reinforced with diagonal micropiles. One deposit was reinforced with a single micropile and was reinforced with two diagonally opposed micropiles, as shown in Figure 5. Titan 26-14 self-drilling micropiles supplied by Ischebeck (NZ) Ltd were used as reinforcement. Titan micropiles consist of high-strength hollow steel threaded bars installed by a self-drilling process with a sacrificial drill bit. Grout is injected during drilling at low pressure to mix with the surrounding soil and provide bonding and corrosion protection.

For this study, the micropiles were installed into loose sand at shallow (2 m) depth and so the bars were installed simply by pushing with hydraulic rams (a cone penetrometer pushing rig), as shown in Figure 6. An oversize cone-shaped drill head was fixed to the pile tip to create an annular space that was progressively filled with grout during pushing. A photograph of the completed installation with two diagonally opposed micropiles is shown in Figure 7.

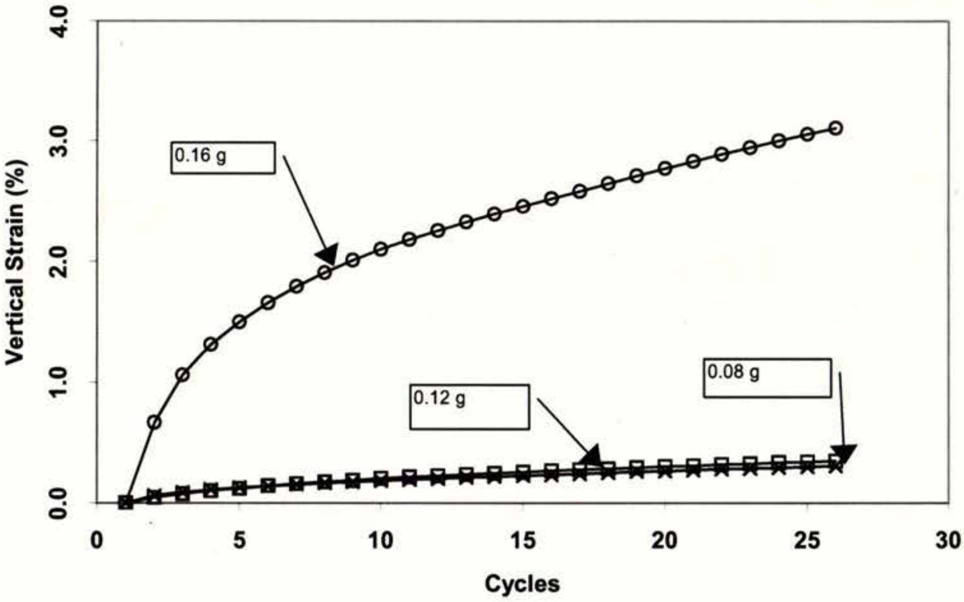

FIG. 4. Settlement of unreinforced soil deposits (D_r = 0.2)

The grout mix was 50:50 by weight of ordinary Portland cement:water, with 3 percent bentonite by weight of cement added to stabilize the grout and reduce water loss to the dry sand. The unconfined compressive strength of the cured grout was 9 MPa at 7 days and 11 MPa at 28 days. Micropiles were exhumed from the soil after each test and were found to be highly uniform in cross-section with a diameter of 100 mm +/- 15 mm.

The two reinforced soil deposits (one micropile and two micropiles) were subjected to the same levels of shaking as unreinforced deposits of similar density (D_r = 0.4). The response of the reinforced deposits is compared to equivalent unreinforced deposits in Figures 8 and 9, showing average peak cyclic shear strain and settlement during shaking. Response of the soil deposit with one inclined micropile was quite similar to the unreinforced deposit. The average peak cyclic shear strains were similarly high (0.54 percent for the unreinforced deposit and 0.64 percent for the reinforced deposit after 13 cycles) and the total settlements were also quite similar (1.2 percent and 1.1 percent). The main notable difference in response was that the deposit with one micropile initially had a larger response in terms of both cyclic shear strain and settlement than the unreinforced deposit, with the response steadily declining during the test.

Response of reinforced soil deposits

The response of the soil deposit with two diagonally opposed micropiles was reduced to about half of the cyclic shear strain of the unreinforced deposit (0.24 percent after 13 cycles) and about one fifth of the settlement (0.24 percent). This level of cyclic shear strain is somewhat above the threshold of 0.1 percent for liquefaction suggested by Dobry and Ladd (1980), but the settlement was reduced substantially suggesting that liquefaction in an equivalent saturated deposit might have been prevented.

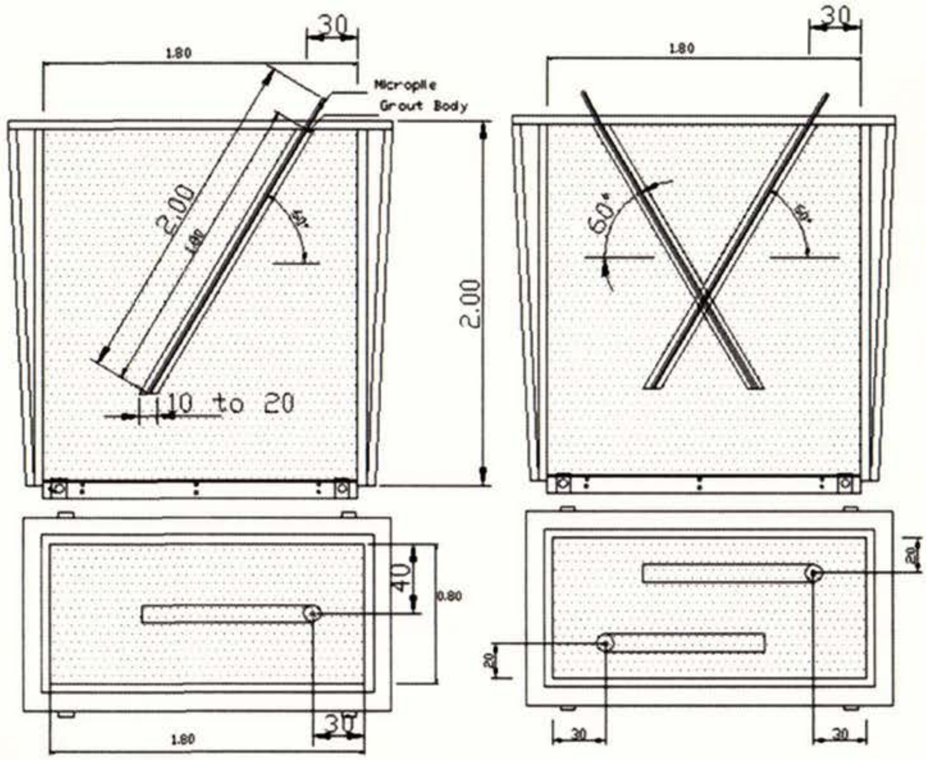

FIG. 5. Layout of micropile reinforcement in laminar tank

Nevertheless, the increase in shear stiffness of the deposit provided by the reinforcement was low considering the steel cross-section introduced. From the measured cyclic shear strains shown in Figure 8, the equivalent shear modulus, G, at mid-depth of the deposit (1 m) may be calculated as 380 KN/m^2 for the unreinforced deposit and 1010 KN/m^2 for the deposit with two micropiles. The equivalent shear modulus provided by the steel reinforcement, if the steel cross-section were fully mobilised, is 52,000 KN/m^2. Obviously, the capacity of the micropiles is hardly mobilised suggesting that reinforcement of much lower strength and stiffness may provide similar benefit at lower cost.

CONCLUSIONS

A large-size laminar tank performed well on the shaking table with linear simple shear being generated in deposits of loose sand in all but the upper 0.2 m. Shaking of loose, unreinforced sand deposits with accelerations of 0.08 g and 0.12 g caused peak cyclic shear strains of up to 0.11 percent and settlements of up to 0.35 percent. Shaking at higher level (0.16 g) caused a transformation in response with large cyclic shear strains (0.65 percent) and large settlements (3.1 percent). Installation of Titan

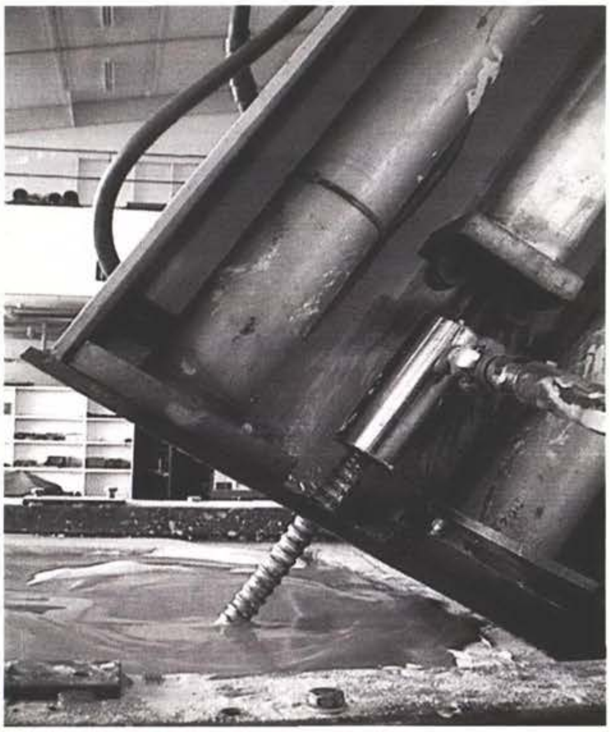

FIG. 6. Installation of inclined micropiles

FIG. 7. Completed installation of two inclined micropiles

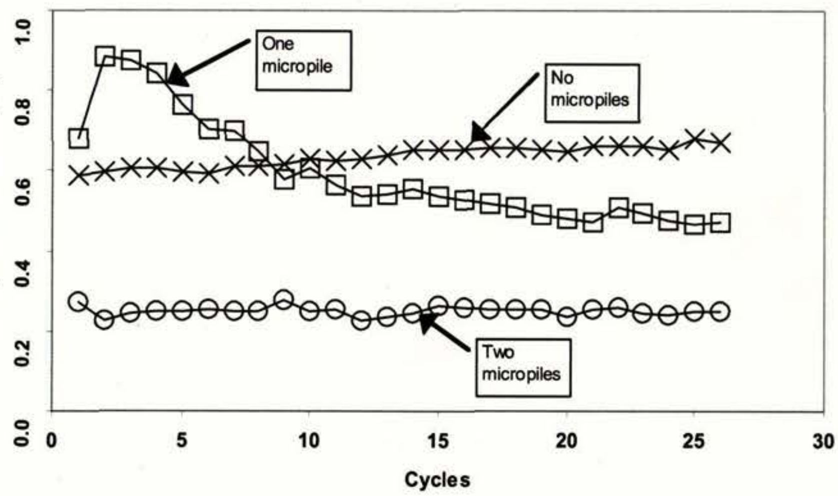

FIG. 8. Average peak cyclic shear strain: Acceleration = 0.16 g, D_r = 0.4

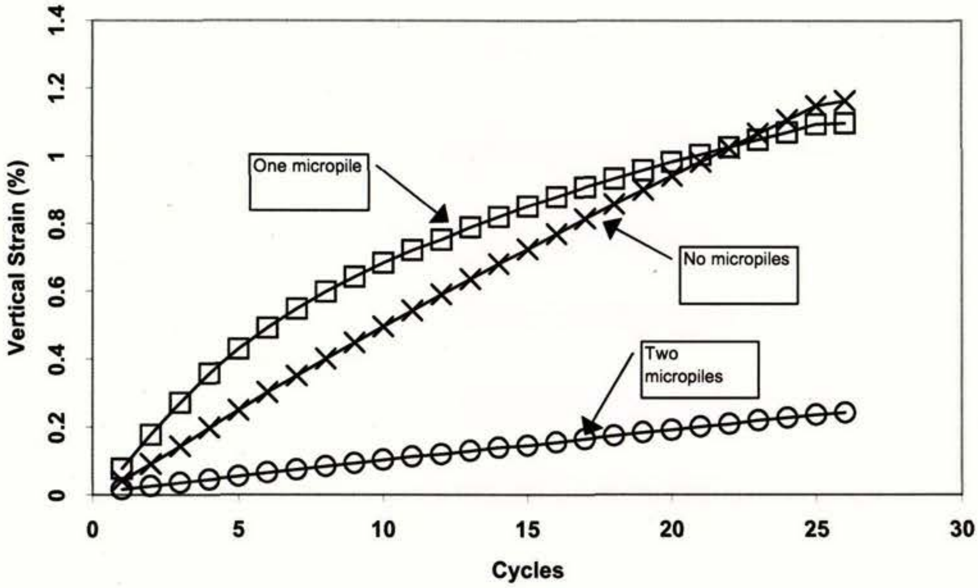

FIG. 9. Settlement during shaking: Acceleration = 0.16 g, D_r = 0.4

self-drilling micropiles at inclinations of 30 degrees was achieved readily by direct-push with simultaneous grout injection at low pressure. Reinforcement of sand deposits with a single inclined micropile had little effect on response to shaking. Reinforcement with two, diagonally opposed micropiles had a significant effect, reducing cyclic shear strain by half and settlement to one fifth that of a similar unreinforced deposit. It is probable that the two micropiles would have prevented liquefaction of a saturated soil deposit in this case ($D_r = 0.4$, 0.16 g). Reinforcement efficiency was low, with relatively little of the potential increase in stiffness from the steel cross-section utilised. Future research should investigate use of lighter reinforcement elements which may provide similar benefits at greater economy.

ACKNOWLEDGMENTS

This project received funding from the New Zealand Earthquake Commission Research Foundation. Ischebeck(NZ) Ltd. provided the micropiles and John Yonge provided advice on installation. Alistair Chambers designed and developed the laminar tank. John Maley assisted with construction and setup of the apparatus and operated the shake table. Richard Pascoe operated the CPT rig and installed the micropiles.

REFERENCES

Dobry, R. and Ladd, R.S. (1980). Discussion to "Soil liquefaction and cyclic mobility evaluation for level ground during earthquakes, : by H.B. Seed and "Liquefaction potential: science versus practice," by R.B. Peck, *J. of the Geotechnical Engineering Division,* ASCE, Vol. 106, No. GT6, pp. 720-724.

Dobry, R., Ladd, R.S., Yokel, F.Y., Chung, R.M., and Powell, D. (1982). "Prediction of pore water pressure buildup and liquefaction of sands during earthquakes by cyclic strain method," *NBS Building Science Series 138,* National Bureau of Standards, Gaithersburg, Maryland, 150 p.

Hushmand, B., Scott R.F. & Crouse C.B. (1988). "Centrifuge liquefaction tests in a laminar box", *Geotechnique,* Vol. 38, No 2, pp. 253-262.

Iai, S. (1991). "A Strain Space Multiple Mechanism Model For Cyclic Behavior of Sand and its Application," *Research Note No.43*, Earthquake Engineering Research Group, Port and Harbour Research Institute, Ministry of Transport, Japan. May 1991.

Silver, N.L. and Seed, H.B. (1971). "Volume changes in sands during cyclic loading," *J. of the Soil Mechanics and Foundations Division,* ASCE, Vol. 97, No. SM9, pp. 1171-1182.

Vucetic, M. and Dobry, R. (1991). "Effect of soil plasticity on cyclic response," *J. of Geotechnical Engineering,*ASCE, Vol. 117, No. 1, pp. 89-107.

Whitman, R.V., Lambe, P.C. & Kutter, B.L. (1981). "Initial Results from a Stacked-Ring Apparatus for Simulation of a Soil Profile". *Proceedings, International Conference on Recent Advances in Geotechnical Earthquake Engineering and Soil Dynamics*, St Louis, Mo., April 26 – May 3, 1981.

Youd, T.L. (1972). "Compaction of sands by repeated shear straining," *J. of the Soil Mechanics and Foundations Division,* ASCE, Vol. 98, No. SM7, pp. 709-725.

ENG 334. 01/477

Inclined reinforcement to prevent soil liquefaction

K.J. McManus

University of Canterbury., Christchurch, N.Z.

J.P. Turner

University of Wyoming, Laramie, Wyoming, U.S.A.

G. Charton

University of Canterbury, Christchurch, N.Z.

2005 NZSEE Conference

ABSTRACT: The use of inclined micropiles as reinforcement to prevent soil liquefaction in level ground has been investigated experimentally. Deposits of loose (Dr = 0.2 to 0.4), dry sand were prepared inside a large (2.0 m deep by 1.8 m long by 0.8 m wide) laminated box and subjected to shaking of different intensities on a one-dimensional shake table. For low intensity shaking (PGA up to 0.28 g) the cyclic shear strains were modest (up to 0.11 percent) and there was a modest settlement (0.31 percent). For higher intensity shaking, (PGA up to 0.40 g) there was a significant transformation in response with much greater cyclic shear strain (0.65 percent) and settlement (3.1 percent).

Other deposits were reinforced by use of Titan 26-14 self-drilling micropiles installed at 30 degrees inclination. Reinforcement by one inclined micropile was found to have little effect on response to shaking but installation of two diagonally opposed, inclined micropiles was found to reduce cyclic shear strain by half and settlement to one fifth that of similar un-reinforced deposits.

1 INTRODUCTION

Soil liquefaction is a significant hazard in earthquake prone regions. The recognized extent of the hazard is growing rapidly in size as regional studies continue to identify large areas of liquefiable soils. There is a growing problem of knowing how to treat sites where small, low cost structures including dwellings are planned. Large projects can more easily absorb the costs of traditional ground improvement techniques such as deep dynamic compaction, stone columns, and vibro-compaction and large structures can economically be founded on piles. But these techniques are seldom found to be economical for smaller projects and they are not applicable to retrofitting numerous existing affected structures.

Traditional ground improvement techniques are highly invasive, require large-size equipment, generate considerable amounts of noise and vibration, make a big mess, and need a large site to operate in. They are unsuited to small or congested sites or where there are near neighbours. By contrast micropiles can be installed with lightweight equipment, quietly, and in confined spaces, even inside of existing buildings.

Horizontal micropiles (usually called "soil nails") have become widely accepted as a means of reinforcing slopes against sliding failures both from static gravity induced forces and earthquakes. This study has investigated the possibility of adapting micropiles to stabilize level ground during earthquakes by installing them as diagonal reinforcement.

Traditional installation techniques for micropiles and soil nails involve drilling, insertion of steel reinforcing, followed by grouting, and are not suited for loose granular soil below the water table (the most typical case for soils susceptible to liquefaction) without the use of temporary casing. However, self-drilling micropiles (e.g. Ischebeck Titan micropiles) are now available which are ideally suited to installation in loose, liquefiable sands without use of temporary casing.

There is growing understanding that cyclic shear strains rather than cyclic shear stresses determine the onset of soil liquefaction. Soil liquefaction is a result of the tendency of loose sands to densify with shaking, the resulting effort of the soil to expel the excess pore water causing a temporary increase in pore water pressure and loss of effective confining stress. A number of researchers (Silver and Seed, 1971, Youd, 1972) have shown experimentally that the densification of dry sands is controlled by cyclic shear strains and not shear stresses. Further, the existence of a threshold cyclic shear strain has been found below which soil densification does not occur.

Therefore, if the cyclic shear strain in the soil can be kept below this threshold value, then pore pressure should not be generated and liquefaction should not occur. Dobry and Ladd (1980) have found that for different sands, prepared by different methods, and tested at different effective confining pressures the threshold cyclic shear strain for significant pore pressure generation is approximately 0.1 percent.

Dobry et. al. (1982) have proposed a method for estimating the cyclic shear strain amplitude at a point in the ground as:

$$\gamma_{cyc} = 0.65 \frac{a_{\max}}{g} \frac{\sigma_v r_d}{G(\gamma_{cyc})} \tag{1}$$

in which $a_{\max}$ = estimated peak ground acceleration at the site and r_d = an empirical reduction factor. The soil shear modulus G is highly non-linear and is a function of the cyclic shear strain. $G_{\max}$, the small strain modulus may be found for the soil profile by use of seismic CPT profiling, for instance. Modulus reduction curves as a function of cyclic shear strain are available (e.g. Vucetic and Dobry, 1991).

From Equation (1), if the shear modulus, G, for the soil mass is enhanced sufficiently by diagonal reinforcement, and the cyclic shear strain maintained below the threshold value of 0.1 percent, then there should be minimal generation of pore water pressure and no liquefaction. Further, by reducing cyclic shear strain the reinforcement should also act to maintain the soil's own initial stiffness which otherwise tends to degrade rapidly.

This study has examined experimentally the effectiveness of inclined micropiles as reinforcement to reduce soil cyclic shear strains during shaking. Full-size prototype micropiles (Titan 26-14) were installed in loose sand in a large (2 m deep x 1.8 m long x 0.8 m wide) laminated shear box then subjected to different levels of shaking. Results were compared to similar soil deposits without micropile reinforcement.

2 LAMINATED SAND TANK

Prototype inclined micropiles were tested in a large laminar sand tank on a one degree of freedom shaking table at the University of Canterbury. The purpose of the laminar tank was to simulate free-field shaking response by allowing the soil to deform in simple shear with minimal boundary effects from the tank (e.g. Hushmand et. al. 1988, Iai 1991, Whitman et. al. 1981). The tank design used for this study follows from that of Hushmand et al., and is shown in Figure 1. The tank has internal dimensions of 1.8 m long by 0.8 m wide by 2.0 m deep.

The laminates were made from 100 mm by 50 mm cold-formed steel channel that was laid on its flat and welded into rectangular frames. Teflon strips of 150 mm long by 10 mm wide by 1 mm thick were glued to both sides of the laminates at six locations to minimize friction. Tests showed that the strips produced a coefficient of friction of 0.07, indicating that at normal stresses equivalent to those at the base of the tank, the load required to shear the laminates was only 2 percent of the load required to shear the soil mass.

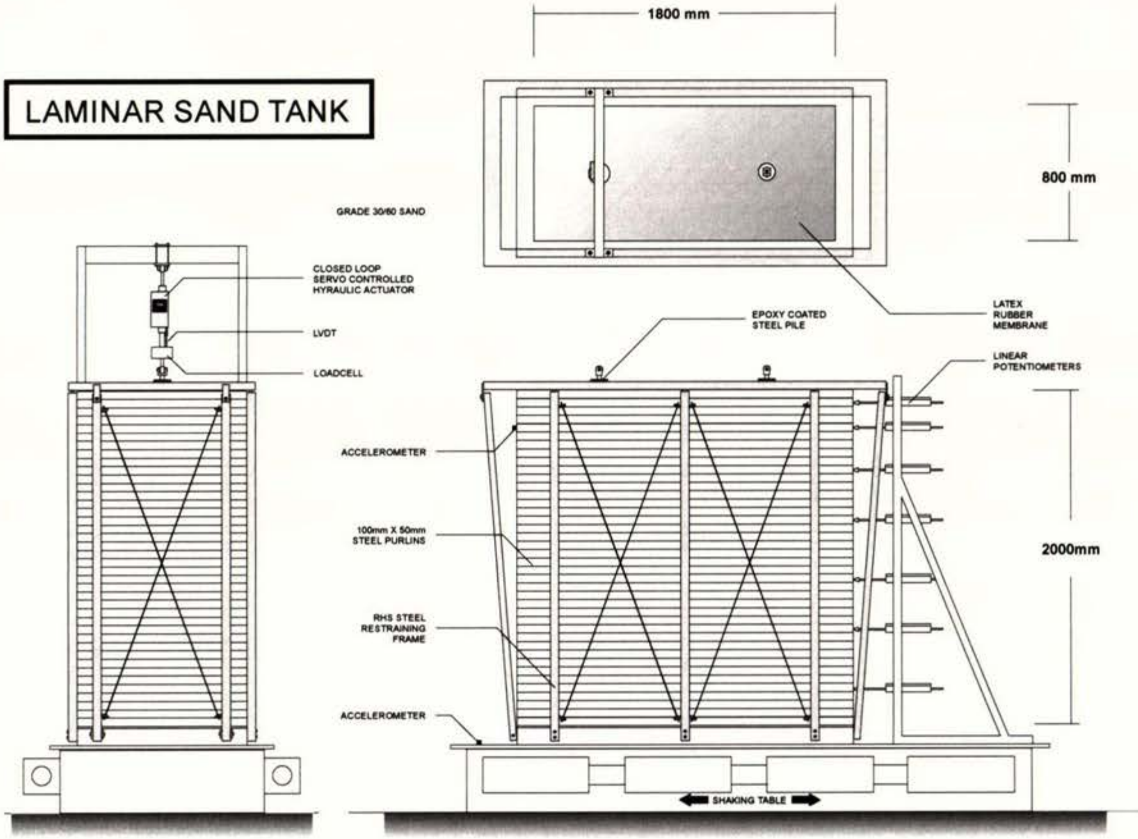

Figure 1. Laminar sand tank

Soil was contained within the tank by a flexible membrane liner. Latex rubber sheets, each 1 mm thick, were draped over the inside of the laminates and glued to the top laminate.

The laminates were supported by a steel frame that was constructed from 50 mm by 50 mm rectangular hollow section (RHS), with 10 mm diameter rods acting as cross-bracing members. The frame restricted the laminates to move only in the direction of the shaking table and also supported the stack of laminates when the tank was empty. Both the top-cap and the side members of the supporting frame were coated with Teflon strips to reduce friction during shaking.

3 INSTRUMENTATION

Five potentiometers (Showa type 50LP300) were placed in contact with tank laminates at various heights above the tank base (1.07 m, 1.34 m, 1.55 m, and 1.97 m) and fixed rigidly to the shaking table in order to measure relative lateral displacements of the tank laminates during shaking.

An accelerometer (Kyowa AS-5GA) was fixed to one of the tank laminates near to the soil surface (1.77 m above tank base) in order to measure soil acceleration and a similar accelerometer was fixed directly to the shaking table.

Settlement of the soil surface was measured by fixing a vertically oriented potentiometer to the tank support frame and making contact with an aluminium plate resting on the sand surface.

4 SOIL DEPOSITS

The soil used was an industrial grade 30/60 silica sand supplied by Commercial Minerals Ltd, Auckland, New Zealand, with properties given in Table 1. This soil was selected because it is suitable for air pluviation and can be re-used without degradation.

Table 1. Soil Properties

Property	Symbol	Value
Density of Solid Particles	ρ_s	2.65 t/m^3
10% finer	D_{10}	0.30 mm
60% finer	D_{60}	0.45 mm
minimum voids ratio	e_{min}	0.53
maximum voids ratio	e_{max}	0.83
Steady State Friction Angle	ϕ_{ss}	33°

Soil deposits were prepared by air pluviation. Sand flowed from a hopper through a gate, was collected in a suspended funnel, then flowed down a 95 mm diameter flexible hose, discharging through a wire mesh diffuser into the laminated tank. The diffuser was made from a 100 mm diameter by 300 mm long section of plastic tube that was packed with wire mesh. By discharging sand from the diffuser directly onto the surface of the deposit, a low initial relative density (six deposits, Dr = 0.17 – 0.26) was achieved. The sand densified somewhat during each episode of shaking enabling some tests to be performed in higher densities (as high as Dr = 0.4).

Two cone penetrometer tests (CPT) were performed in one of the deposits after deposition and prior to shaking. The penetration was found to be consistent throughout the deposit with cone resistance q_c ranging from 1 MPa to 1.4 MPa.

5 SHAKING TABLE

The characteristics of the University of Canterbury shaking table are given in Table 2. The table is driven by a closed-loop, servo-controlled hydraulic actuator with an MTS Teststar 2 system controller. Each test was performed under displacement control, with the cyclic table displacements generated by entering the required amplitude, frequency, and number of cycles into the controller.

Table 2. Characteristics of the University of Canterbury Shaking Table

Property	Value
Plan Dimensions	4.0 m x 2.0 m
Maximum Allowable Load	200 kN
Maximum Horizontal Force	200 kN
Maximum acceleration with a mass of 5 tonne	2.7 g
Maximum Velocity	1.0 m/s
Maximum Displacement	0.30 m

6 SOIL RESPONSE TO SHAKING

Four deposits were constructed without micropile reinforcement and subjected to shaking to verify behaviour of the laminar tank and to determine baseline soil response. Soil deposits were subjected to individual "earthquakes" consisting of 26 cycles of 1 Hz sine wave shaking at three amplitudes: +/- 20 mm, +/- 30 mm, and +/- 40 mm.

Shake table acceleration response was somewhat "jerky", as shown for a typical +/- 40 mm test in

Figure 2. The ideal, "smooth" response of the table would have been perfect sine waves of +/- 0.16 g, instead the response was unsymmetrical and overlain by high frequency noise with average peak values of approximately 0.26 g. This "jerky" response is arguably more representative of real earthquakes than a pure sine wave would have been.

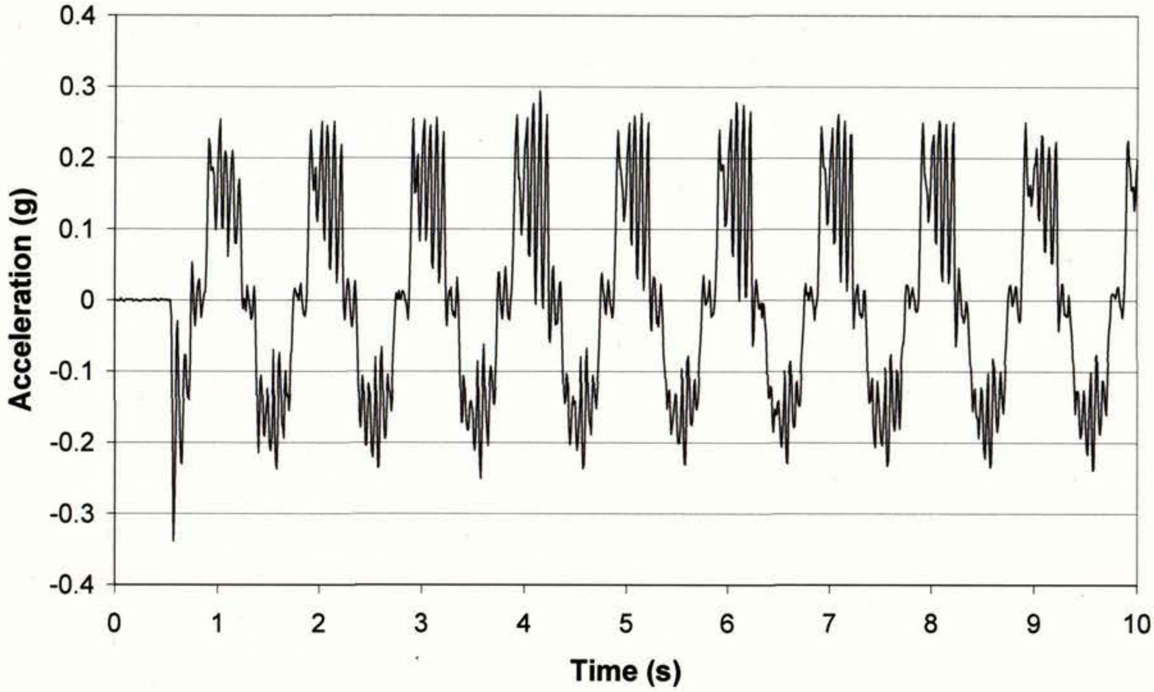

Figure 2. Acceleration Response of Shake Table for +/- 40 mm, 1 Hz shaking.

Laboratory experiments using sine wave excitation of soils are considered to be more severe than real earthquakes where there are usually relatively few excursions near to the peak ground acceleration (PGA). Seed (1970) argued that peak ground accelerations used for sine wave based laboratory experiments should be scaled up by a factor of 1/0.65 when making predictions of soil response for real earthquakes. The levels of shaking used for this study are summarised in Table 3 together with equivalent PGA values as recommended by Seed (1970).

Table 3. Levels of Shaking and Equivalent Peak Ground Accelerations

Programmed Displacement (26 cycles, 1 Hz)	Average Peak Cyclic Acceleration (g)	Equivalent PGA (g)
+/- 20 mm	0.15	0.23
+/-30 mm	0.18	0.28
+/-40mm	0.26	0.40

During shaking, the displacement measurements showed that the soil mass deformed in a linear, simple shear mode from the tank base to a height of 1.6 m, then deformed in a non-linear, irregular mode from 1.6 m to the surface at 2.0 m. The deformation of the surface soil seems to have been affected by surface waves of complex shape that were observed during shaking. Typical displacement measurements are shown in Figure 3.

The cyclic shear strain during shaking is shown in Figure 4 for the three amplitudes of shaking. The peak displacement of each transducer for each cycle of shaking was captured and divided by the height above the tank base then averaged over all of the transducers to give an average peak shear strain for each cycle. Peak strain decreased during each "earthquake" as the initially loose soil densified. For the lower amplitude shaking (0.23 g and 0.28 g) the cyclic shear strains were modest (0.23 percent and 0.11 percent for cycle 13) but for the higher amplitude shaking (0.40 g) the cyclic shear strain was much greater (0.65 percent for cycle 13).

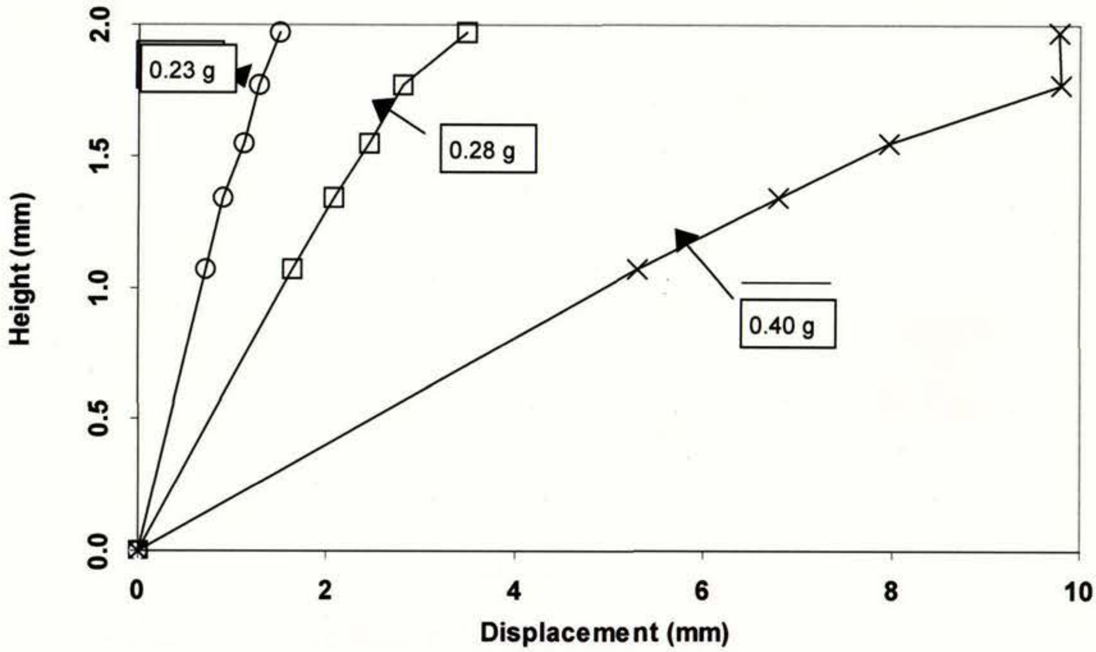

Figure 3. Displacement profiles for unreinforced soil deposits.

Significant settlements occurred at the surface of each soil deposit during shaking as the initially loose sand densified. The amount of settlement varied significantly depending on the amplitude of shaking, as shown in Figure 5. For the shaking at 0.23 g and 0.28 g the settlement was modest and similar(0.31 percent and 0.35 percent), but, for the higher level shaking at 0.40 g the settlement was much greater (3.1 percent).

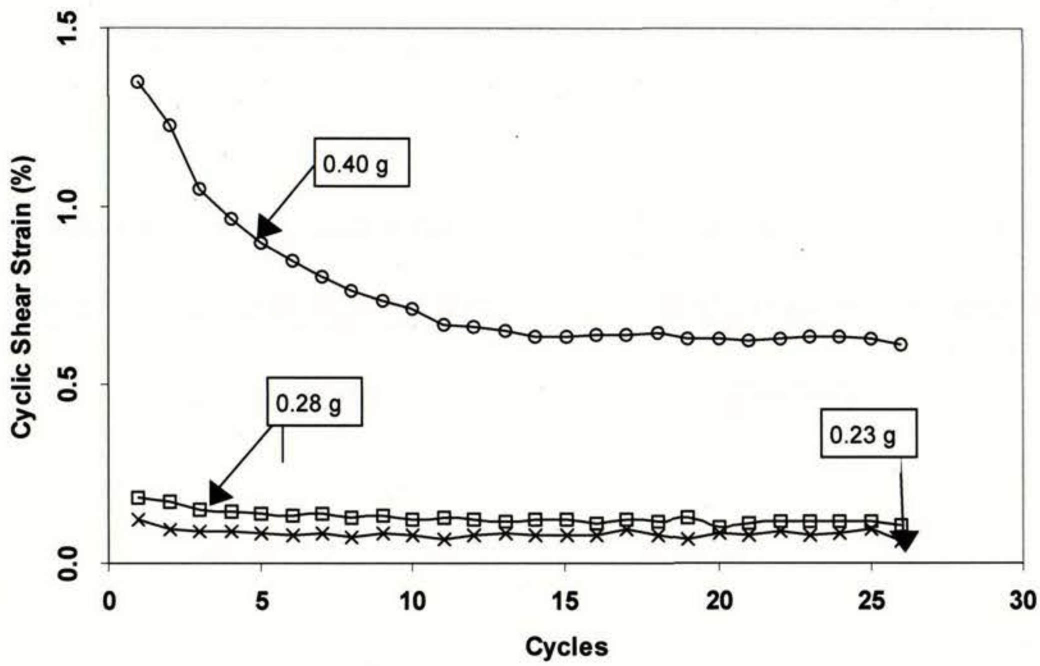

Figure 4. Average peak cyclic shear strain for unreinforced soil deposits (Initial Dr = 0.2)

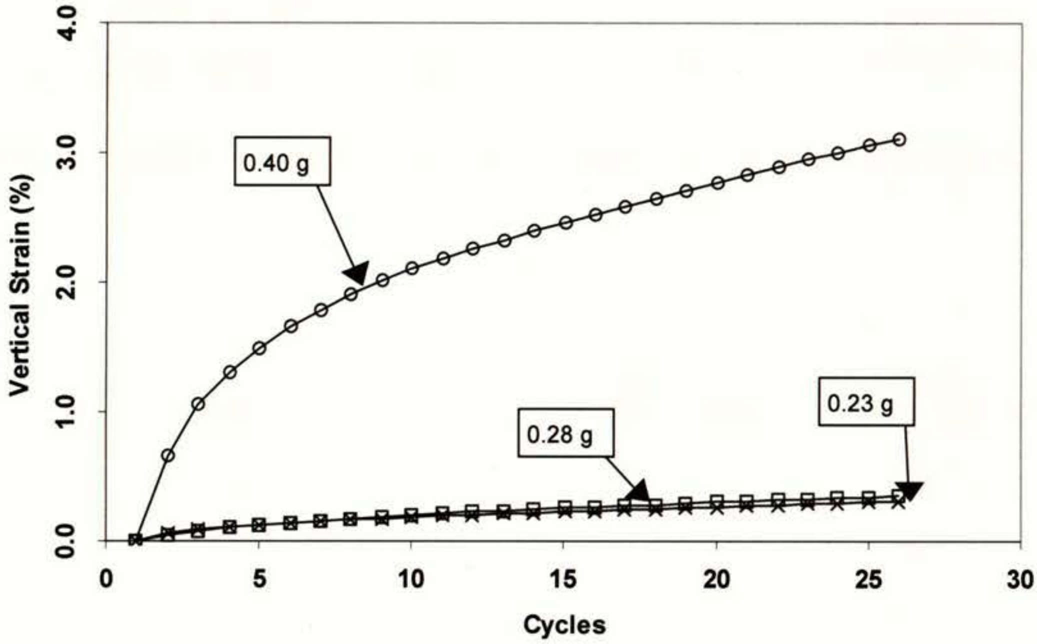

Figure 5. Settlement of unreinforced soil deposits (Initial Dr = 0.2).

Clearly, a significant transformation in response occurred between the shaking at 0.28 g and the shaking at 0.40 g, with settlement jumping from 0.35 percent to 3.1 percent. The shaking at 0.28 g caused a cyclic shear strain of 0.11 percent which is very close to the threshold value for liquefaction of 0.1 percent suggested by Dobry and Ladd (1980). Increasing the shaking intensity further to 0.40 g may have triggered a "collapse" of the soil fabric with a large reduction in shear stiffness and increase in settlement. This "collapse" may be equivalent to liquefaction occurring in a saturated sand deposit.

7 MICROPILE INSTALLATION

Two soil deposits were reinforced with diagonal micropiles. One deposit was reinforced with a single micropile and was reinforced with two diagonally opposed micropiles, as shown in Figure 6. Titan 26-14 self-drilling micropiles supplied by Ischebeck (NZ) Ltd were used as reinforcement. Titan micropiles consist of high-strength hollow steel threaded bars installed by a self-drilling process with a sacrificial drill bit. Grout is injected during drilling at low pressure to mix with the surrounding soil and provide bonding and corrosion protection.

For this study, the micropiles were installed into loose sand at shallow (2 m) depth and so the bars were installed simply by pushing with hydraulic rams (a cone penetrometer pushing rig), as shown in Figure 7. An oversize cone-shaped drill head was fixed to the pile tip to create an annular space that was progressively filled with grout during pushing. A photograph of the completed installation with two diagonally opposed micropiles is shown in Figure 8.

The grout mix used was 50:50 by weight of ordinary Portland cement:water, with 3 percent bentonite by weight of cement added to stabilize the grout and reduce water loss to the dry sand. The unconfined compressive strength of the cured grout was 9 MPa at 7 days and 11 MPa at 28 days.

The micropiles were exhumed from the soil after each test and were found to be highly uniform in cross-section with a diameter of 100 mm +/- 15 mm.

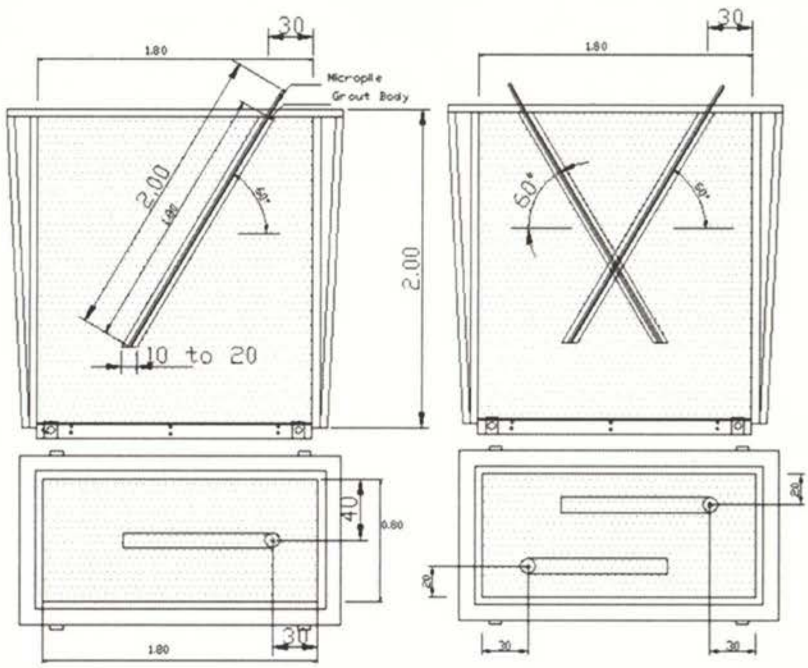

Figure 6. Layout of micropile reinforcement in laminar tank.

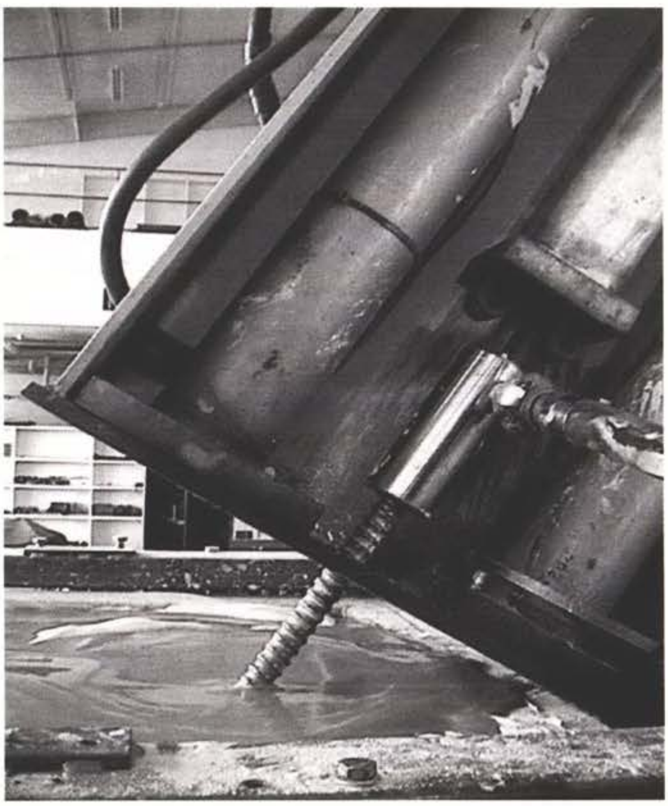

Figure 7. Installation of inclined micropiles.

Figure 8. Completed installation of two inclined micropiles.

8 RESPONSE OF REINFORCED SOIL DEPOSITS

The two reinforced soil deposits (one micropile and two micropiles) were subjected to the same levels of shaking as unreinforced deposits of similar density (Initial Dr = 0.4). The response of the reinforced deposits is compared to equivalent unreinforced deposits in Figures 9 and 10, showing average peak cyclic shear strain and settlement during shaking.

The response of the soil deposit with one inclined micropile was quite similar to the unreinforced deposit. The average peak cyclic shear strains were similarly high (0.54 percent for the unreinforced deposit and 0.64 percent for the reinforced deposit after 13 cycles) and the total settlements were also quite similar (1.2 percent and 1.1 percent). The main notable difference in response was that the deposit with one micropile initially had a larger response in terms of both cyclic shear strain and settlement than the unreinforced deposit, with the response steadily declining during the test.

The response of the soil deposit with two diagonally opposed micropiles was reduced to about half of the cyclic shear strain of the unreinforced deposit (0.24 percent after 13 cycles) and about one fifth of the settlement (0.24 percent). This level of cyclic shear strain is somewhat above the threshold of 0.1 percent for liquefaction suggested by Dobry and Ladd (1980), but the settlement was reduced substantially suggesting that liquefaction in an equivalent saturated deposit might have been prevented.

Nevertheless, the increase in shear stiffness of the deposit provided by the reinforcement was low considering the steel cross-section introduced. From the measured cyclic shear strains shown in Figure 9, the equivalent shear modulus, *G*, at mid-depth of the deposit (1 m) may be calculated as 380 KN/m^2 for the unreinforced deposit and 1010 KN/m^2 for the deposit with two micropiles. The equivalent shear modulus provided by the steel reinforcement, if the steel cross-section were fully mobilised, is 52,000 KN/m^2. Obviously, the capacity of the micropiles is hardly mobilised suggesting that reinforcement of much lower strength and stiffness may provide similar benefit at lower cost.

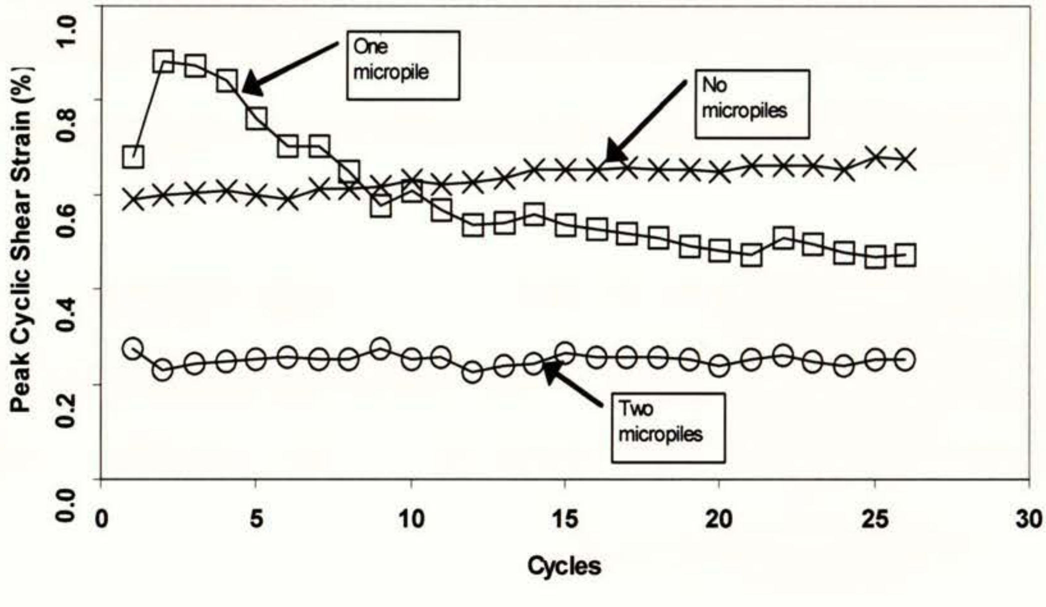

Figure 9. Average peak cyclic shear strain: PGA = 0.40 g, initial Dr = 0.4.

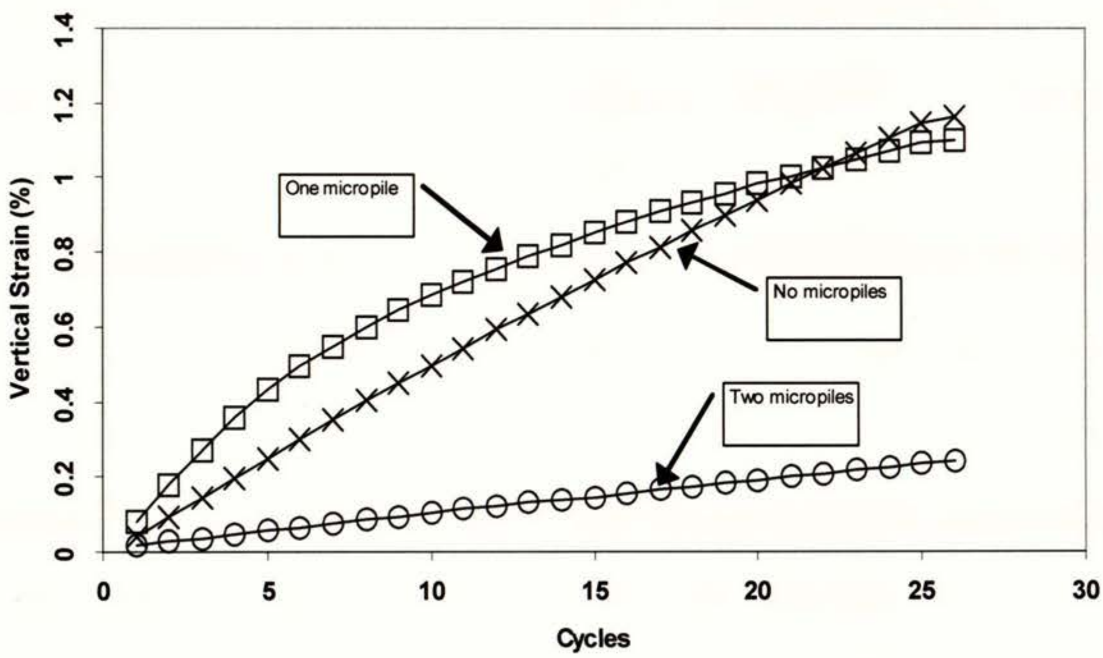

Figure 10. Settlement during shaking: PGA = 0.40 g, initial Dr = 0.4

9 CONCLUSIONS

The large-size laminar tank performed well on the shaking table with linear simple shear being generated in deposits of loose sand in all but the upper 0.2 m. Shaking of loose, unreinforced sand deposits with accelerations of 0.23 g and 0.28 g caused peak cyclic shear strains of up to 0.11 percent and minimal settlements of up to 0.35 percent. Shaking at higher level (0.40 g) caused a transformation in response with large cyclic shear strains (0.65 percent) and large settlements (3.1 percent).

Installation of Titan self-drilling micropiles at inclinations of 30 degrees was achieved readily by direct-push with simultaneous grout injection at low pressure.

Reinforcement of sand deposits with a single inclined micropile had little effect on response to shaking. Reinforcement with two, diagonally opposed micropiles had a significant effect, reducing cyclic shear strain by half and settlement to one fifth that of a similar unreinforced deposit. It is probable that the two micropiles would have prevented liquefaction of the soil deposit in this case (initial Dr = 0.4, PGA = 0.40 g) if it had been saturated with water.

The efficiency of the reinforcement was low, with relatively little of the potential increase in stiffness from the steel cross-section utilised.

Future research should investigate use of much lighter reinforcement elements which may provide similar benefits at greater economy.

10 ACKNOWLEDGEMENTS

This project received funding from the New Zealand Earthquake Commission Research Foundation under grant EQC 01/477. Ischebeck(NZ) Ltd. provided the micropiles and John Yonge provided much advice on installation. Alistair Chambers designed and developed the laminar tank. John Maley assisted with construction and setup of the apparatus and operated the shake table. Richard Pascoe operated the CPT rig and installed the micropiles. Neil Charters contributed to the analysis.

REFERENCES:

Dobry, R. and Ladd, R.S. (1980). Discussion to "Soil liquefaction and cyclic mobility evaluation for level ground during earthquakes, : by H.B. Seed and "Liquefaction potential: science versus practice," by R.B. Peck, *J. of the Geotechnical Engineering Division*, ASCE, Vol. 106, No. GT6, pp. 720-724.

Dobry, R., Ladd, R.S., Yokel, F.Y., Chung, R.M., and Powell, D. (1982). "Predictionof pore water pressure buildup and liquefaction of sands during earthquakes by cyclic strain method," *NBS Building Science Series 138*, National Bureau of Standards, Gaithersburg, Maryland, 150 pp.

Hushmand, B., Scott R.F. & Crouse C.B. (1988). "Centrifuge liquefaction tests in a laminar box", *Geotechnique*, Vol. 38, No 2, pp. 253-262.

Iai, S. (1991). "A Strain Space Multiple Mechanism Model For Cyclic Behavior of Sand and its Application," *Research Note No.43*, Earthquake Engineering Research Group, Port and Harbour Research Institute, Ministry of Transport, Japan. May 1991.

Seed, H. B.and Idriss, I. M. (1970). *A simplified procedure for evaluating soil*

liquefaction potential, Earthquake Engineering Research Center, Univeristy of California, Berkeley, Nov. 1970, 38 p.

Silver, N.L. and Seed, H.B. (1971). "Volume changes in sands during cyclic loading," *J. of the Soil Mechanics and Foundations Division*, ASCE, Vol. 97, No. SM9, pp. 1171-

Vucetic, M. and Dobry, R. (1991). "Effect of soil plasticity on cyclic response," *J. of Geotechnical Engineering*, ASCE, Vol. 117, No. 1, pp. 89-107.

Whitman, R.V., Lambe, P.C. & Kutter, B.L. (1981). "Initial Results from a Stacked-Ring Apparatus for Simulation of a Soil Profile". *Proceedings, International Conference on Recent Advances in Geotechnical Earthquake Engineering and Soil Dynamics*, St Louis, Mo., April 26 – May 3, 1981.

Youd, T.L. (1972). "Compaction of sands by repeated shear straining," *J. of the Soil Mechanics and Foundations Division*, ASCE, Vol. 98, No. SM7, pp. 709-725.

01/477
ENC 334.

USE OF MICROPILES FOR REMEDIATION OF LIQUEFACTION PRONE SITES AND RETRO-FITTING OF SMALL STRUCTURES

EQC 01/477

Final Report, October 2005

Prepared by

UNIVERSITY OF CANTERBURY
Department of Civil Engineering
Christchurch
New Zealand

Principal Investigator
Kevin J McManus

Prepared for
Earthquake Commission
Box 311
Wellington
New Zealand

Director of Research Fund
R. Ivan Skinner

Abstract

The use of inclined micropiles as reinforcement to prevent soil liquefaction in level ground has been investigated experimentally. Deposits of loose (Dr = 0.2 to 0.4), dry sand were prepared inside a large (2.0 m deep by 1.8 m long by 0.8 m wide) laminated box and subjected to shaking of different intensities on a one-dimensional shake table. For low intensity shaking (PGA up to 0.28 g) the cyclic shear strains were modest (up to 0.11 percent) and there was a modest settlement (0.31 percent). For higher intensity shaking, (PGA up to 0.40 g) there was a significant transformation in response with much greater cyclic shear strain (0.65 percent) and settlement (3.1 percent).

Other deposits were reinforced by use of Titan 26-14 self-drilling micropiles installed at 30 degrees inclination. Reinforcement by one inclined micropile was found to have little effect on response to shaking but installation of two diagonally opposed, inclined micropiles was found to reduce cyclic shear strain by half and settlement to one fifth that of similar un-reinforced deposits.

A second phase of experimentation investigated a simpler and more economical method of forming the micropiles by simply pushing a 90 mm diameter hollow steel mandrel into the loose sand deposits, placing a 6 mm deformed steel bar, injecting cement grout , and then removing the mandrel. Shaking of up to 0.86 g was used, with the micropiles successfully reinforcing the sand at accelerations up to 0.6 g. Settlement was reduced to less than a quarter of that of the unreinforced soil, and cyclic shear strains were reduced to between 0.08 and 0.5 %.

A finite element numerical model was developed using the PLAXIS software code, and this was able to successfully simulate the main aspects of the experiments in the laminated tank on the shake table. Standard PLAXIS geotextile elements were used to represent the diagonal micropiles.

Numerical analysis of two simple but realistic field applications was performed by extrapolating the PLAXIS finite element model which had been calibrated against the tank experiments. Reductions in ground response were much greater for the case studies than for the laminated tank models (peak shear strain reduced from 1.12 percent for an unreinforced site to only 0.2 percent for a reinforced site). Both case

studies were costed and found to be competitive with a quote for a traditional ground improvement project utilising stone columns. ($43/m3 for Case Study 1 and $41/m3 for Case Study 2, compared with $60/m3 for stone columns).

The use of inclined micropile reinforcing appears to hold substantial promise as an alternative strategy for preventing soil liquefaction.

Acknowledgements

This project was funded principally by the Earthquake Commission under research grant EQC 01/477. Ischebeck(NZ) Ltd. provided the micropiles and John Yonge provided much advice on installation. Alistair Chambers designed and developed the laminar tank. John Maley assisted with construction and setup of the apparatus and operated the shake table. Richard Pascoe operated the CPT rig and installed the micropiles. Guillaume Charton carried out the Phase I experiments. Neil Charters carried out the Phase II experiments and his Masters Thesis forms part of this final report. John Turner of the University of Wyoming provided oversight throughout the study.

Contents

1 Introduction

Soil liquefaction is a significant hazard in earthquake prone regions. The recognized extent of the hazard is growing rapidly in size as regional studies continue to identify large areas of liquefiable soils. There is a growing problem of knowing how to treat sites where small, low cost structures including dwellings are planned. Large projects can more easily absorb the costs of traditional ground improvement techniques such as deep dynamic compaction, stone columns, and vibro-compaction and large structures can economically be founded on piles. But these techniques are seldom found to be economical for smaller projects and they are not applicable to retrofitting numerous existing affected structures.

Traditional ground improvement techniques are highly invasive, require large-size equipment, generate considerable amounts of noise and vibration, make a big mess, and need a large site to operate in. They are unsuited to small or congested sites or where there are near neighbours. By contrast micropiles can be installed with lightweight equipment, quietly, and in confined spaces, even inside of existing buildings.

Figure 1.1. Kawagishi-Cho apartments, Nigata Earthgquake, 1964.

Horizontal micropiles (usually called "soil nails") have become widely accepted as a means of reinforcing slopes against sliding failures both from static gravity induced forces and earthquakes. This study has investigated the possibility of adapting micropiles to stabilize level ground during earthquakes by installing them as diagonal reinforcement.

Traditional installation techniques for micropiles and soil nails involve drilling, insertion of steel reinforcing, followed by grouting, and are not suited for loose granular soil below the water table (the most typical case for soils susceptible to liquefaction) without the use of temporary casing. However, self-drilling micropiles (e.g. Ischebeck Titan micropiles) are now available which are ideally suited to installation in loose, liquefiable sands without use of temporary casing.

There is growing understanding that cyclic shear strains rather than cyclic shear stresses determine the onset of soil liquefaction. Soil liquefaction is a result of the tendency of loose sands to densify with shaking, the resulting effort of the soil to expel the excess pore water causing a temporary increase in pore water pressure and loss of effective confining stress. A number of researchers (Silver and Seed, 1971, Youd, 1972) have shown experimentally that the densification of dry sands is controlled by cyclic shear strains and not shear stresses. Further, the existence of a threshold cyclic shear strain has been found below which soil densification does not occur.

Therefore, if the cyclic shear strain in the soil can be kept below this threshold value, then pore pressure should not be generated and liquefaction should not occur. Dobry and Ladd (1980) have found that for different sands, prepared by different methods, and tested at different effective confining pressures the threshold cyclic shear strain for significant pore pressure generation is approximately 0.1 percent.

Dobry et. al. (1982) have proposed a method for estimating the cyclic shear strain amplitude at a point in the ground as:

$$\gamma_{cyc} = 0.65 \frac{a_{\max}}{g} \frac{\sigma_v r_d}{G(\gamma_{cyc})} \tag{1}$$

in which $a_{\max}$ = estimated peak ground acceleration at the site and r_d = an empirical reduction factor. The soil shear modulus G is highly non-linear and is a function of the cyclic shear strain. $G_{\max}$, the small strain modulus may be found for the soil profile by use of seismic CPT profiling, for instance. Modulus reduction curves as a function of cyclic shear strain are available (e.g. Vucetic and Dobry, 1991).

From Equation (1), if the shear modulus, G, for the soil mass is enhanced sufficiently by diagonal reinforcement, and the cyclic shear strain maintained below the threshold value of 0.1 percent, then there should be minimal generation of pore water pressure and no liquefaction. Further, by reducing cyclic shear strain the reinforcement should also act to maintain the soil's own initial stiffness which otherwise tends to degrade rapidly.

This study has examined both experimentally and by numerical analysis the effectiveness of inclined micropiles as reinforcement to reduce soil cyclic shear strains during shaking in four distinct phases of investigation:

In the Phase I experiments, full-size prototype micropiles (Ischebeck Titan 26-14 self-drilling anchors) were installed in loose sand in a large (2 m deep x 1.8 m long x 0.8 m wide) laminated shear box then subjected to different levels of shaking. Results were compared to similar soil deposits without micropile reinforcement.

Next, the Phase I results were modelled numerically using PLAXIS Finite Element Code for Soil and Rock. The objectives for this second phase of the investigation were to gain additional understanding of the mechanisms controlling response of the soil reinforcement by observing distributions of stress and strain surrounding the reinforcement. From this understanding it was found possible to economise substantially on the amount of steel in each micropile and so a second phase of experiments (Phase II experiments) were conducted using much lighter, 6 mm diameter steel rods for the micropiles.

The final phase of the investigation was to use the finite element numerical modelling to extrapolate the results of the tank shaking table experiments to full-size prototype case study situations.

Additional introductory material describing the phenomenon of liquefaction is included in Appendix B.

2 Phase I Experimental Model

2.1 Laminated sand tank

Prototype inclined micropiles were tested in a large laminar sand tank on a one degree of freedom shaking table at the University of Canterbury. The purpose of the laminar tank was to simulate free-field shaking response by allowing the soil to deform in simple shear with minimal boundary effects from the tank (e.g. Hushmand et. al. 1988, Iai 1991, Whitman et. al. 1981). The tank design used for this study follows from that of Hushmand et al., and is shown in Figure 2.1. The tank has internal dimensions of 1.8 m long by 0.8 m wide by 2.0 m deep.

The laminates were made from 100 mm by 50 mm cold-formed steel channel that was laid on its flat and welded into rectangular frames. Teflon strips of 150 mm long by 10 mm wide by 1 mm thick were glued to both sides of the laminates at six locations to minimize friction. Tests showed that the strips produced a coefficient of friction of 0.07, indicating that at normal stresses equivalent to those at the base of the tank, the load required to shear the laminates was only 2 percent of the load required to shear the soil mass.

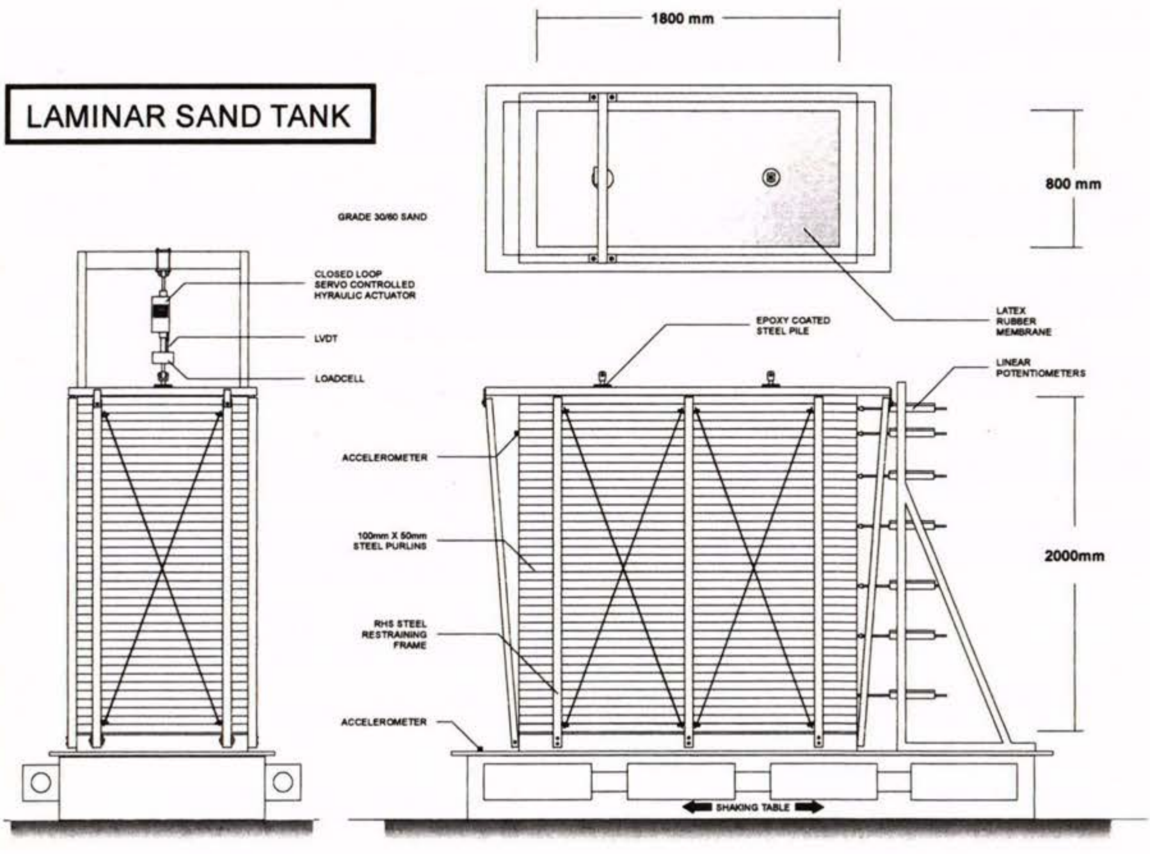

Figure 2.1 Laminar sand tank.

Soil was contained within the tank by a flexible membrane liner. Latex rubber sheets, each 1 mm thick, were draped over the inside of the laminates and glued to the top laminate.

The laminates were supported by a steel frame that was constructed from 50 mm by 50 mm rectangular hollow section (RHS), with 10 mm diameter rods acting as cross-bracing members. The frame restricted the laminates to move only in the direction of the shaking table and also supported the stack of laminates when the tank was empty. Both the top-cap and the side members of the supporting frame were coated with Teflon strips to reduce friction during shaking.

2.2 Instrumentation

Five potentiometers (Showa type 50LP300) were placed in contact with tank laminates at various heights above the tank base (1.07 m, 1.34 m, 1.55 m, and 1.97 m) and fixed rigidly to the shaking table in order to measure relative lateral displacements of the tank laminates during shaking.

An accelerometer (Kyowa AS-5GA) was fixed to one of the tank laminates near to the soil surface (1.77 m above tank base) in order to measure soil acceleration and a similar accelerometer was fixed directly to the shaking table.

Settlement of the soil surface was measured by fixing a vertically oriented potentiometer to the tank support frame and making contact with an aluminium plate resting on the sand surface.

2.3 Soil deposits

The soil used was an industrial grade 30/60 silica sand supplied by Commercial Minerals Ltd, Auckland, New Zealand, with properties given in Table 2.1. This soil was selected because it is suitable for air pluviation and can be re-used without degradation.

Table 2.1. Soil Properties

Property	Symbol	Value
Density of Solid Particles	ρ_s	2.65 t/m^3
10% finer	D_{10}	0.30 mm
60% finer	D_{60}	0.45 mm
minimum voids ratio	e_{min}	0.53
maximum voids ratio	e_{max}	0.83
Steady State Friction Angle	ϕ_{ss}	33^o

Soil deposits were prepared by air pluviation. Sand flowed from a hopper through a gate, was collected in a suspended funnel, then flowed down a 95 mm diameter flexible hose, discharging through a wire mesh diffuser into the laminated tank. The diffuser was made from a 100 mm diameter by 300 mm long section of plastic tube that was packed with wire mesh. By discharging sand from the diffuser directly onto the surface of the deposit, a low initial relative density (six deposits, Dr = 0.17 – 0.26) was achieved. The sand densified somewhat during each episode of shaking enabling some tests to be performed in higher densities (as high as Dr = 0.4).

Two cone penetrometer tests (CPT) were performed in one of the deposits after deposition and prior to shaking. The penetration was found to be consistent throughout the deposit with cone resistance q_c ranging from 1 MPa to 1.4 MPa.

2.4 Shaking Table

The characteristics of the University of Canterbury shaking table are given in Table 2.2. The table is driven by a closed-loop, servo-controlled hydraulic actuator with an MTS Teststar 2 system controller. Each test was performed under displacement control, with the cyclic table displacements generated by entering the required amplitude, frequency, and number of cycles into the controller.

Table 2.2. Characteristics of the University of Canterbury Shaking Table

Property	Value
Plan Dimensions	4.0 m x 2.0 m
Maximum Allowable Load	200 kN
Maximum Horizontal Force	200 kN
Maximum acceleration with a mass of 5 tonne	2.7 g
Maximum Velocity	1.0 m/s
Maximum Displacement	0.30 m

2.5 Soil response to shaking

Four deposits were constructed without micropile reinforcement and subjected to shaking to verify behaviour of the laminar tank and to determine baseline soil response. Soil deposits were subjected to individual "earthquakes" consisting of 26 cycles of 1 Hz sine wave shaking at three amplitudes: +/- 20 mm, +/- 30 mm, and +/- 40 mm.

Shake table acceleration response was somewhat "jerky", as shown for a typical +/- 40 mm test in Figure 2.2. The ideal, "smooth" response of the table would have been perfect sine waves of +/- 0.16 g, instead the response was unsymmetrical and overlain by high frequency noise with average peak values of approximately 0.26 g. This "jerky" response is arguably more representative of real earthquakes than a pure sine wave would have been.

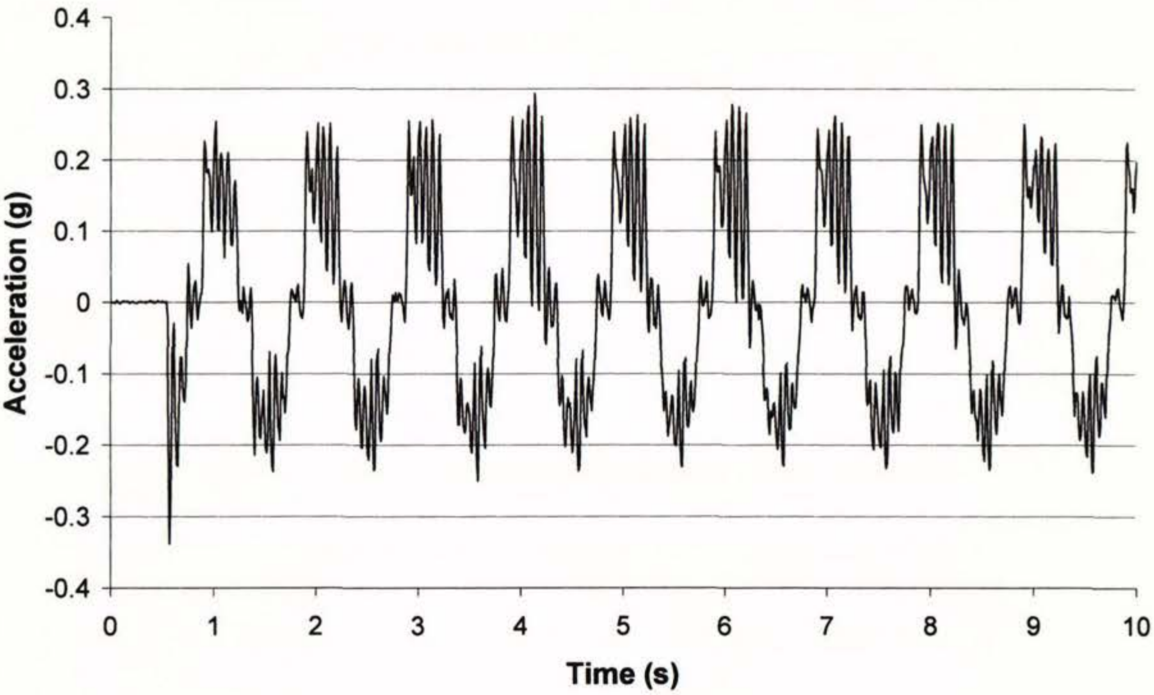

Figure 2.2. Acceleration Response of Shake Table for +/- 40 mm, 1 Hz shaking.

Laboratory experiments using sine wave excitation of soils are considered to be more severe than real earthquakes where there are usually relatively few excursions near to the peak ground acceleration (PGA). Seed (1970) argued that peak ground accelerations used for sine wave based laboratory experiments should be scaled up by a factor of 1/0.65 when making predictions of soil response for real earthquakes. The levels of shaking used for this study are summarised in Table 2.3 together with equivalent PGA values as recommended by Seed (1970).

Table 2.3. Levels of Shaking and Equivalent Peak Ground Accelerations

Programmed Displacement (26 cycles, 1 Hz)	Average Peak Cyclic Acceleration (g)	Equivalent PGA (g)
+/- 20 mm	0.15	0.23
+/-30 mm	0.18	0.28
+/-40mm	0.26	0.40

During shaking, the displacement measurements showed that the soil mass deformed in a linear, simple shear mode from the tank base to a height of 1.6 m, then deformed in a non-linear, irregular mode from 1.6 m to the surface at 2.0 m. The deformation of the surface soil seems to have been affected by surface waves of complex shape that were observed during shaking. Typical displacement measurements are shown in Figure 2.3.

The cyclic shear strain during shaking is shown in Figure 2.4 for the three amplitudes of shaking. The peak displacement of each transducer for each cycle of shaking was captured and divided by the height above the tank base then averaged over all of the transducers to give an average peak shear strain for each cycle. Peak strain decreased during each "earthquake" as the initially loose soil densified. For the lower amplitude shaking (0.23 g and 0.28 g) the cyclic shear strains were modest (0.23 percent and 0.11 percent for cycle 13) but for the higher amplitude shaking (0.40 g) the cyclic shear strain was much greater (0.65 percent for cycle 13).

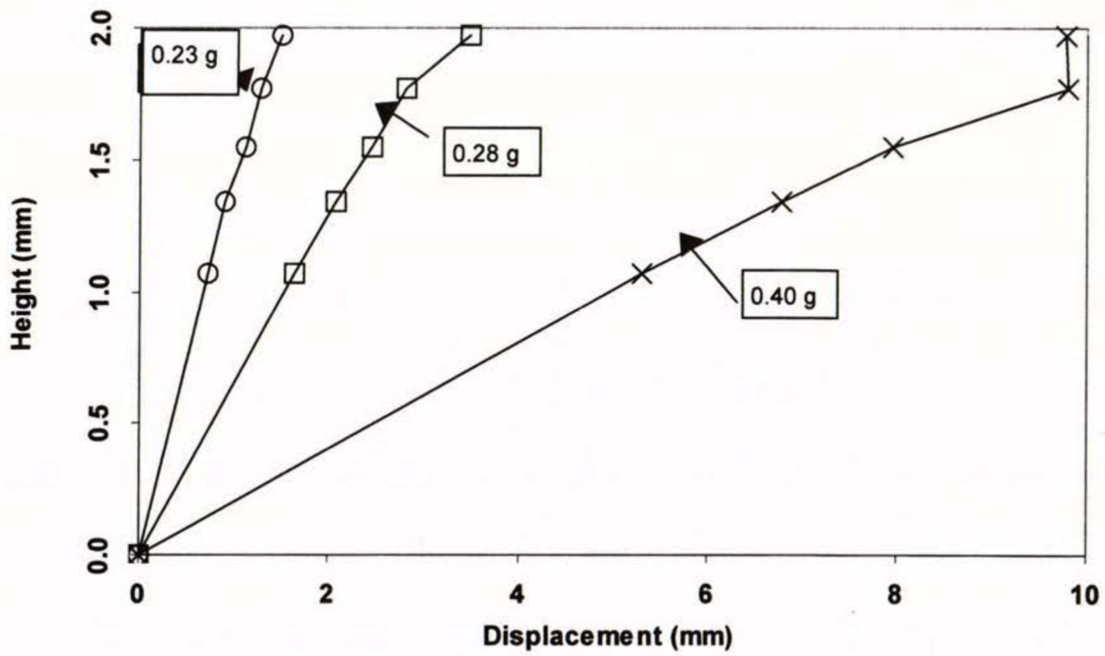

Figure 2.3. Displacement profiles for unreinforced soil deposits.

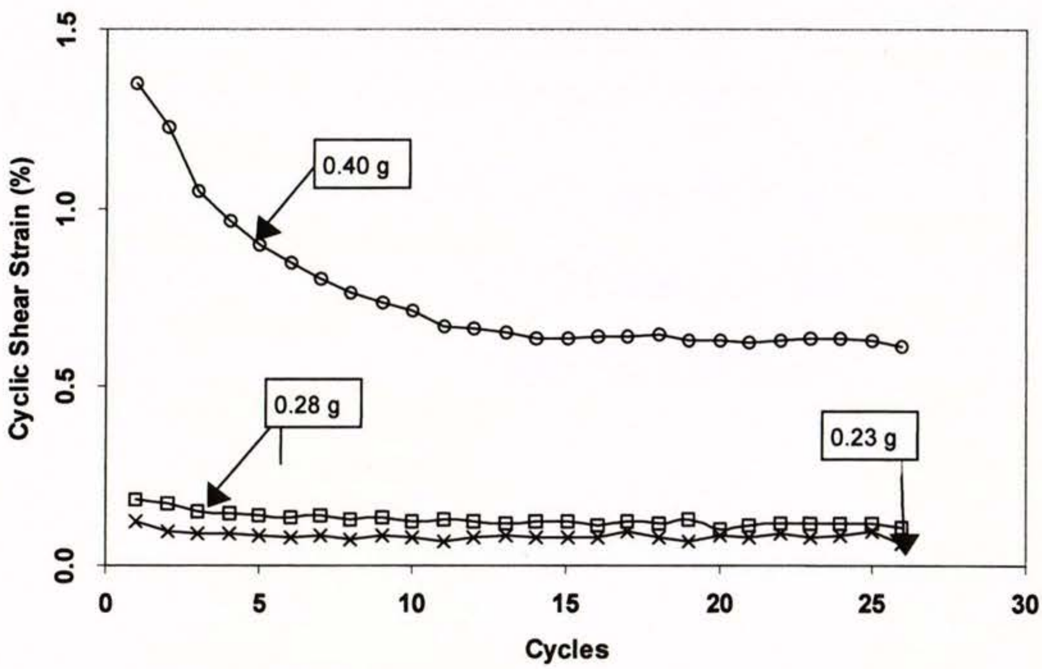

Figure 2.4. Average peak cyclic shear strain for unreinforced soil deposits (Initial Dr = 0.2)

Significant settlements occurred at the surface of each soil deposit during shaking as the initially loose sand densified. The amount of settlement varied significantly depending on the amplitude of shaking, as shown in Figure 2.5. For the shaking at 0.23 g and 0.28 g the settlement was modest and similar (0.31 percent and 0.35 percent), but, for the higher level shaking at 0.40 g the settlement was much greater (3.1 percent).

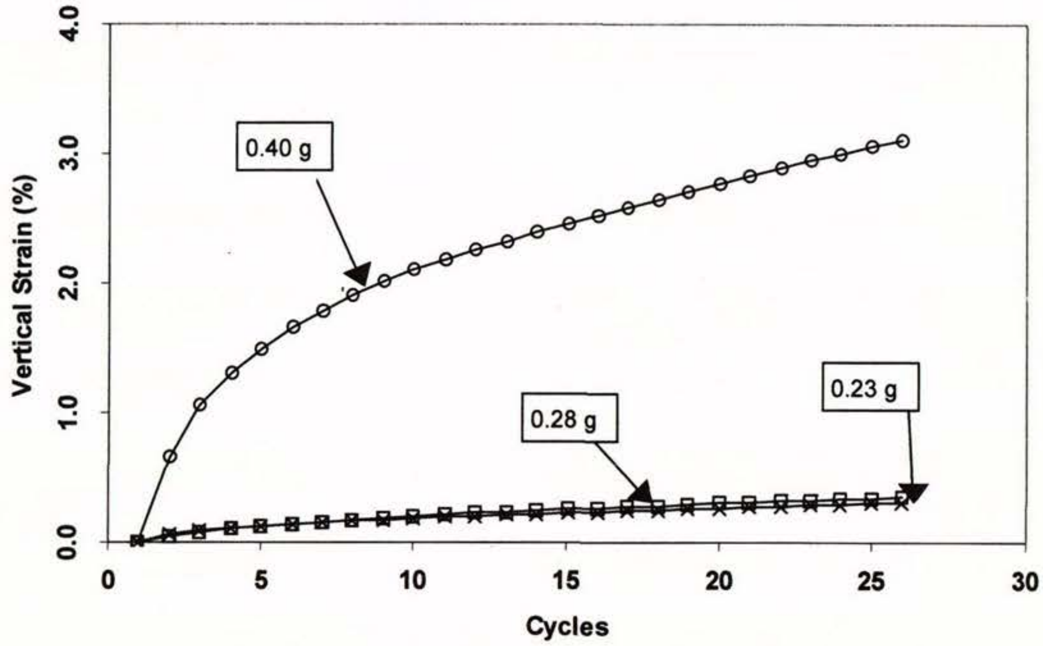

Figure 2.5. Settlement of unreinforced soil deposits (Initial Dr = 0.2).

Clearly, a significant transformation in response occurred between the shaking at 0.28 g and the shaking at 0.40 g, with settlement jumping from 0.35 percent to 3.1 percent. The shaking at 0.28 g caused a cyclic shear strain of 0.11 percent which is very close to the threshold value for liquefaction of 0.1 percent suggested by Dobry and Ladd (1980). Increasing the shaking intensity further to 0.40 g may have triggered a "collapse" of the soil fabric with a large reduction in shear stiffness and increase in settlement. This "collapse" may be equivalent to liquefaction occurring in a saturated sand deposit.

2.6 Micropile installation

Two soil deposits were reinforced with diagonal micropiles. One deposit was reinforced with a single micropile and was reinforced with two diagonally opposed micropiles, as shown in Figure. 2.6. Titan 26-14 self-drilling micropiles supplied by Ischebeck (NZ) Ltd were used as reinforcement. Titan micropiles consist of high-strength hollow steel threaded bars installed by a self-drilling process with a sacrificial drill bit. Grout is injected during drilling at low pressure to mix with the surrounding soil and provide bonding and corrosion protection.

For this study, the micropiles were installed into loose sand at shallow (2 m) depth and so the bars were installed simply by pushing with hydraulic rams (a cone penetrometer pushing rig), as shown in Figure 2.7. An oversize cone-shaped drill head was fixed to the pile tip to create an annular space that was progressively filled with grout during pushing. A photograph of the completed installation with two diagonally opposed micropiles is shown in Figure 2.8.

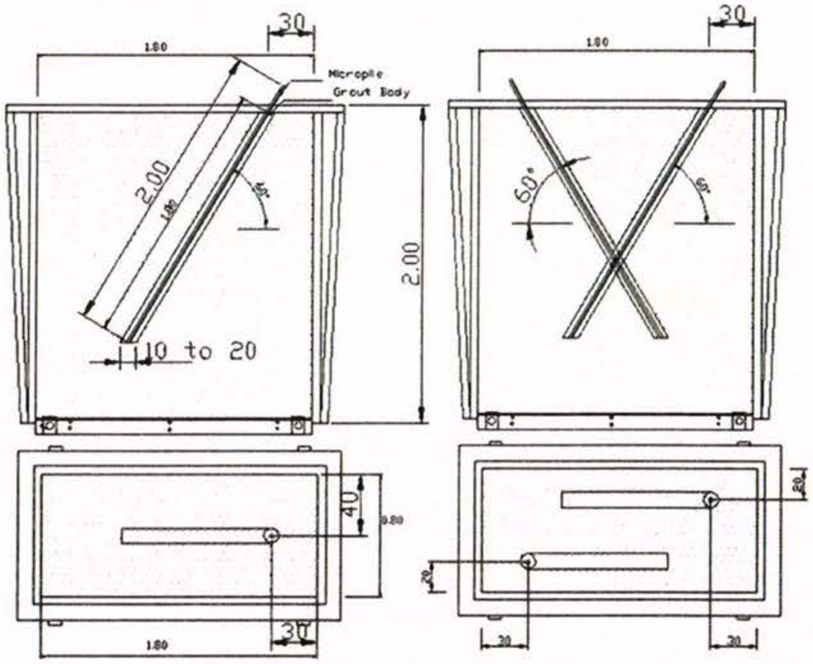

Figure 2.6. Layout of micropile reinforcement in laminar tank.

Figure 2.7. Installation of inclined micropiles.

The grout mix used was 50:50 by weight of ordinary Portland cement:water, with 3 percent bentonite by weight of cement added to stabilize the grout and reduce water loss to the dry sand. The unconfined compressive strength of the cured grout was 9 MPa at 7 days and 11 MPa at 28 days.

The micropiles were exhumed from the soil after each test and were found to be highly uniform in cross-section with a diameter of 100 mm +/- 15 mm.

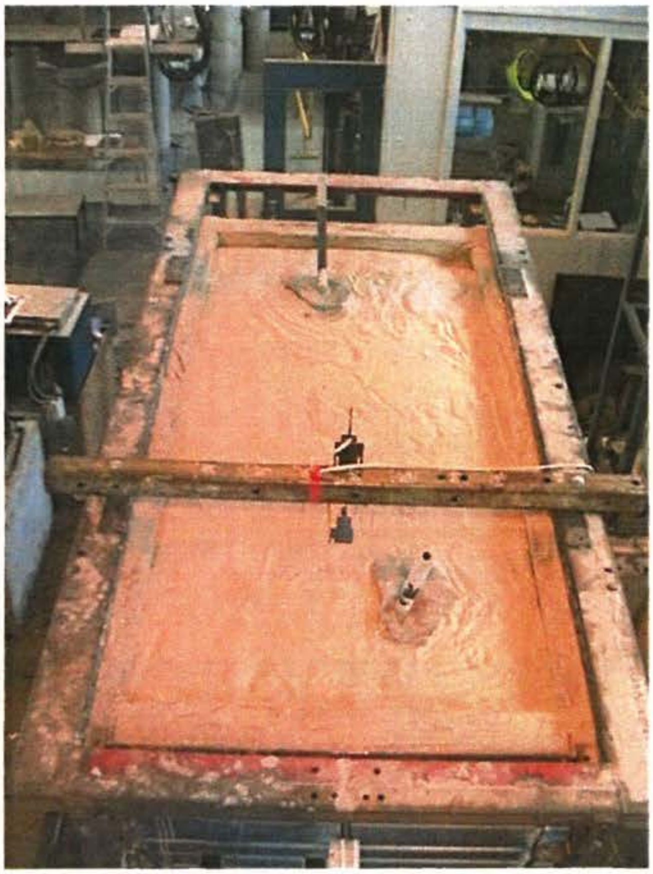

Figure 2.8. Completed installation of two inclined micropiles.

2.7 Response of reinforced soil deposits

The two reinforced soil deposits (one micropile and two micropiles) were subjected to the same levels of shaking as unreinforced deposits of similar density (Initial Dr = 0.4). The response of the reinforced deposits is compared to equivalent unreinforced deposits in Figures 2.9 and 2.10, showing average peak cyclic shear strain and settlement during shaking.

The response of the soil deposit with one inclined micropile was quite similar to the unreinforced deposit. The average peak cyclic shear strains were similarly high (0.54 percent for the unreinforced deposit and 0.64 percent for the reinforced deposit after 13 cycles) and the total settlements were also quite similar (1.2 percent and 1.1 percent). The most notable difference in response was that the deposit with one micropile initially had a larger response in terms of both cyclic shear strain and settlement than the unreinforced deposit, with the response steadily declining during the test.

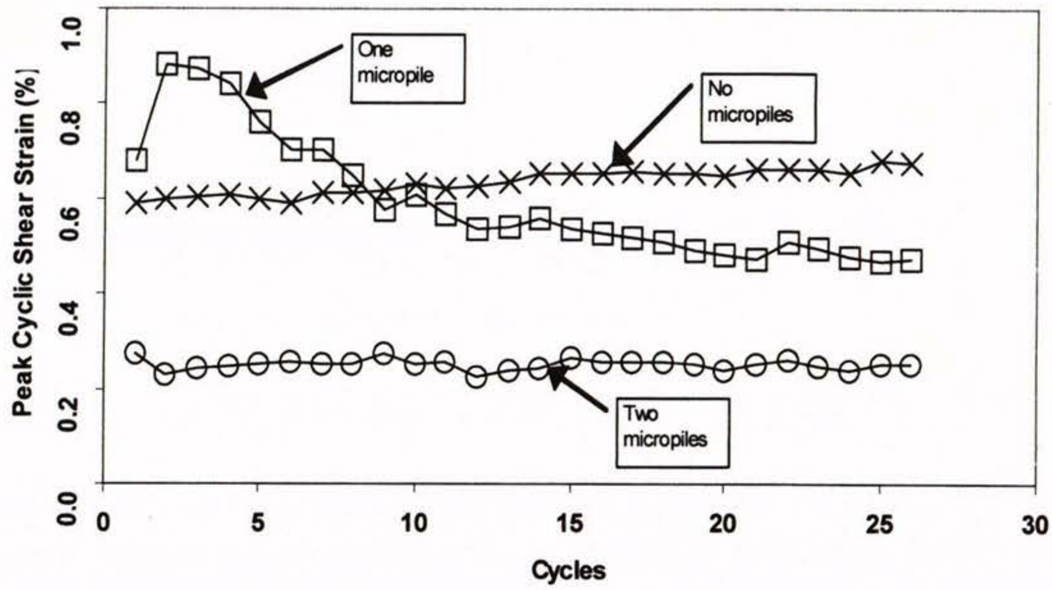

Figure 2.9. Average peak cyclic shear strain: PGA = 0.40 g, initial Dr = 0.4.

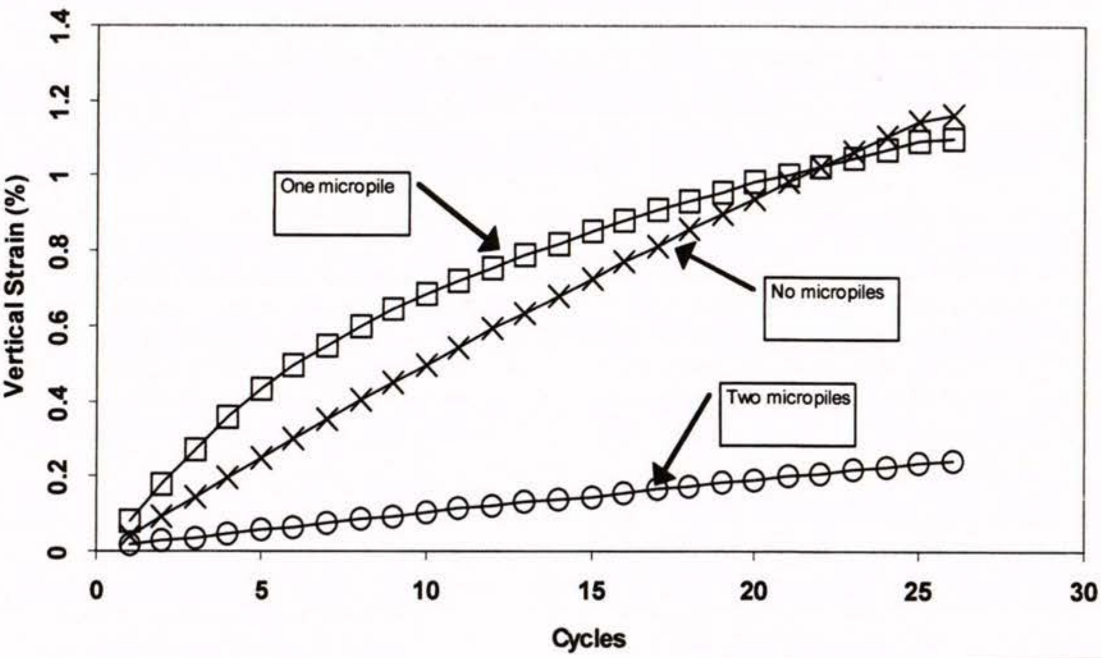

Figure 2.10. Settlement during shaking: PGA = 0.40 g, initial Dr = 0.4

The response of the soil deposit with two diagonally opposed micropiles was reduced to about half of the cyclic shear strain of the unreinforced deposit (0.24 percent after 13 cycles) and about one fifth of the settlement (0.24 percent). This level of cyclic shear strain is somewhat above the threshold of 0.1 percent for liquefaction suggested by Dobry and Ladd (1980), but the settlement was reduced substantially suggesting that liquefaction in an equivalent saturated deposit might have been prevented.

Nevertheless, the increase in shear stiffness of the deposit provided by the reinforcement was low considering the steel cross-section introduced. From the measured cyclic shear strains shown in Figure 2.9, the equivalent shear modulus, *G*, at mid-depth of the deposit (1 m) may be calculated as 380 KN/m^2 for the unreinforced deposit and 1010 KN/m^2 for the deposit with two micropiles. The equivalent shear modulus provided by the steel reinforcement, if the steel cross-section were fully mobilised, is 52,000 KN/m^2. Obviously, the capacity of the micropiles is hardly mobilised suggesting that reinforcement of much lower strength and stiffness may provide similar benefit at lower cost.

2.8 Phase I Conclusions

The large-size laminar tank performed well on the shaking table with linear simple shear being generated in deposits of loose sand in all but the upper 0.2 m. Shaking of loose, unreinforced sand deposits with accelerations of 0.23 g and 0.28 g caused peak cyclic shear strains of up to 0.11 percent and minimal settlements of up to 0.35 percent. Shaking at higher level (0.40 g) caused a transformation in response with large cyclic shear strains (0.65 percent) and large settlements (3.1 percent).

Installation of Titan self-drilling micropiles at inclinations of 30 degrees was achieved readily by direct-push with simultaneous grout injection at low pressure.

Reinforcement of sand deposits with a single inclined micropile had little effect on response to shaking. Reinforcement with two, diagonally opposed micropiles had a significant effect, reducing cyclic shear strain by half and settlement to one fifth that of a similar unreinforced deposit. It is probable that the two micropiles would have prevented liquefaction of the soil deposit in this case (initial Dr = 0.4, PGA = 0.40 g) if it had been saturated with water.

The efficiency of the reinforcement was low, with relatively little of the potential increase in stiffness from the steel cross-section utilised.

The Phase II experiments were undertaken to investigate the use of much lighter reinforcement elements which might provide similar benefits at greater economy.

3 Finite Element Model

3.1 Introduction

The main objective of the finite element modelling was to be able extend the observed physical behaviour of the soil reinforcement system from the modest-size laboratory tank experiments to full-size prototype case study situations.

A second objective was to try to gain additional understanding of the mechanisms controlling response of the soil reinforcement by observing distributions of stress and strain surrounding the reinforcement.

A further objective was to experiment with different configurations of reinforcement in an effort to try and optimise economy of reinforcement size and spacing.

Successful accomplishment of all of these objectives was dependant on first being able to successfully model the observed response of the reinforced sand tank deposits. The analyses were made using PLAXIS Finite Element Code for Soil and Rock Analyses (Brinkgreve and Vermeer, 1998) which features dynamic, non-linear, finite element analysis of soil systems. PLAXIS is routinely used to model a wide range of geotechnical systems and includes special beam, tie, and anchor elements suitable for mdelling of the micropile reinforcing elements.

A significant limitation of the PLAXIS study is the inability of the available soil models to model the contractive behaviour of sand to cyclic loading. Rather than predict soil contraction and thus liquefaction directly, the purpose of the numerical modelling was to be able to predict the cyclic strain within the reinforced soil mass and thus the likelihood of contractive behaviour and liquefaction indirectly.

3.2 Sand Tank Model

3.2.1 Model Details

The laminated sand tank is simple in concept but is quite complex in detailed implementation. The concept is to physically contain a deposit of sand and constrain it to deform in simple shear whilst being accelerated horizontally at the base. To achieve this objective, it is usual to adopt a laminated system, with each laminate having sufficient strength and stiffness to contain the sand and provide the necessary horizontal confining stress.

Rather than try and model every detail of the tank system with some 40 individual laminates, the tank walls were modelled as a pair of stiff beam elements tied together at the top and bottom with stiff tie elements, as shown in Figure 3.1. The whole structure was thus constrained to deform in simple shear, just like the physical tank model. No constraints were placed above the base of the model and the only stability was provided by the shear stiffness of the sand fill.

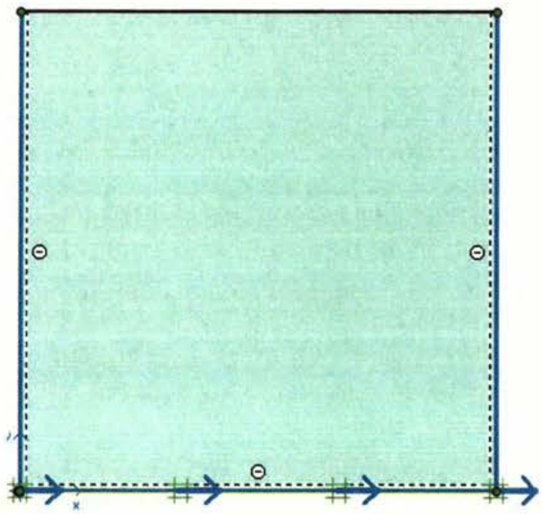

Figure 3.1. PLAXIS model representing a deposit of unreinforced sand in the laminated tank.

Previous experience by experimenters with laminated tanks has found that there are difficulties with shear stresses at the tank boundaries and that it is necessary to provide a load path for complementary shear stresses at the corners. The best way to achieve such a load path is to provide a continuous strip of geotextile wrapping along the base of the tank and up both walls. PLAXIS has special elements that are used to model geotextiles and a geotextile element was placed along the base of the deposit and this proved effective in providing stability to the numerical model.

The sand was modelled using both a Mohr-Coulomb elastic-plastic model and a hardening soil model with a hyperbolic stiffness function. Initial experimentation showed that there was little difference in output from the two models and so all of the modelling reported herein was performed using the Mohr-Coulomb model to save computation time. The numerical model parameters are summarised in Table 3.1. Stiffness parameters were selected to provide reasonable similarity to the observed average soil stiffness in the physical model results.

Table 3.1. Soil properties used for finite element model.

Parameter	**Value**	**Units**
Unit weight	20	KN/m^3
Cohesion	1	KN/m^2
Friction angle	33	degrees
Dilation angle	0	degrees
Young's Modulus	2,000	KN/m^2
Poisson's ratio	0.3	-

Shaking was achieved for the PLAXIS model by use of an imposed horizontal displacement at the base of the model. This imposed displacement was modulated as a sine wave as the time stepping dynamic procedure proceeded, mimicking the behaviour of the physical shake table.

No specific dynamic energy absorbing boundaries were used for the PLAXIS model. Instead, damping was achieved in this case by soil yielding and hysteresis. The basic time step selected for the dynamic calculations was 0.02 seconds with 10 intermediate integration steps. A total of 20 cycles of 1 Hz sine wave cycles was applied to allow decay of the starting transients and a steady state response to be observed.

3.2.2 Response of unreinforced deposit

The benchmark response of the unreinforced soil model to shaking is shown in Figure 3.2 for a point on the sand surface at the centre of the deposit. This response is somewhat lower than but broadly similar to the response of the physical model shown in Figure 2.4. The degree of similarity between the numerical and physical models was considered to be adequate given the relatively simple numerical model being employed. The initial decay in peak response for the numerical model is caused by damping of the starting transient as the first cycle of motion is applied. The physical model shows a higher initial rate of decay because, in addition to the starting transient, there was also a marked densification of the soil taking place. This densification was not simulated in the numerical model.

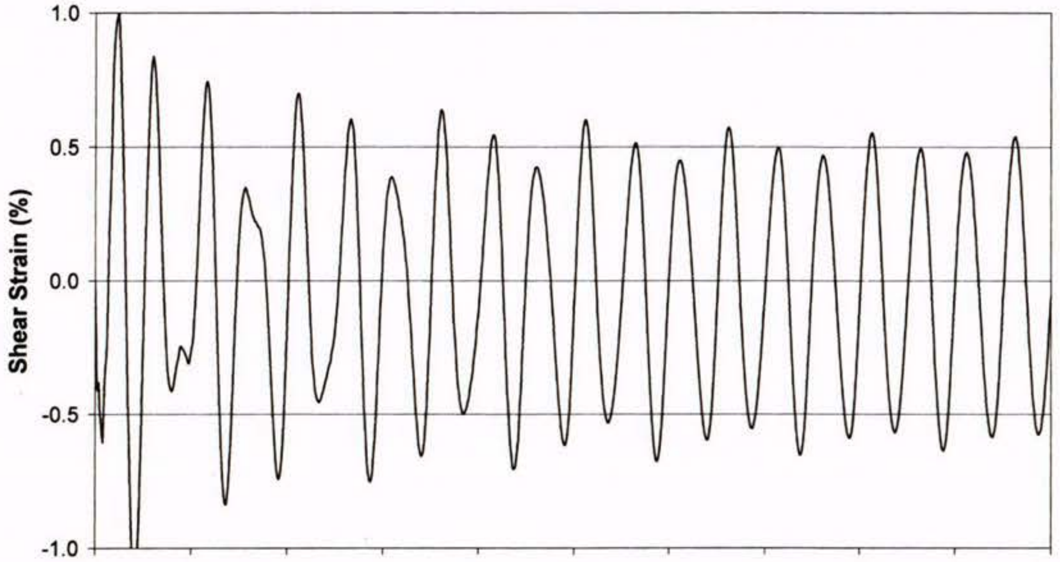

Figure 3.2. Response of unreinforced soil model to forced shaking at base of +/- 40 mm at 1 Hz. Shear stain = [surface displacement – base displacement] / soil height.

3.2.3 Response with inclined reinforcement

The inclined micropile reinforcing elements were modelled in PLAXIS by using geotextile elements, as shown in Figure 3.3. Initial attempts using beam elements proved unsuccessful, probably because of the unrealistic constraint where the two elements crossed at the centre of the soil deposit. The PLAXIS model used was 2-D plane strain and so called beam elements are actually modelling plates, and the crossing point of the two diagonally opposed plates must be pinned. By using geotextile elements there is less constraint at the crossing point and the results achieved were much more realistic.

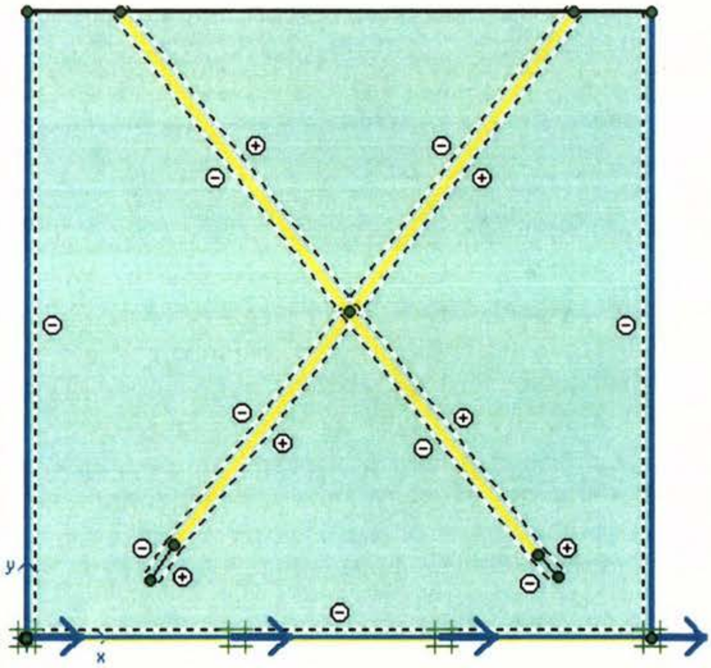

Figure 3.3. PLAXIS model representing a deposit of double reinforced sand in the laminated tank.

The key parameter for the geotextile element in PLAXIS is axial stiffness. Axial stiffness is expressed solely in tension and the element has no effect in compression. Interface elements were also added to the perimeter of the geotextile elements to provide better modelling of the soil structure interface (Brinkgreve and Vermeer, 1998). The stiffness of the geotextile elements was selected to model the reinforcing elements used in the physical tank experiments with values given in Table 3.2. Two different values were selected, one for each phase of the physical experiments.

Table 3.2. Stiffness values for the inclined reinforcing elements.

Axial Stiffness[1] (KN/m)	Physical Model
2.8×10^5	Phase I: Ischebeck Titan Micropile 26-14
1.6×10^5	Phase II: 6 mm reinforcing bar in 100 mm diameter grout micropile

[1]Assumes piles are spaced at 1 m centres.

The response of the numerical model with reinforcing elements when subjected to 20 cycles of +/- 40 mm, 1 Hz shaking at the base is shown in Figure 3.4. The main effect of adding the reinforcing elements was to significantly reduce the magnitude of the peak soil shear strains by 40 to 50 percent. This result compares well with the observed reduction for the physical experiment of 40 percent after 10 cycles and 50 percent after 20 cycles, as shown in Figure 2.9.

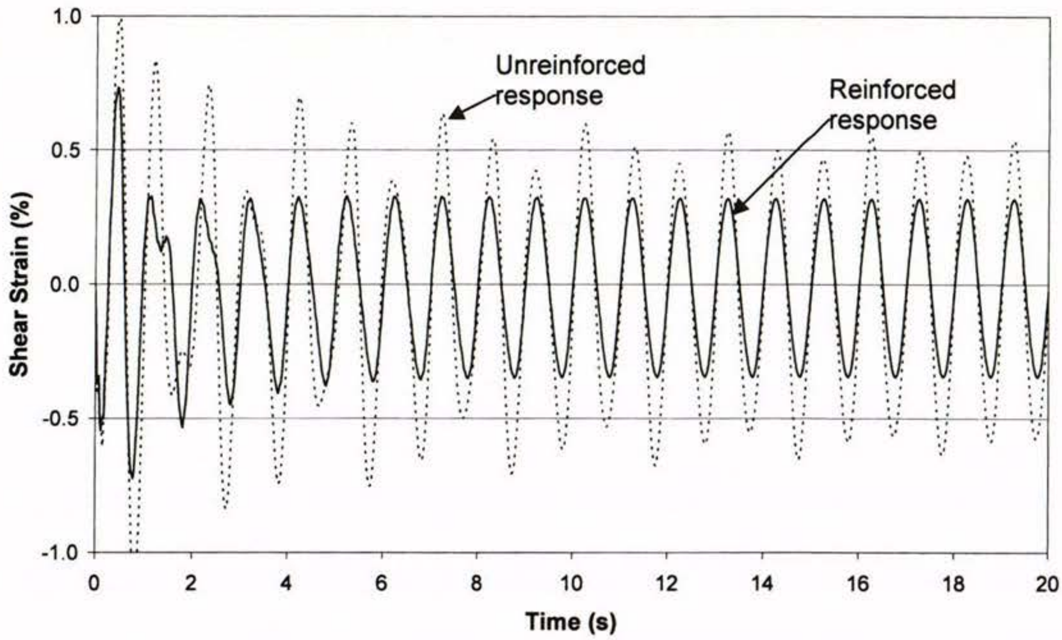

Figure 3.4. Response of unreinforced soil model to forced shaking at base of +/- 40 mm at 1 Hz. Shear stain = [surface displacement – base displacement] x soil height. Response of unreinforced soil model is shown dashed.

Another significant effect of adding the reinforcing elements was to increase the rate of damping of the initial starting transient. Steady state response was achieved after one cycle compared with five or six for the unreinforced model.

No discernable difference in response was found for the two different values of reinforcing element stiffness analysed (1.6 x 10^5 KN/m and 2.8 x 10^5 KN/m), at least not for the plotting scale adopted for Figure 3.4. It would seem that the key mechanism affecting the response of the model with reinforcing elements is some stiffening effect from the presence of the soil/structure interface and not the axial stiffness of the structural element per se.

3.3 Conclusions

The PLAXIS finite element package was able to successfully model the response of both the unreinforced sand tank deposits and the reinforced deposits.

The PLAXIS analysis was able to successfully predict that the addition of the opposing, inclined reinforcing elements would reduce the peak cyclic shear strains by about 50 percent.

The PLAXIS analysis also predicted that the axial stiffness of the reinforcing elements was not a significant parameter, with a negligible change in response for a 75 percent increase in axial stiffness.

It would seem that the key mechanism affecting the response of the model with reinforcing elements is a stiffening effect from the presence of the soil/structure interface and not the stiffness of the structural elements per se.

4 Phase II Experimental Modelling

An important conclusion from the numerical modelling was that the axial stiffness of the reinforcing elements was not a key parameter in reducing the shear strain response of the sand deposits to shaking. Therefore, it was decided to extend the study by repeating the Phase I experiments in the laminated sand tank but using much more lightly reinforced micropiles. This Phase II experimental study is described in detail in the thesis of Charters (2005) included in Appendix B.

5 Case Study Numerical Modelling

5.1 Introduction

The objective of the case study numerical modelling was to extrapolate the results from the tank experiments to realistic field applications. Two applications were considered: a "green field" site where it is possible to install reinforcement everywhere across the site prior to construction of a building, and a "retrofit" site where reinforcement has to be installed around an existing building.

In both cases, the approach was to take the finite element model which had been calibrated against the tank experiments and extend it to simulate the two field cases. A typical subsoil profile was adopted for both cases: two metres of stiff silt-sand overlying four metres of loose sand, overlying stiff silt-sand.

5.2 Case study 1: Undeveloped Site

5.2.1 Site Description

The first case study is for a "green field" site where it is possible to install an optimum pattern of reinforcements prior to constructing any building on the site. The subsoil profile adopted is given in Table 5.1 and represents an amalgam of typical sites known to be prone to liquefaction. The upper two metre stratum represents the "crust" of stiffer soils typically found above the water table. Next there is a four metre thickness of liquefiable sand. The very low value for the modulus of the liquefiable layer was adopted from the actual values found from the tank experiments. Stiff soils were assumed for the remainder of the profile to simplify the model.

Table 5.1. Subsoil profile for the case study models.

Stratum	Description	c	ϕ	E
0 – 2m	Silt-sand	1 KPa	33	15 MPa
2m – 6m	Loose sand	1 KPa	33	2 MPa
6m – 15m	Silt-Sand	1 KPa	33	40 MPa

5.2.2 Reinforcements

The pattern of reinforcements used was: 11 m long elements, 45 degree inclination, 2 m spacing, installed in all four directions, north, south, east, and west. Each element was considered to be a 24 mm diameter reinforcing bar, grouted into a 100 mm diameter hole created using a mandrel, similar to the procedure used for the Phase II tank experiments. The axial stiffness of each 24 mm bar was calculated to be 9 x 10^4 KN, ignoring the stiffness contribution of the grout column because of likely cracking.

5.2.3 Numerical Model

The numerical model used for the case studies was essentially the same as the finite element model successfully used to model the tank experiments. The only variations were to increase the size of the deposit, insert more reinforcing elements, and adopt a simple layered soil profile with a water table at a depth of 2 m.

The PLAXIS finite element model used to represent this pattern is shown in Figure 5.1. The model adopted is 2-D plain strain and therefore only the east and west elements are shown. A total width of 20 m of reinforced ground was considered, of a total width of 60 m for the finite element model.

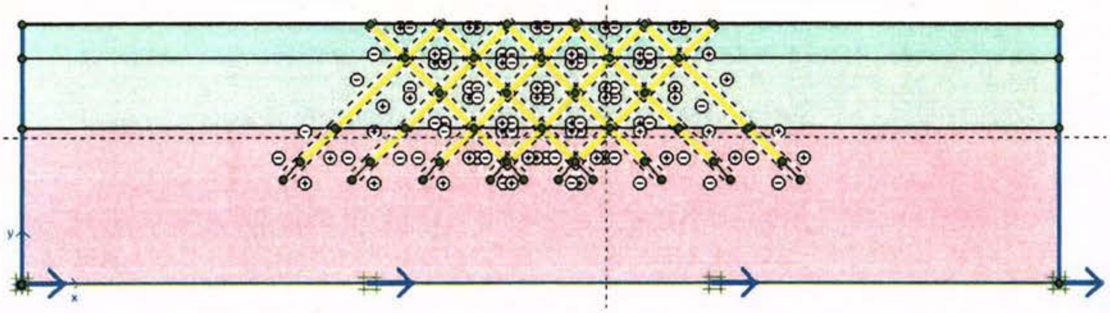

Figure 5.1. PLAXIS model for an undeveloped site with 20 m wide reinforced strip.

The base of the model is fully constrained but the walls are unconstrained. Instead, rigid beam elements were used to contain the soil and these were linked by a rigid node-to-node tie across the top, allowing the whole soil deposit to deform freely in simple shear.

The inclined reinforcements (shown in yellow in Figure 5.1) are shown spaced at 4 m centres in the PLAXIS model, rather than the 2 m centres intended for the field installation. The reason for this increased spacing was to simplify the finite element mesh, with the stiffness of individual elements increased by a factor of 2 to account for the stiffness of the missing elements. The dashed lines surrounding each reinforcement are special interface elements, used by PLAXIS to better model soil structure interface effects.

A stiff geotextile element was placed along the base of the soil deposit to provide continuity for complementary shear stresses, as for the tank model.

To properly benchmark the effectiveness of the reinforcement pattern, the model was subjected to shaking both with and without the reinforcing elements.

5.2.4 Earthquake record

A strong motion earthquake record was used to best investigate the performance of the reinforcement system. The Izmit S90E record from the M7.4 Turkey earthquake of 1999, with an epicentral distance of 10 km was used, scaled to give a peak ground acceleration of 0.43 g. This record was considered to be relevant in terms of both magnitude and geologic setting to many of the earthquake prone regions of New Zealand. The peak ground acceleration of 0.43 g is towards the upper range usually considered for New Zealand sites.

5.2.5 Results

The response of the unreinforced site, prior to installation of the reinforcement pattern, to the scaled strong motion record is shown in Figure 5.2 The average shear strain was calculated by tracking the displacement of individual node points at the top and bottom of the loose sand stratum, subtracting these displacements, and dividing by the thickness of the stratum. The peak strain was 1.12 percent, with 10 excursions beyond 0.5 percent.

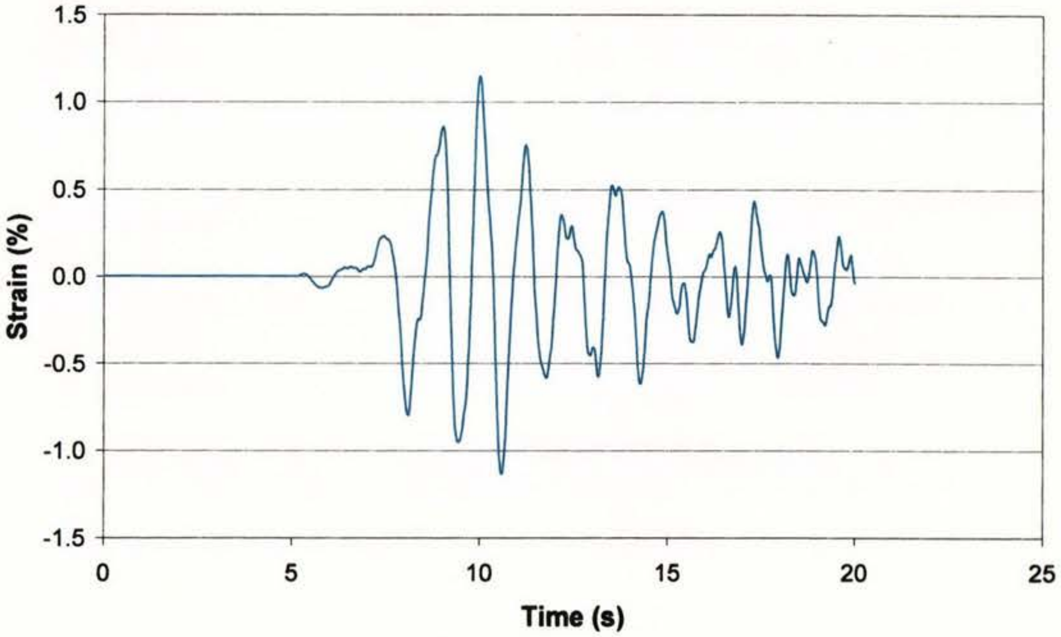

Figure 5.2. Shear strain versus time for the site without reinforcing subject to Izmit EW record. Surface PGA = 0.43 g.

The response of the site after installation of the full reinforcement pattern is shown in Figure 5.3. The level of shear strain within the loose sand layer has been substantially reduced from a peak value of 1.12 percent without reinforcement to only 0.2 percent with the reinforcement. The peak ground acceleration (PGA) at the ground surface was reduced from 0.43 g to 0.35 g, presumably because of the additional stiffness and/or damping effect of the reinforcing elements.

It is likely that the level of shear strain shown in Figure 5.2 would be sufficient to initiate liquefaction in the loose sand layer whereas the much reduced shear strains shown in Figure 5.3 would be unlikely to cause liquefaction. Dobry and Ladd (1980) found that the threshold strain required to cause significant pore pressure generation was 0.1 percent. While the peak shear strain did exceed this low threshold in Figure 5.3, there are only a few excursions beyond 0.15 percent and so some pore pressure increase is possible but probably insufficient to cause liquefaction. It is impossible to be precise about evaluating the risk of liquefaction because many other factors need to be considered especially specific characteristics of the site soils.

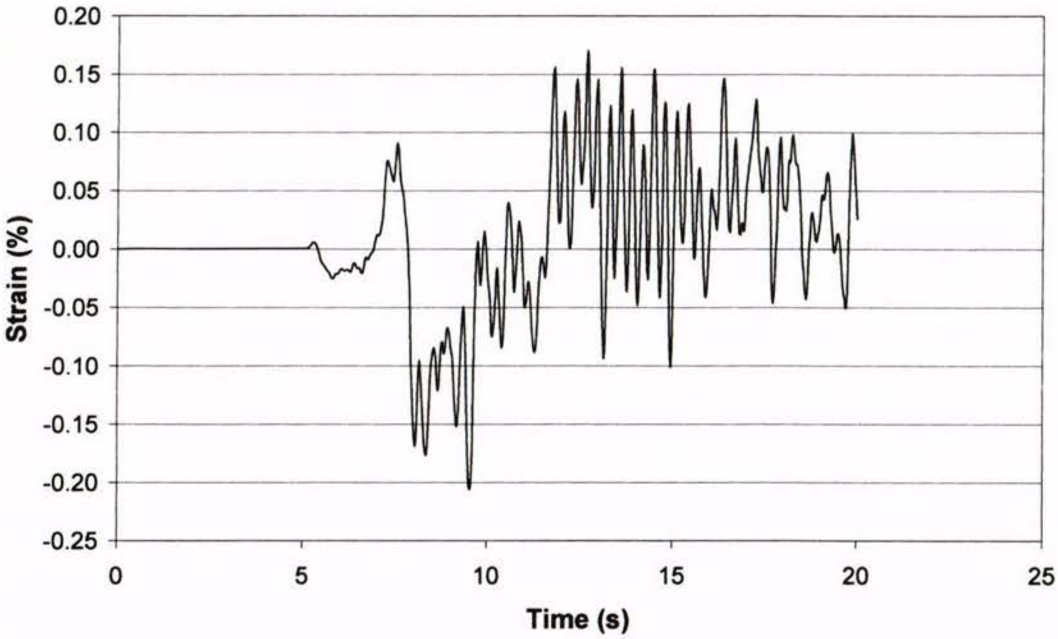

Figure 5.3. Shear strain versus time for the "green field" site after installation of reinforcing and subject to Izmit EW record. Surface PGA = 0.35

The axial force in each reinforcing element was monitored during the time history analysis and the peak axial force in a single element was found to be 45 KN. This force is equivalent to a peak steel stress of 100 MPa allowing use of standard grade 275 deformed reinforcing bars. (It might also be possible to further optimise the design by reducing the diameter of the reinforcing bars).

5.2.6 Costing

A costing exercise was carried out to estimate a cost per unit area and cost per unit volum for the reinforcement pattern, with an estimated cost including materials, labour, plant, overheads, and profit of $257/m^{2}or $43/m^3 . Detailed cost calculations are attached in Appendix A. This cost may be compared to a rate of $60/m^3 quoted for a recent project utilising a traditional ground improvement process with stone columns.

5.3 Case Study 2: Retrofit Site

5.3.1 Site Description

The second case study was for a "retrofit" site where a small building such as a telephone exchange or pumping station is already in place. The same subsoil profile as for Case Study 1 was adopted with the parameters given in Table 5.1.

5.3.2 Reinforcements

The presence of an existing structure obviously prevents installation of the ideal reinforcement pattern chosen for the "green field" site in Case Study 1. In certain circumstances it may be possible to drill through the floor of an existing building and install the ideal pattern used in Case Study 1, with the same resultant performance expected. Instead, for Case Study 2, the performance of an alternative pattern was investigated assuming that it is impossible to install reinforcements through the floor of the existing building. For most structures it will also be impossible to install outwardly inclined reinforcements close to the existing walls.

After some trial and error, satisfactory performance was obtained using the pattern of reinforcement shown in Figure 5.4. This pattern is somewhat more complex than that for Case Study 1 with the following features:

- Building assumed to be 10 m wide with a relatively strong floor.
- 14 m long reinforcements at 1 m centres, fixed to the outer edge of the floor, inclined at 45 degrees underneath the building.
- 8 m long vertical reinforcements at 2 m centres, fixed to the outer edge of the floor.
- 11 m long reinforcements on a 2 m grid inclined in the north, south, east, and west directions for a strip 8 m wide both sides of the building

Each element was assumed to be the same 24 mm reinforcing bar, grouted into a 100 mm diameter hole as used for Case Study 1, with a stiffness of 9 x 10^4 KN.

5.3.3 Numerical Model

The PLAXIS finite element model used to represent this reinforcement pattern is shown in Figure 5.4. Apart from the more complex pattern, the model is identical in all other respects to that used for Case Study 1.

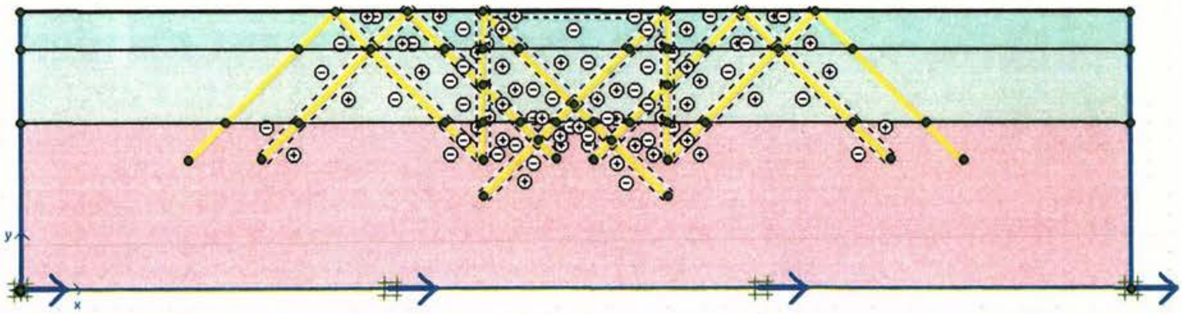

Figure 5.4. PLAXIS model for a retrofit site with a 10 m wide existing building.

5.3.4 Results

The response of the site after installation of the full reinforcement pattern is shown in Figure 5.5, and may be compared with the response of the unreinforced site shown in Figure 5.2. The presence of the reinforcement has significantly reduced the level of shear strain in the loose sand layer during the shaking, although the reduction is not as great as for the more ideal pattern of reinforcement for the undeveloped "green field" site shown in Figure 5.3. The peak shear strain was reduced to 0.27 percent compared with 1.12 percent for the unreinforced deposit shown in Figure 5.2. There are ten peaks exceeding 0.2 percent strain and most of the shear strain peaks are between 0.1 and 0.15 percent.

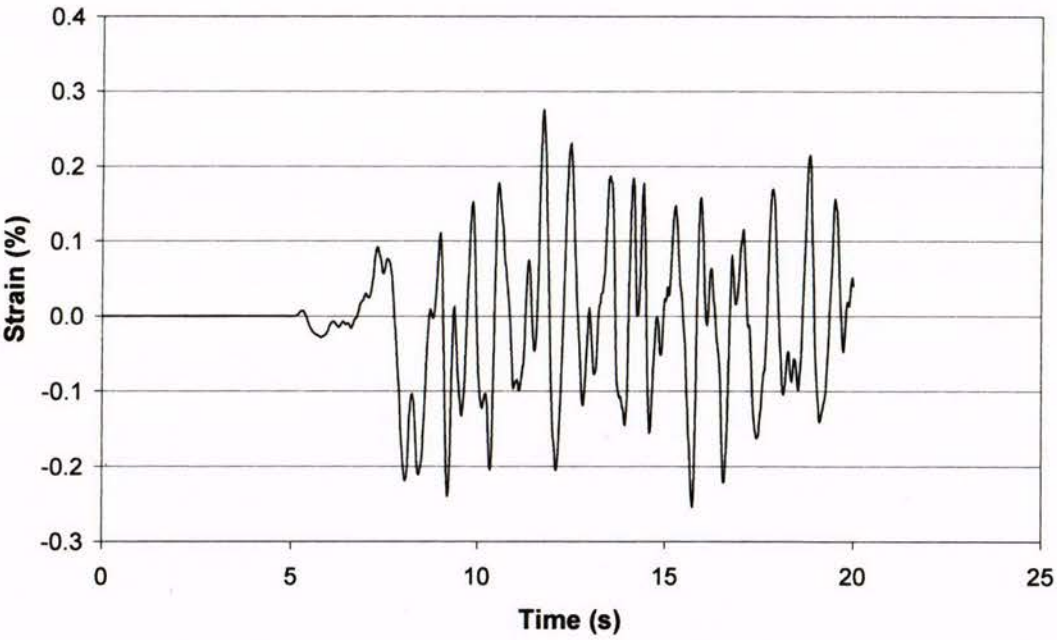

Figure 5.5. Shear strain versus time for the retrofit site after installation of reinforcing pattern subject to Izmit EW record.

It is impossible to say for certain whether or not the shear strain response shown in Figure 5.5 would cause liquefaction, but it is certainly much less likely to cause liquefaction than the shear strain response for the unreinforced site shown in Figure 5.2. It is impossible to be precise about evaluating the risk of liquefaction because many other factors need to be considered especially specific characteristics of the site soils.

The axial force in each reinforcing element was monitored during the time history analysis and the peak axial force in a single element was found to be 114 KN for the reinforcement elements inclined back underneath the existing building. This force is equivalent to a peak steel stress of 250 MPa allowing use of standard grade 400 deformed reinforcing bars.

5.3.5 Costing

A costing exercise was carried out to estimate a cost per unit area and cost per unit volume for the reinforcement pattern, with an estimated cost including materials, labour, plant, overheads, and profit of \$243/m^{2}or \$41/m^3 . Detailed cost calculations are attached in Appendix A. These rates are slightly less than for the undeveloped "green field" site because of the larger overall area and reduced quantity of reinforcement underneath the existing building. This cost may be compared to a rate of \$60/m^3 quoted for a recent project utilising a traditional ground improvement process with stone columns.

6 Conclusions and Design Recommendations

The Phase I experimental study in the laminated tank showed that diagonal micropile reinforcement is able to substantially reduce the cyclic shear strain in a deposit of loose sand during shaking. Two diagonally opposed micropiles were able to reduce cyclic shear strain by one half and the resultant settlement to one fifth that of similar unreinforced deposits. Such a significant reduction in contractive behaviour for loose, dry sand probably indicates that liquefaction would have been prevented if the deposits had been fully saturated with water.

The efficiency of the reinforcement was found to be low, with relatively little of the potential increase in stiffness from the steel cross-section being effective in reducing the shear displacement of the tank deposits.

A finite element numerical model was developed using the PLAXIS software code, and this was able to successfully simulate the main aspects of the Phase I laminated tank experiments. Standard PLAXIS geotextile elements were used to represent the diagonal micropiles.

The numerical model predicted that the response of the reinforced soil deposit was insensitive to the stiffness of the reinforcing elements. Reducing the stiffness from 2.8×10^5 KN/m to 1.6×10^5 KN/m caused no significant change in the numerical response of the soil deposit. Presumably, the main benefit of introducing the reinforcement is some stiffening effect from the presence of the soil/structure interfaces and not from the axial stiffness of the structural elements per se.

To test the prediction of the numerical model that element stiffness was not significant, a second phase of laminated tank experiments were conducted. These Phase II experiments used smaller micropiles with reduced axial stiffness of 1.6×10^5 KN each. The first experiments in Phase II used a smaller diameter micropile (65 mm compared with 100 mm for Phase I) and these seemed to suffer some kind of axial failure mechanism, presumably by yielding at the soil/structure interface. Subsequent tests were made using 90 mm diameter micropiles.

The 90 mm diameter micropiles with axial stiffness of 1.6×10^4 KN were found to be successful in reducing settlement to less than one quarter that for unreinforced deposits for shaking with accelerations of up to 0.6 g.

Numerical analysis of two simple but realistic field applications was performed by extrapolating the PLAXIS finite element model which had been calibrated against the tank experiments. Input shaking was from the Izmit EW record of the 1999 turkey earthquake scaled to give a peak ground acceleration of 0.43 g.

Reductions in ground response were much greater for the case studies than for the laminated tank models (peak shear strain reduced from 1.12 percent for an unreinforced site to only 0.2 percent for a reinforced site). Probably, this improved performance was because the ends of the micropile reinforcements were effectively anchored into stiffer, non-liquefiable strata above and below the liquefiable stratum.

The peak ground acceleration at the ground surface was found to be reduced by the presence of the reinforcement (Peak ground acceleration reduced from 0.43 g to 0.35 g).

The second case study was for a "retro-fit" example where an existing building makes it impossible to install an ideal pattern of reinforcements. Reductions in ground response were slightly less than for the "green field" case study but were still considered very good (peak shear strain reduced from 1.12 percent to 0.27 percent).

The risk of liquefaction occurring at either of the case study sites was considered to be greatly reduced by the installation of the reinforcements. However, it is impossible to make a precise prediction because of the many other factors involved including various specific soil characteristics.

Both case studies were costed and found to be competitive with a quote for a traditional ground improvement project utilising stone columns. ($43/m^3 for Case Study 1 and $41/m^3 for Case Study 2, compared with $60/m^3 for stone columns). The true economic feasibility of the reinforcement methodology needs to be tested in the marketplace and would depend to some extent on the ingenuity of a contractor to develop suitable equipment to efficiently install the inclined micropiles.

The use of inclined micropile reinforcing appears to hold substantial promise as an alternative strategy for preventing soil liquefaction. It is premature to issue design guidelines at this point although the reinforcement pattern adopted for the two case studies could be applied directly to certain sites with similar ground conditions. Other applications would need to be the subject of special study utilising the PLAXIS model developed herein.

7 Recommendations for Further Study

The issue of soil/micropile interface stresses needs further investigation. The Phase II experiments using 65 mm diameter micropiles seemed to result in shear failure at the soil/micropile interface with the head of the micropiles being pushed up from the soil surface. No interface failures were predicted by the PLAXIS numerical modelling but the micropile reinforcements were modelled by using 2-D geotextile elements that have a greater surface area than the equivalent micropiles. Additional PLAXIS modelling could be used to determine the necessary shear transfer to the reinforcement elements. The shear transfer could then be compared to the available side resistance of the design micropiles.

Additional PLAXIS case studies are recommended to examine a wider range of subsoil profiles and regional shaking scenarios. Such case studies could be used to develop a database of acceptable solutions for soil liquefaction sites.

Full-scale field trials are the only final way to prove that the concept of inclined micropile reinforcement is fully effective in preventing liquefaction. Given the difficulty in arranging full-scale earthquake level shaking in the field, construction of demonstration test sites in high earthquake risk areas might be considered. Alternatively, participation in large-scale explosives driven experiments such as the Treasure Island experiments in San Francisco should be sought.

An alternative to full-scale field trial is true-scale centrifuge study. True-scale modelling of geotechnical systems requires that the acceleration of gravity be increased in accordance with the rules of dimensional analysis. A number of geotechnical centrifuge facilities are available worldwide, the closest to New Zealand being a facility in Perth, Western Australia.

8 References

Brinkgreve, R.B.G. and Vermeer, P.A. (1988). PLAXIS finite element code for soil and rock analyses, Version 7, Balkema, Rotterdam.

Dobry, R. and Ladd, R.S. (1980). Discussion to "Soil liquefaction and cyclic mobility evaluation for level ground during earthquakes, : by H.B. Seed and "Liquefaction potential: science versus practice," by R.B. Peck, *J. of the Geotechnical Engineering Division*, ASCE, Vol. 106, No. GT6, pp. 720-724.

Dobry, R., Ladd, R.S., Yokel, F.Y., Chung, R.M., and Powell, D. (1982). "Prediction of pore water pressure buildup and liquefaction of sands during earthquakes by cyclic strain method," *NBS Building Science Series 138*, National Bureau of Standards, Gaithersburg, Maryland, 150 pp.

Hushmand, B., Scott R.F. & Crouse C.B. (1988). "Centrifuge liquefaction tests in a laminar box", *Geotechnique*, Vol. 38, No 2, pp. 253-262.

Iai, S. (1991). "A Strain Space Multiple Mechanism Model For Cyclic Behavior of Sand and its Application," *Research Note No.43*, Earthquake Engineering Research Group, Port and Harbour Research Institute, Ministry of Transport, Japan. May 1991.

Seed, H. B.and Idriss, I. M. (1970). *A simplified procedure for evaluating soil liquefaction potential*, Earthquake Engineering Research Center, Univeristy of California, Berkeley, Nov. 1970, 38 p.

Silver, N.L. and Seed, H.B. (1971). "Volume changes in sands during cyclic loading," *J. of the Soil Mechanics and Foundations Division*, ASCE, Vol. 97, No. SM9, pp. 1171-

Vucetic, M. and Dobry, R. (1991). "Effect of soil plasticity on cyclic response," *J. of Geotechnical Engineering*, ASCE, Vol. 117, No. 1, pp. 89-107.

Whitman, R.V., Lambe, P.C. & Kutter, B.L. (1981). "Initial Results from a Stacked-Ring Apparatus for Simulation of a Soil Profile". *Proceedings, International Conference on Recent Advances in Geotechnical Earthquake Engineering and Soil Dynamics*, St Louis, Mo., April 26 – May 3, 1981.

Youd, T.L. (1972). "Compaction of sands by repeated shear straining," *J. of the Soil Mechanics and Foundations Division*, ASCE, Vol. 98, No. SM7, pp. 709-725.

Appendix A Cost Estimates for Case Studies

Case Study 1: Undeveloped Site

Reinforcing pattern: Grid = 2m x 2m with micropiles inclined 45 degrees in north, south, east, and west directions, each 11 m long

Length of micropile per m^2 of reinforced ground = 4 x 11 / 4 = 11 m

Cost calculation for 20 m x 20 m site:

Materials:

HD24 rebar	11x20x20=4400 m / 281 = 15.7 tonne x $1300 =	$20,356
Centralisers	4400/2 = 2200 each @ say $2	$4,400
Cement	4400x0.008=35 m^3 grout @ 30 l/bag = 1167 bags @ 10.00	$11,667
Admixtures, overbreak and waste say 25 %		$2,917

Plant:

Assume use of modified tracked 20 tonne excavator to either push mandrel or drill.

Productivity Cycle	Locate over grid	5 mins
	Drive mandrel	15 mins
	Insert bar, grout	10 mins
		30 mins

Plant time = 400 x 0.5 = 200 hours / 10 = 20 days @ 1000		$20,000
Grouting plant	200 hours / 10 = 20 days @ 500	$10,000

Labour:

3 man crew x 200 hours @ 40.00	$24,000
	$93,340

Overhead and profit:

93340 x 0.10	$9,334
	$102,674

Cost / m^2 = 102374 / 400 = **$257/m^2**

Cost / m^3 = 257 / 6 = **$43/m^2** (considering the depth of reinforced ground = 6 m)

Case Study 2: Retrofit Site

Reinforcing pattern:

- 14 m long reinforcements at 1 m centres, fixed to the floor, inclined at 45 degrees underneath the building.
- 8 m long vertical reinforcements at 2 m centres, fixed to the floor.
- 11 m long reinforcements at 2 m centres in the north, south, east, and west directions for a strip 8 m wide both sides of the building

Cost calculation for 26 m x 26 m site with 10 m x 10 m existing building:

Materials:

HD24 rebar 40x14m + 20x8m + 576x11m=7056
7056 m / 281 = 25.1 tonne x $1300 = $32,643

Centralisers 7056/2 = 3528 each @ say $2$7,056

Cement 4400x0.008=56 m^3 grout @ 30 l/bag = 1882 bags @ 10.00 $18,816

Admixtures, overbreak and waste say 25 % $4,704

Plant:

Assume use of modified tracked 20 tonne excavator to either push mandrel or drill.
Productivity Cycle Locate over grid 5 mins
Drive mandrel 15 mins
Insert bar, grout 10 mins
30 mins

Plant time = 636 x 0.5 = 318 hours / 10 = 32 days @ 1000 $32,000

Grouting plant 318 hours / 10 = 32 days @ 500 $16,000

Labour:

3 man crew x 318 hours @ 40.00 $38,160
$149,379

Overhead and profit:

149379 x 0.10 $14,938

$164,317

Cost / m^2 = 164317/26^2 = **$243/m^2**

Cost / m^3 = 243 / 6 = **$41/m^2** (considering the depth of reinforced ground = 6 m)

Appendix B Phase II Experiments

(Masters Thesis of Neil Charters)

The Use of Micropiles to Resist Liquefaction

A project submitted in partial fulfilment of the requirements for the degree of

Master of Engineering

Neil Charters

Department of Civil Engineering

University of Canterbury

Christchurch

New Zealand

February 2005

Abstract

Previous research has shown that the use of micropiles (inclined soil nails) to reduce settlement in loose sands is a successful method. This work extends previous work to investigate a simpler and more economical method of forming the micropiles. Previous work used micropiles that had 25 mm diameter hollow steel bars in a 100 mm diameter grout column while this work used 6 mm deformed steel bars within a 90 mm diameter grout column.

Loose sand deposits ($D_r \approx 0.10$) were formed by air pluviation into a 2 m deep by 1.8 m long by 0.8 m wide laminated (50 mm intervals) shear tank. A shaking test was carried out on the unreinforced sand on a one dimensional shake table to establish the baseline response of the sand and to ensure all instruments and equipment were working correctly. Settlement of 5 % and cyclic shear strain of 0.75 % was recorded in the initial unreinforced soil deposit.

Micropiles were then formed by pushing a steel casing into the soil using a hydraulic ram. The casing was then filled with grout, and while the grout was still liquid, the casing was removed and the pile allowed to cure in the soil. Two diagonally opposed micropiles were installed in each deposit tested.

A range of sizes of micropile were tested using similar shaking parameters. Shaking of up to 0.86 g was used, with the micropiles successfully reinforcing the sand at accelerations up to 0.6 g. Settlement was reduced to less than a quarter of that of the unreinforced soil, and cyclic shear strains were reduced to between 0.08 and 0.5 %. Dry sand was used for all tests, and settlement was taken as an indication that liquefaction may have occurred had the sand been saturated. Those piles that successfully reduced settlement of the tank are hypothesised to be capable of preventing liquefaction in saturated sands.

Table of Contents

List of Figures

List of Tables

1 Introduction

1.1 Soil Liquefaction

Liquefaction has been recognised as a major cause of earthquake related damage since 1964 when two major earthquakes occurred in a three month period. At Niigata (Japan) there was major liquefaction leading to foundation failure, bridges being damaged due to lateral spreading and extensive liquefaction induced settlement. While the earthquake magnitude was large (M7.5), the epicentre was located 60 km from the town, so peak ground accelerations were relatively low at 0.16 g (Seed and Idriss, 1982). In the Anchorage, Alaska (M8.3) earthquake of 1964 there were major landslides triggered by liquefaction of sand lenses within a glacial till deposit. Damage was catastrophic and led to the relocation of several towns (Seed, 1968). In both these cases, and most cases since, the impact of liquefaction has largely been economic loss rather than loss of life or injury.

Liquefaction is the process whereby the grain structure of a loose sand collapses upon shaking. This collapse attempts to expel water from the voids, and leads to pore pressure increases when the water cannot flow freely away. As pore pressure rises, effective stress decreases, and in the limit, pore pressure rises to the total stress value, leaving zero effective stress. This is termed liquefaction, and represents a soil behaving as a liquid, with no intergranular forces acting. Thus, shear stress cannot be resisted and the behaviour of the soil changes. Effects of liquefaction include foundation, slope and wall failures together with lateral spreading, flotation of light structures and modification of the ground acceleration.

Current research suggests that liquefaction is triggered by shear strain as the particles move past one another during soil fabric collapse (Butterfield et al., 2003 and Dobry et al., 1982). If the strain or excess pore pressures can be reduced, then the tendency of a soil to liquefy will be less. Pore pressure dissipation can be achieved with drainage, and strain can be reduced either by densifying the material or by reinforcing the soil. Densifying the material pre-collapses the structure to remove the tendency to contract during shaking. This is an expensive and intrusive albeit proven method to reduce liquefaction risk before construction begins. Micropiles can be used to increase the shear stiffness of the soil, and are sufficiently small that they employ unintrusive construction methods. This means that they can be used post construction with relatively little disruption to occupants or services. Micropiles are essentially the same as soil nails, but are used on level ground to prevent liquefaction rather than on slopes to provide stability.

1.2 Project Objectives

This study focussed on the use of micropiles to increase the stiffness of the soil. These elements reduce the tendency of the soil structure to collapse and can be easily retrofitted around buildings. Previous work has used large diameter (25 mm) steel micropiles that were pushed into the soil while simultaneously pumping grout into the hole. McManus et al (2004) found that very little of the strength of the steel within the micropile was mobilised in resisting the shearing.

This study will aim to reduce the cost of installation by using micropiles that are pushed into the ground inside a steel casing. The casing is then filled with grout (poured, not pumped) and pulled out of the ground. This leaves a grout column encasing a 6 mm diameter reinforcing bar. By reducing the amount of steel and grout required to fabricate the micropiles and employing a simpler installation method, significant economic benefits can be achieved. The micropiles were installed in the same tank and at the same spacing and orientation as previously used by Charton (2004) to allow a direct comparison between construction methods to be made.

Laboratory tests were carried out on the University of Canterbury shaking table, in a 2 m x 1.8 m x 0.8 m laminated (50 mm intervals) shear tank. These tests aimed to determine the effectiveness of the micropiles in reducing settlement and shearing at a number of acceleration levels. The tests were also intended to develop limits within which the micropiles could be relied upon to prevent liquefaction of the soil. A range of tests were carried out on different sized micropiles, at different shaking intensities and at a range of relative densities of the soil. A baseline test was also carried out with no micropiles to establish a soil response pre-reinforcing.

1.3 Synopsis of Report

Chapter two presents the fundamentals of liquefaction, including the mechanics of the process, effects of liquefaction, trigger mechanisms and counter measures. A number of methods to determine liquefaction susceptibility are discussed.

Chapter three describes the test equipment, methods and parameters. Chapter four follows with a discussion of micropiles and their usage as well as a description of the new method developed for installing the micropiles.

Chapter five presents and briefly discusses results from the five tests carried out on different deposits. Analysis and further discussion of the results are in chapter 6.

Chapter seven briefly discusses local seismology to bring the use of micropiles into context. Finite Element Modelling carried out using Plaxis (version 7.2) is presented and discussed in chapter eight. Chapter nine concludes the report and raises questions and recommendations for further work.

2 Liquefaction

2.1 What is liquefaction?

Liquefaction is the process of soil losing all of its shear strength and effectively becoming a liquid. This occurs due to rising pore pressures, and ultimately when pore pressure exceeds the total stress, the effective stress (that part of the stress carried between soil particles) tends to zero. According to Terzaghi's principle of effective stress:

$$\sigma_{total} = \sigma' + u \tag{2.1}$$

When the effective stress is zero, there is no soil strength because there are no contact forces between the soil grains. This leaves a soil that behaves like a liquid (i.e. has no shear strength) with the soil particles in suspension.

The rise in pore pressure is due to a densification of the soil during shaking, and the inability of pore pressures to dissipate. Thus, for liquefaction to occur, a soil must generally be (Kramer, 1996):

- loose - to enable densification upon shearing;
- cohesionless - so it behaves as grains in water;
- relatively low permeability - to impede drainage so pore pressures can rise;
- saturated.

These criteria show that fine sand or cohesionless silt is the most likely soil to liquefy as clays are too cohesive and coarser sands allow rapid drainage. However, there are situations when a coarser sand or gravel can liquefy when the pore water is confined between impermeable strata. Figure 2.1 (from PHRI, 1997) is a schematic diagram showing how the soil particles rearrange during liquefaction. Note that effective stress is defined as the contact force between grains, so in Figure 2.1b the effective stress is zero.

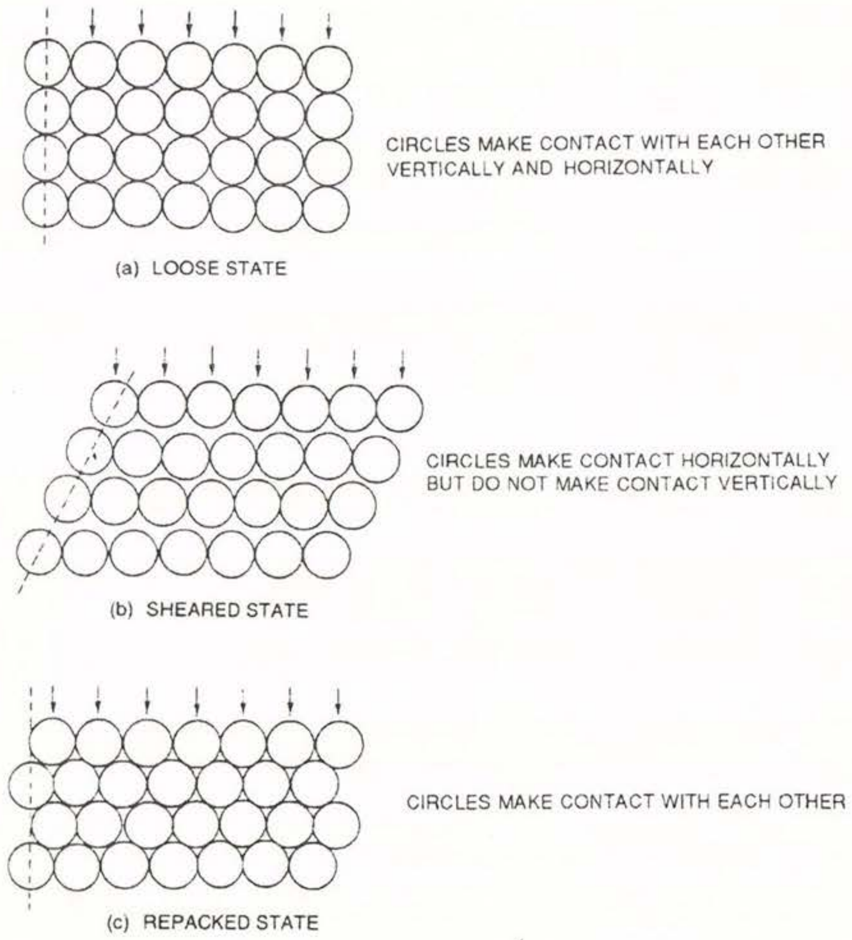

Figure 2.1. Schematic diagram showing the process of liquefaction

There are two types of liquefaction: flow failures and cyclic mobility (as defined in Kramer, 1996). Flow failure occurs when the static shear strength required for equilibrium is less than the reduced strength of the soil. This leads to major slope failures or lateral spreading near banks. Cyclic mobility occurs in a denser soil than flow failures. As cyclic shear stresses rise, and the pore pressure becomes equal to the effective stress, a failure initiates. However, as soon as motion occurs, the cyclic stresses are lost, so motion stops. Pore pressures then rise again, and the cycle continues. During the short period of zero effective stress, permanent displacements can occur. There is also a sub-category of liquefaction for that which occurs on level ground. Clearly, if the ground is level, no shear stress is required for static equilibrium. The water table is often at a one or two metres depth, so no liquefaction can occur in the surface layers. However, below the water table, liquefaction can occur, and the surface layer becomes a raft, floating on the liquefied layer at depth. Differential movement between the rafts leads to damage, especially to lifelines (such as water mains, power and phone lines) which are usually buried above the water table.

2.2 Effects of Liquefaction

Liquefaction usually results in damage and economic losses rather than threatening life or injury. The effects are widespread and can be seen after and during the event. The effects are due to loss of shear strength, and thus a weakness in the soil. This change in soil properties modifies the forces imposed by the soil on structures and also modifies the ability of the soil to resist forces imposed by structures. Of particular concern in Christchurch is lateral spreading affecting many pumping stations that are on river banks.

2.2.1 Lateral spreading

Lateral spreading is the motion of a shallow slope or flat surface (near to a small free face) in a horizontal direction. It typically occurs adjacent to rivers or streams, resulting in motion of the ground towards the river and multiple, river parallel tension cracks extending away from the river for up to 300m (as at Whakatane, 1987). Figure 2.2 (Kramer, 1996) shows the Showa River bridge in Niigata where the simply supported spans fell off the piers as the piers moved and rotated as a result of lateral spreading.

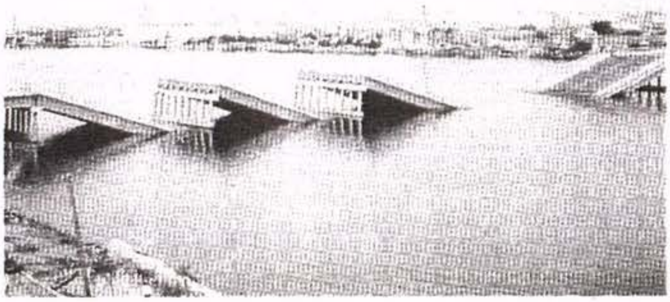

Figure 2.2. Lateral Spreading resulting in damage to the Showa River Bridge, Niigata

Lateral spreading occurs as a result of an imbalance in the forces applied to either end of the liquefiable layer. Pre-shaking, using standard soil pressure models, the forces acting on the river side of the layer are proportional to ρ_{water} and the depth of the layer. At the inland end of the layer, the forces are proportional to ρ_{soil}, K_a and the depth. A static analysis would show that the forces are approximately equal, and that any imbalance can be resisted by the strength of the soil. However, during shaking, the soil loses shear strength and thus K_a tends to 1. This increases the forces acting towards the river, and the soil is weaker, so it can no longer resist a force imbalance and it yields and moves towards the river. This causes cracking and extension of the non-liquefiable crust layer.

2.2.2 Retaining wall failure

Retaining wall failures are associated with liquefaction as a result of decreasing soil strength. This results in an increased pressure being exerted on the wall coupled with a reduced strength of the foundation of the wall. In most cases the design pressure on the wall is taken as the active earth pressure, which relies on all of the soil yielding and thus mobilising its full shear strength. During liquefaction this strength is lost and the horizontal earth pressure increases. However, retaining walls are often used to retain artificial backfill and are well drained. The effect of this is that the water table is drawn to a level below the wall and the material retained is non-liquefiable. Therefore, many retaining walls fail as a result of liquefaction beneath the foundation of the wall allowing settlement or rotation of the wall. An example of a retaining wall failure from the Kobe earthquake of 1995 is shown in Figure 2.3 (from Kramer, 1996).

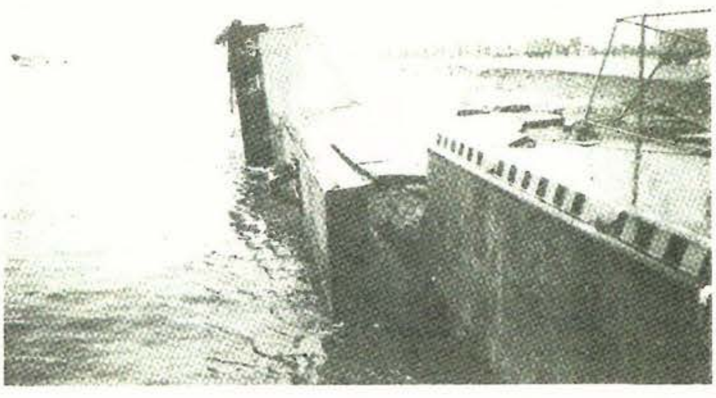

Figure 2.3. Retaining Wall Failure

2.2.3 Sand Boils

Sand boils are not so much destructive features associated with liquefaction as indicators of liquefaction. They can be very useful to indicate that underlying strata have liquefied and can indicate historical liquefaction events when they are preserved in the geological record. Figure 2.4 shows a sand boil resulting from the 1964 Niigata earthquake (Kramer, 1996).

Figure 2.4. Photograph of a sand boil

The development of sand boils is a result of excess pore pressures near the surface. A vertical pressure gradient develops, and if this reaches a critical value, the effective stress will be zero, and the soil will be in a quick condition (Kramer, 1996). In these cases, the flow velocity of the water may be great enough to carry sand particles to the surface. Because soil is rarely homogeneous, the flow is concentrated through cracks in the soil and sand boils develop at irregular intervals.

2.2.4 Modification of the acceleration at the surface

As soil is liquefied and loses shear strength, the ability of it to transfer energy decreases because transmission of shear waves relies upon shear strength. At high shaking frequency, a liquefied soil will absorb almost all of the energy. Once liquefied, the shaking transmitted to the ground surface is strongly shifted to the low frequency end of the spectrum. This is illustrated in Figure 2.5, a strong motion seismogram recording from the 1964 Niigata earthquake (Kramer, 1996). It can be seen that at about 7 s the acceleration changes from high frequency to low frequency. This corresponds to the onset of liquefaction.

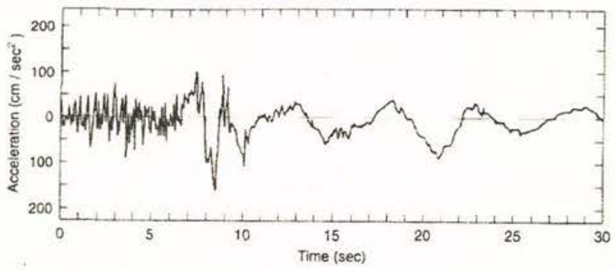

Figure 2.5. Accelerogram showing liquefaction

This modification in shaking can be advantageous because it reduces the likelihood of the structure above sustaining major damage, provided it is not damaged by the liquefaction.

2.2.5 Foundation Failure

When a soil has liquefied and lost strength, any foundations relying upon the soil strength are liable to fail. This covers both deep and shallow foundations. Shallow foundations may fail due to total loss of shear strength of the soil or by unravelling of a strong, dry layer into an underlying liquefied layer, as happened at the Kawagishi-Cho apartments in Niigata, 1964, shown in Figure 2.6 (Kramer, 1996).

Figure 2.6. Kawagishi-Cho apartments, showing foundation failure

Deep foundations are more complex structures and so have more possible failure mechanisms. Piles may fail in bending at the interface of liquefied layers due to lateral spreading (as at Kobe, 1995 – Nanjyo et al., 1998), as shown in Figure 2.7. Note the SPT graph adjacent to the pile schematic indicates that the lower fractures are at the same depth as a rapid increase in soil density.

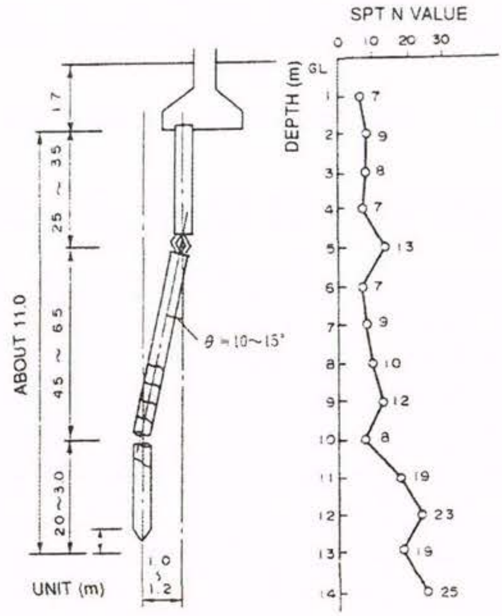

Figure 2.7. Pile failure schematic diagram

Lateral spreading causes large passive forces to be exerted on in-ground structures. This may also cause pile failure, and was first recognised after the 1987 earthquake in Whakatane, where "bow waves" of soil were observed adjacent to the bridge piers (see Figure 2.8, from Berrill et al., 2001). The bow wave can be see on the right hand side of the pier, and is a result of the bridge remaining static while the soil moved from right to left in the picture. This indicated that passive failure had occurred in the soil as it had been forced past the piers.

Figure 2.8. Bow wave of soil adjacent to bridge pier

During an earthquake, the structure supported by the piles will be shaking and imposing an increased load on the piles. This will be a cyclic load, which can either lead to failure in compression, tension or 2 way failure as a result of densification of the pile-soil interface, as defined by the Poulos stability chart. Negative skin friction can reduce the pile capacity because during settlement, the soil surrounding the pile will drag the pile downwards.

2.2.6 Flotation of Lightweight structures

During liquefaction, lightweight (lighter than the soil) structures become buoyant and rise upwards. Examples of this type of structure are pipelines, manholes and tunnels. Clearly a loss of alignment is severe damage to these structures. Figure 2.9 shows a manhole that has been damaged by flotation of the underlying pipeline (from PHRI, 1997).

Figure 2.9. Damage to Manhole caused by flotation of sewer pipe

2.2.7 Settlement

The fundamental mechanism driving sand liquefaction is the collapse of the soil fabric. At point A in Figure 2.10 (Kramer, 1996), pre-earthquake, the soil state is on the normal consolidation curve. During the earthquake, the soil fabric tends to collapse and densify the soil. This collapse is resisted by the pore water and results in an increase in pore pressure (point B). As fluid pressures dissipate, the void ratio will reduce (point C). Generally, any volume change is constrained to be in the vertical direction, and so the densification causes settlement.

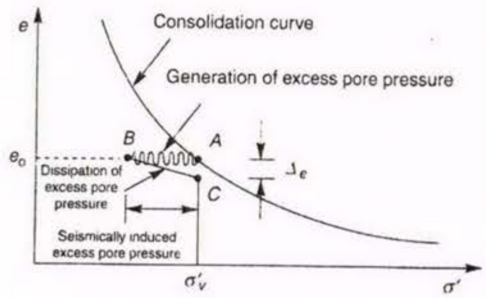

Figure 2.10. Settlement mechanism in liquefaction

2.2.8 Slope Failure

Any ground slope requires some shear strength for equilibrium, but during liquefaction, the soil shear strength is reduced. If it is reduced to below the amount required for stability, then a slope failure will occur. Driving forces for failure are also increased during earthquakes due to horizontal ground accelerations. There have been many cases of slope failures in earthquakes as a result of both liquefaction and the shaking, such as in Anchorage, Alaska in 1964 (Seed, 1968).

2.3 Liquefaction trigger mechanisms

Butterfield et al (2003) examined liquefaction triggers to attempt to determine whether a stress threshold (when the soil first reaches its Mohr-Coulomb yield surface) or a strain threshold (as proposed by Dobry et al., 1982) is relevant for the onset of liquefaction. It was found that the strain hypothesis held true, and that the trigger mechanism for liquefaction is shaking leading to an increase in strain. As the particles are shaken, they begin to slide over one another. Assuming spherical particles, the contact stresses are greatest in the centre of the particles, reducing with distance from the point contact. Slip is initially confined to an annular area, but as the shaking intensity increases, the strain moves closer to the centre of the particle contact. Once the whole area is straining, particle rearrangement can begin. It is this particle rearrangement that causes pore pressures to rise as the particles attempt to reach a more dense arrangement and reduce the soil volume. This pore pressure rise leads to liquefaction.

The strain values required for this densification are large enough that the soil is no longer operating in its elastic region. The boundary for elasticity is at approximately 10^{-6} while the onset of liquefaction is at (Butterfield)

$$\gamma_t = 1.25 * 10^{-5} . \sigma'_v{}^{\frac{2}{3}} \qquad (2.2)$$

Equation 2.2 includes the depth as effective stress because as the soil gets deeper, it gets stiffer and is therefore harder to liquefy. The threshold identified by Butterfield et al (2003) lies within the range proposed by Dobry et al (1982).

2.4 Liquefaction Countermeasures

Conventional countermeasures against liquefaction involve either densifying the soil or installing drainage to allow rapid dissipation of excess pore pressures (PHRI, 1997). These are both intrusive processes that must be carried out before construction of the protected facilities begins. This Section summarises liquefaction remediation as presented by PHRI (1997) and Kramer (1996).

Densifying the soil increases the strength and stiffness of the soil by increasing the density of packing. This compaction of the soil can be done using vibroflotation, stone columns or deep dynamic compaction, with varying energy inputs and frequencies achieving densification to greater depths. Increasing the density of the soil reduces the tendency to generate increased pore pressures during shaking because the soil can no longer densify upon shaking. These techniques of ground improvement have been tried and tested, and have been used in constructions such as Te Papa in Wellington, NZ (Deep dynamic compaction) and on many reclaimed islands in seismic areas such as the Kobe and San Francisco harbours. In deep dynamic compaction, the soil is compacted by repeated blows with a large block which is dropped from a crane, as shown in Figure 2.11 (Kramer, 1996). The grid pattern of the drops is evident, as is the settlement caused by densification.

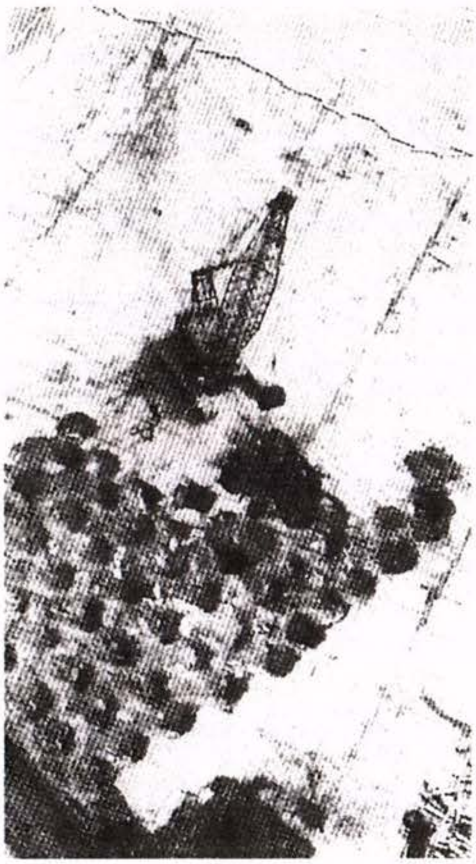

Figure 2.11. Deep dynamic compaction

Widely spaced blows with a large mass are used to densify the soil at depth, followed by a closer grid of smaller blows to bring the compaction to the surface. This is effective in preventing liquefaction, but is very expensive and intrusive during construction. There are a number of side effects that can be experienced: Strength and stiffness of granular soils depend upon the density, so by changing the density, the response of the soil to seismic waves will change. This will often reduce displacement, but accelerations may be increased as a function of reduced damping and energy absorption. The settlements associated with reducing void ratio that would have occurred during liquefaction occur during construction. Depending upon the amount of settlement that occurs, the ground may need replacing to original level with imported free draining fill, which further adds to the expense of the process.

Wick drains are the most common drainage option. These are vertical holes filled with free draining material, and are usually wrapped in a geotextile to prevent loss of sand. The drains are spaced relatively closely to ensure the excess pore pressures dissipated during shaking are dissipated rapidly. These have been used at the eastern abutment of the new San Francisco Bay crossing.

Many methods combine the two above methods to densify and drain the soil in a single process. These include vibroflotation and stone columns, and usually involve the densification of the soil followed by the insertion of free draining material to provide stiffness and drainage.

Soil strength can also be increased by mixing with either cement or lime, depending upon the clay content. In the case of liquefaction reduction, cement is usually more appropriate. This method is also an expensive and disruptive option because all the soil must be mixed and a large volume of cement (usually 5% of the soil mass) is required. The cement is mixed into the soil using augers and as it cures, the soil is stiffened and strengthened. This method has been widely used in roading projects (to a very limited depth) in NZ to provide extra strength in the subgrade, and has been used to depths of 60 m in Japan for reducing liquefaction (Kramer, 1996).

The soil can also be reinforced structurally. This is the type of countermeasure that will be tested in this project. The soil is reinforced with (in this case) micropiles that act to reduce the shear strains in the soil and therefore prevent densification and liquefaction. The micropiles increase the shear strength of the soil by carrying much of the imposed shear stress imposed on the soil. This method of reinforcement can be carried out after construction of the facilities, and generally for a significantly lower price than the ground treatment options previously discussed. This makes it suitable for retrofitting and for use to protect smaller infrastructure such as water pumping stations. Micropiles are discussed in detail in section 4.

2.5 Liquefaction susceptibility assessment

Most methods for assessing liquefaction susceptibility have been based on a correlation with in-situ density tests. Originally they were based on the SPT (Standard Penetration Test), but they are increasingly based on the CPT (Cone Penetration Test). Robertson and Campanella (1985) produced a preliminary liquefaction assessment diagram (see Figure 2.12). This allows for a rapid assessment of liquefaction potential based on the tip resistance and side friction values from a CPT test. If the soil falls in, or close to the zone of potential liquefaction (zone A), more complex calculation methods are justified to determine the liquefaction susceptibility more accurately.

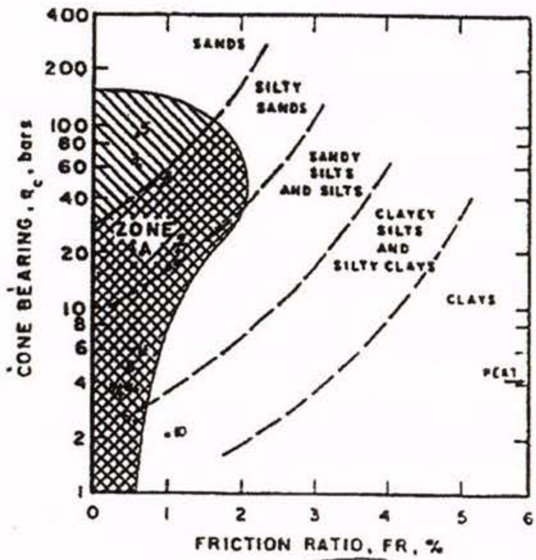

Figure 2.12. Robertson and Campanella's preliminary liquefaction assessment diagram

There are two groups of procedure used for determining the liquefaction susceptibility more accurately: those based on cyclic stress ratios (CSR) (Seed and Idriss, NCEER) and those based on energy dissipation (Davis and Berrill). The original Seed and Idriss method, Davis and Berrill's energy dissipation method and the more recent NCEER method are discussed below. The effect of particle size grading is also very important in determining liquefaction susceptibility. It is taken into account by the

NCEER method when determining the cyclic resistance ratio (CRR) of the soil. It is also used in a number of empirical methods for determination of lateral spread distance (for example, Bartlett and Youd, 1992).

In most cases, it is recommended that all three methods be applied due to the approximate nature of the calculations. In marginal cases, each method may give a different susceptibility, and it is up to engineering judgement to determine which method is most appropriate for the particular site. Carr (2003) notes that the liquefaction prediction models are generally correct, but that the models are too simple to capture the complex nature of liquefaction and all of the seismological factors in an earthquake.

2.5.1 Seed and Idriss (1971)

The Seed and Idriss liquefaction evaluation is based upon a comparison between the stress required to start liquefaction in the soil (as a function of SPT-N value) and the cyclic stress induced in the soil by the earthquake. Cyclic stress is calculated as a proportion of the overburden stress in the soil as follows:

$$CSR = \frac{\tau}{\sigma'_{v0}} = 0.65 * \frac{a_{\max}}{g} * \frac{\sigma_{v0}}{\sigma'_{v0}} * \frac{r_D}{MSF} \tag{2.3}$$

The variables are as follows: r_D is a term accounting for the flexibility of the soil column, which reduces cyclic stress in a column as the column gets longer. MSF is a magnitude scaling factor, introduced to account for the longer shaking periods associated with larger magnitude earthquakes.

The calculated CSR is then compared to a critical CSR, obtained from a graph of critical CSR values vs SPT-N value. If the calculated CSR is greater than the critical CSR, the model predicts liquefaction.

The 0.65 multiplier accounts for the fact that earthquake motions are irregular signals. 0.65 was determined empirically as a scalar to bring the maximum acceleration down to a realistic average value for the earthquake. This is further discussed in the analysis, section 6. The equation was derived empirically, and therefore uncertainties should be considered when applying it. It should be used in conjunction with other methods of liquefaction prediction. Carr found that this method was generally conservative when predicting liquefaction (Carr, 2003).

2.5.2 Davis and Berrill (1982)

This method is based on calculating the amount of excess pore pressure generated at a site and comparing this to the in situ vertical effective stresses to see if liquefaction occurs. If the calculated pore pressure rise is greater than the in situ effective stress, then the model is predicting that liquefaction will occur. The excess pore pressure rise is calculated using the amount of energy input at the site (a combination of the magnitude of the earthquake and the amount of geometric attenuation taking place), the original effective stress and the normalised SPT N value (see Equation 2.4). The geometric attenuation term is calculated assuming a simple inverse square relationship. Clearly this relationship is not appropriate for near-epicentre sites where directivity and rupture propagation effects will alter the energy dissipation pattern. This method is based on two soil properties (SPT-N and σ') and sound laboratory testing and theory so is perhaps more reliable than the earlier Seed and Idriss empirical method. The original method calculated pore pressure as:

$$\Delta u = \frac{450}{R^2 N_1{}^2 \sqrt{\sigma'_{v0}}} 10^{1.5M} \qquad (2.4)$$

Where R is the epicentral distance, N is the corrected SPT value and M is the moment magnitude of the earthquake. This relationship is often rearranged to give an expression for the magnitude of an earthquake required to give liquefaction at a site. It is also well suited to probabilistic analysis to get the probability of liquefaction at a site from the probabilistic seismic hazard assessment for the region.

2.5.3 NCEER (Youd and Idriss, 2001)

The NCEER method is similar to the Seed and Idriss method in that it calculates a cyclic stress ratio, which is compared with the shear strength of the soil expressed as a cyclic resistance ratio (CRR). It differs in the method of calculating the CSR and CRR. The loading term (CSR) is calculated as before, using Equation 2.4. The CRR is based upon normalised CPT values and a soil behaviour constant defined by the friction ratio of the soil. A resistance term is calculated using an iterative process to converge on an equivalent clean sand value, taking into account the gradation of the sand. This reflects the changes to the soil properties resulting form the presence of fines. They increase the strength of the soil by taking the place of intergranular water, but provide some extra cohesion to provide resistance. The net effect on liquefaction resistance is very little.

3 Experimental Design

3.1 Introduction

The objective of the experimental phase was to design and test a new style of micropile together with a new installation method. Micropiles have been researched in the University of Canterbury Civil Engineering department previously, by Chambers (1999) and Charton (2003). Both researchers used a laminated tank and shaking table to simulate free field shaking, and this same equipment was used for this study. A clean grade 30/60 silica sand was chosen because it is an easily liquefiable material, does not produce dust when handled and can be reused. To aid with deposit preparation, the sand was dry and the settlement of this taken as an indication that liquefaction would have occurred if the sand was saturated with water.

The new method of installation uses a hydraulic ram to push a casing into the soil that will be filled with grout before being retracted. A large frame was built in the Structural Engineering laboratory to hold the ram in the correct position and to provide a reaction force to the micropile. The installation method is described in detail in Section 4.

3.2 Laminar Tank

Chambers (1999) designed and constructed a laminar tank to carry out scale model testing of foundation piles in dynamic soils under both static and dynamic loading. The design is based upon that of Hushmand et al (1988), and is shown in Figure 3.1 (modified from McManus et al., 2004).

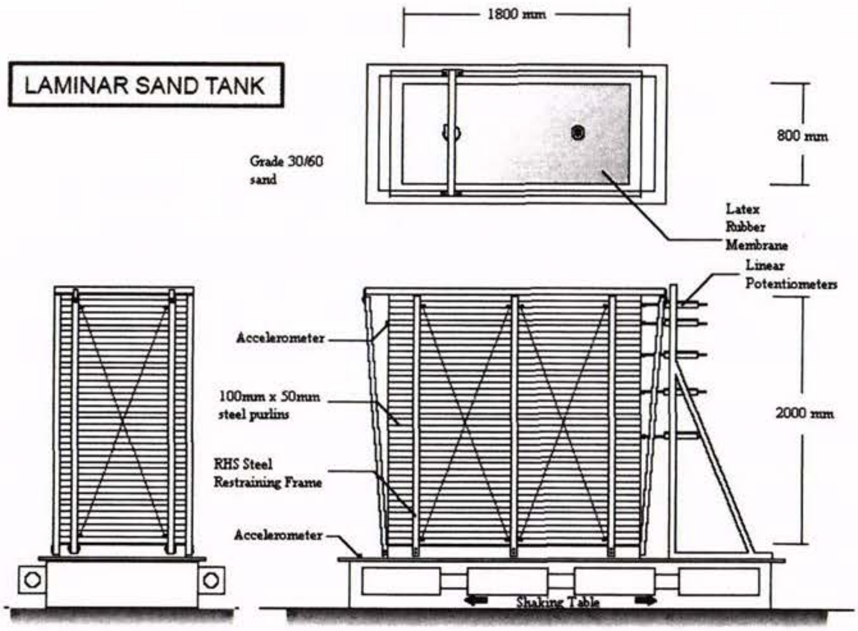

Figure 3.1. Laminar sand tank design

The laminar tank was intended to simulate one dimensional free field shaking by allowing unrestricted deformation of the soil and preventing reflection of any shear waves. It is made up of a stack of 50 mm thick steel laminates separated from those below it by six Teflon strips. A steel frame prevents rotation and motion in two directions by constraining the laminates to move only in the direction of the shaking. This is a simulation of vertically propagating, horizontally polarised shear (SH) waves. This frame also had Teflon strips attached to reduce friction between it and the laminates. The sand was contained within the tank by overlapping 1 mm thick latex membranes that were attached to the top laminate and hung freely down the inside of the tank. Two trapdoors are located in the base of the tank and operated with screw threads to allow the sand to be emptied from the tank. The nuts used to open the trapdoors can be seen on the end of the tank base in Figure 3.2. As a result of the micropiles bleeding, the sand in the laminar tank became damp each time it was used. Using trapdoors was vital as aligning perforated plates (as used in the transfer and storage hoppers) would not allow the damp sand out of the laminar tank.

The whole tank was bolted to the shake table and diagonal bracing was provided with 10 mm steel rods. Figure 3.2 shows the tank bolted to the shake table.

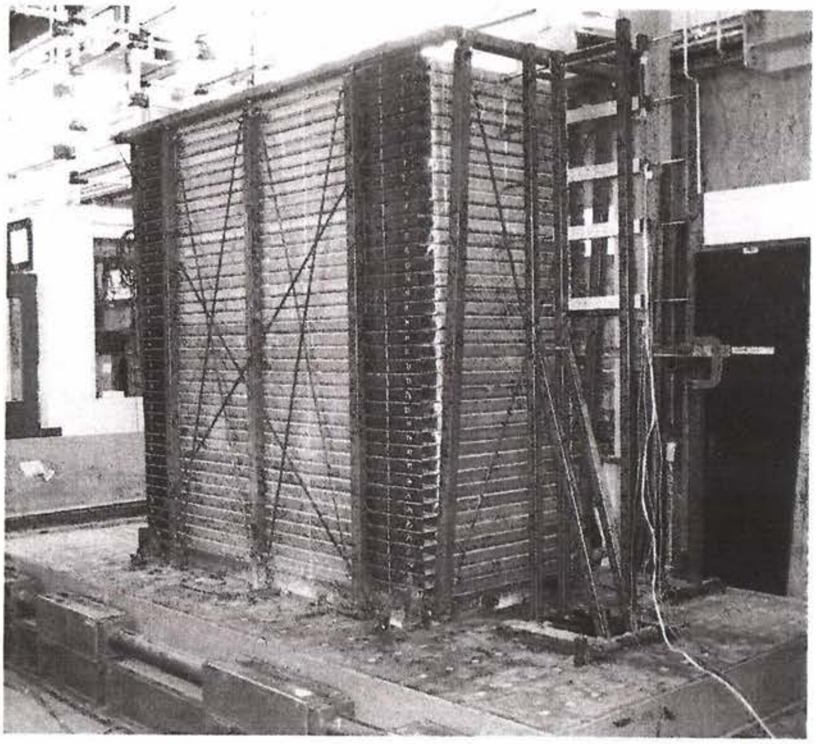

Figure 3.2. Laminated tank on shake table

The force required to deform the tank at 1 Hz shaking is approximately 2 % of that required to deform the soil within the tank at the same shaking (Chambers, 1999).

3.3 Pluviation Method

The sand was transferred into the laminar tank using a pluviator designed by Chambers (1999). This consists of a 1m square transfer hopper with holes in the base to allow sand transfer. The rate of transfer is controlled by a screw thread which moves two plates with holes into or out of alignment. The hopper does not fit inside the laminated tank, so a hose is attached to the funnel to transfer the sand into a diffuser. The diffuser is a stack of four standard 200 mm diameter soil testing sieves (shown in Figure 3.3). The sieves used were two 10 mm and two 5.5 mm sizes.

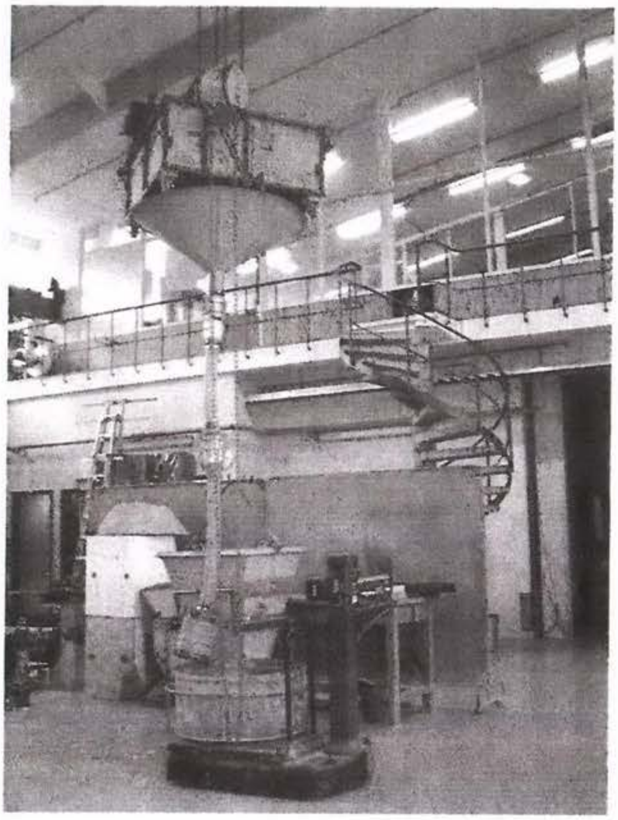

Figure 3.3. Transfer hopper, funnel and hose

This equipment rained the sand into the tank at a low rate and the fall height was carefully controlled to ensure a loose configuration. The amount of energy put into the sand during deposition determines its compaction, so by controlling the fall height uniformly loose deposits were achieved each time.

Chambers (1999) found that this pluviation method was able to produce soil deposits with a range of relative densities of ±6% over 18 tests, and the current tests had a closer range than this.

A further large hopper was used to store the sand when it was not in the laminated tank. This held a larger volume than the laminated tank, and had a pair of perforated plates in its base. One plate was on a screw thread and when the holes were aligned the sand flowed out. It was placed on steel beams to allow the small transfer hopper to be wheeled under it and filled before the funnel, hose and sieve arrangement was attached for pluviation. Figure 3.4 shows the transfer hopper being filled from the storage tank.

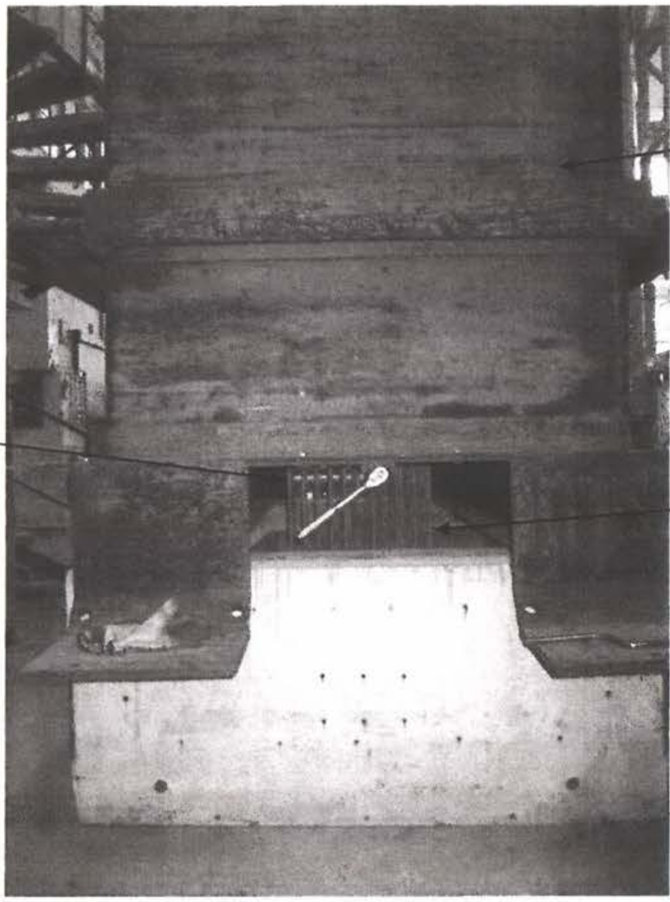

Figure 3.4. Filling of the transfer hopper

3.4 Shake Table

The University of Canterbury has a one dimensional horizontal shake table. It is capable of generating accelerations of up to 2.7 g with a mass of 5 tonnes (approximately that of the laminar tank when full of sand). It is 4 m by 2 m in plan with standard threaded bolt holes at 300 mm centres for attaching items to be subjected to shaking. The maximum horizontal force that can be applied is 200 kN and the maximum displacement is 300 mm.

3.5 Instrumentation of the test

Measurement of the test was done using six potentiometers and two accelerometers. Five potentiometers (Showa type 50LP300) were attached to a frame adjacent to the laminar tank on the shake table, as shown in Figure 3.5. These measurements allowed a deformation profile and horizontal shear strains to be determined. One potentiometer was used to measure settlement of the sand during the test. One of the accelerometers (Kyowa AS-5GA) was attached to the top of the laminar tank to measure acceleration of the soil mass while the other one measured acceleration applied by the shake table.

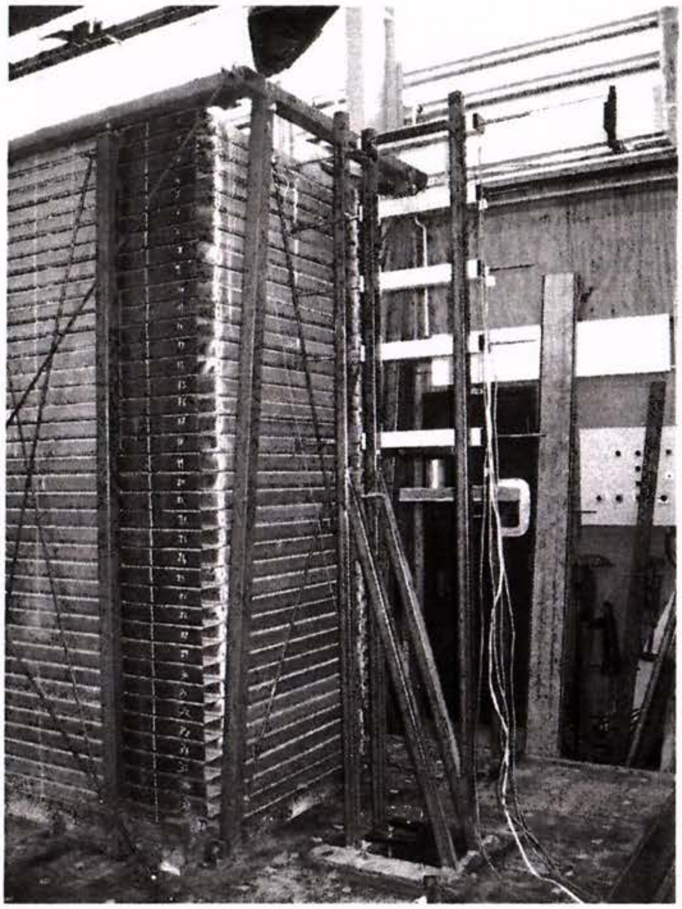

Figure 3.5. Instrument Frame on shake table

The outputs from these instruments were measured on a PC based data acquisition unit. Calibrations were performed on all instruments before use.

3.6 Sand Properties

The sand used in this study has previously been used by both Chambers (1999) and Charton (2003), and is an industrial silica sand with a very low fines content. It was sourced from Australia and supplied by Commercial Minerals Ltd (Auckland). The low fines content means that dust is not formed during pluviation, and the silica composition prevents degradation during testing which allows multiple reuses of the same material. Chambers was the first worker with the sand, and he carried out many tests on the soil to determine its properties. The following table is taken from Chambers (1999).

Table 3.1. Sand properties

Property	Symbol	Value
Density of solid particles	ρ_s	2650 kg/m^3
10% finer	D_{10}	0.3 mm
60% finer	D_{60}	0.45 mm
Minimum void ratio	e_{min}	0.53
Maximum void ratio	e_{max}	0.83
Steady state friction angle	φ_{ss}	33^0

3.7 Shaking intensity and duration

To allow a direct comparison of the new micropiles designed as part of this project and those previously used by Charton (2003), the same shaking parameters were used. The parameters Charton used were 26 cycles of sinusoidal shaking at 1 Hz with an amplitude of ±40 mm, corresponding to a theoretical peak acceleration of 0.16 g. This acceleration was found by Charton to be the minimum required to mobilise the full strength of the micropiles, and so get the full benefit from their installation. Chambers, who built the tank, carried out testing of the response of the tank to differing input frequencies. It was found that at 1 Hz the tank responded linearly with only a small zone of stiffening at the base. 1 Hz also represents a realistic frequency for strong ground motions in an earthquake. 26 cycles is an appropriate number of cycles for a M7.5-8 earthquake (Seed and Idriss, 1970).

After Tests 1-3 it was apparent that the measured accelerations were too high, and that the micropiles would not work at these levels. For Test 5, new shaking parameters were used that were within the expected range of the micropiles despite the lack of a baseline response to compare the results with.

A number of tests were carried out on different sizes of pile with slightly different peak accelerations. These are shown in Table 3.2. Note that the repeat peak accelerations are significantly higher than the theoretical accelerations expected. This is discussed further in the analysis (Section 6).

Table 3.2. Test parameters

Test	Reinforcement tested	Shake table		PGA	
		Amplitude	Frequency	Theoretical	Actual
1	None	±40 mm	1 Hz	0.16 g	0.63 g
2	65 mm	±40 mm	1 Hz	0.16 g	0.64 g
3	90 mm	±40 mm	1 Hz	0.16 g	0.71 g
5/1	90 mm	±20 mm	1 Hz	0.08 g	0.16 g
5/2	90 mm	±38 mm	1 Hz	0.16 g	0.25 g
5/3	90 mm	±40 mm	1 Hz	0.16 g	0.38 g
5/4	90 mm	±40 mm	1 Hz	0.16 g	0.40 g
5/5	90 mm	±50 mm	1 Hz	0.2 g	0.86 g

4 Micropiles

There are two current uses of micropiles. They are either used to carry structural loads or to create an insitu zone of reinforced soil (Bensilame et al., 1998). Micropiles are commonly used to carry structural loads when space is limited or for increasing foundation capacity during seismic retrofit or building extensions (Bedenis et al. 2004). These authors cite an example of an extension at a power station in America which utilised micropiles for foundation reinforcing because they had limited headroom for installing conventional piles, were unable to get access to the site with a pile driving rig, and wanted to cause the minimum disturbance to adjacent structures. The micropiles used were 50 mm Dywidag threaded bars inserted into predrilled 125 mm diameter holes, centred using PVC spacers and grouted into place. As with all micropiles, the dominant source of resistance for axial loads is from side friction.

A micropile is defined as a pile 300 mm or less in diameter, with reinforcement surrounded by cement grout (Kishishita et al., 2000). Their research focused on use of micropiles as foundations and the effects of these on motion of the structure. They found that using high capacity micropiles as raking members significantly reduced the vertical motion of the structure but had very little effect on the horizontal motion, which was controlled by the soil motion. Yang et al. (2000) found that for shaking of less than 0.25 g, a vertical micropile follows exactly the shaking of the soil and so any soil-pile interactions can be neglected. Beyond this, however, non linear soil behaviour significantly affects the response of the pile and the interaction between the soil and pile can no longer be neglected.

For the purposes of this research, the micropiles are looked at primarily as reinforcing members to reduce the risk of liquefaction by stiffening the soil. Their effect on ground motions was not considered, although their effect on ground displacement had a follow through effect on acceleration. By reducing shear strain, displacements are reduced and therefore the acceleration was changed.

Charton (2004) tested Ischebeck Titan 26-14 self drilling micropiles (a proprietary product) that were 100 mm in diameter. The piles were 25 mm diameter high strength hollow threaded steel bars with sacrificial drill bits on their tips. Charton's method used a cone penetrometer rig to push the micropiles into the ground and involved pressure grout pumping. During pushing, grout was injected at low pressure to the base of the pile to keep the hole open and to provide a bond with the surrounding soil. The resulting grout column was 100 mm ± 15 mm in diameter. These piles proved successful in reinforcing the soil to reduce shear strain and thus prevent liquefaction. McManus, Turner and Charton (2004) proved that the piles only mobilised a very small part of their strength in this strengthening. The purpose of this study is to test much smaller diameter piles that are more economical and easier to install. This study will use the same installation pattern and shake parameters to allow accurate comparison of the smaller micropiles with the proprietary product.

The micropiles for this study were designed to be easier to install and more economical to fabricate (due to lower steel and grout demand) while still providing sufficient reinforcement to the soil. Charton found that two opposed micropiles installed at 30^0 from vertical provided the best reinforcement. According to Coulomb's theory of soil failure, and assuming that:

- $\sigma_v > \sigma_h$ (i.e. $a_{max} < 1$ g)
- The steady state angle of internal friction in the sand is 30^0
- The earthquake waves are horizontally propagating shear waves

then the micropiles were installed on the plane of maximum shear stress. Using two opposed piles allows the conjugate stress directions to be strengthened. This inclination means that the axial stiffness of the micropile is mobilised rather than relying on the relatively low bending stiffness.

Jewell (1980), in a study of soil nails, determined that the reinforcement should be as longitudinally stiff as possible, and must be orientated in the direction of principal strain. He found that the bending stiffness of the reinforcement is unimportant because it contributes little to the shear strength improvement of a soil mass.

The two piles were installed 200 mm from the edges of the laminated tank. While this is outside of the recommendations of having all reinforcement more than five pile diameters away from the edge of the tank to avoid edge effects (Bensilame et al., 1998) the tank is too small to avoid such interference with 100 mm diameter piles. This is the same reinforcement pattern used by Charton (2003) to allow direct comparison.

4.1 Design

Following on from Charton's finding that very little of the strength of the steel was mobilised to stiffen the soil, it was decided to use a significantly smaller section of steel to allow for a more simple and economical method of installation. Charton carried out pressure grouting to form his micropiles, which was an awkward process and gave a range of 30 mm on the diameter of the piles (Charton, 2004). This study utilised a hydraulic ram to push the tubes into the ground, followed by gravity grouting and then use of the same hydraulic ram to pull the tube out of the ground. Details of the installation process are in Section 4.2.

Two sizes of micropile were tested. The first micropile design tested was a 6mm deformed bar within a 65 mm grout column. A deformed bar was used to provide a better bond with the surrounding grout. The micropile was installed to a depth such that there were more than five pile diameters between the pile tip and the base of the tank to avoid any edge effects, as suggested by Bensilame et al. (1998).

The second size of micropile tested was 90 mm, and Figure 4.1 shows the tip and rod assembly of one of these micropiles. The lip on the pile tip is for the casing to sit on so that it lies flush with the tip and does not leak grout. The shoulder (labelled on Figure 4.1) is to provide friction with the soil to ensure the tip stays in place when the casing is removed. The deformed bar is welded into a hole in the centre of the tip. The same design of components was used, albeit with a new set of couplers, tubes and adaptors which were needed to increase the diameter. This improvement was as a result of observations that the pile appeared to fail in friction, and backed up by Jewell (1980). Jewell found that the maximum benefit can be gained from the reinforcing when the bond between the soil and the nail is as great as possible, so a rough nail of larger diameter was used.

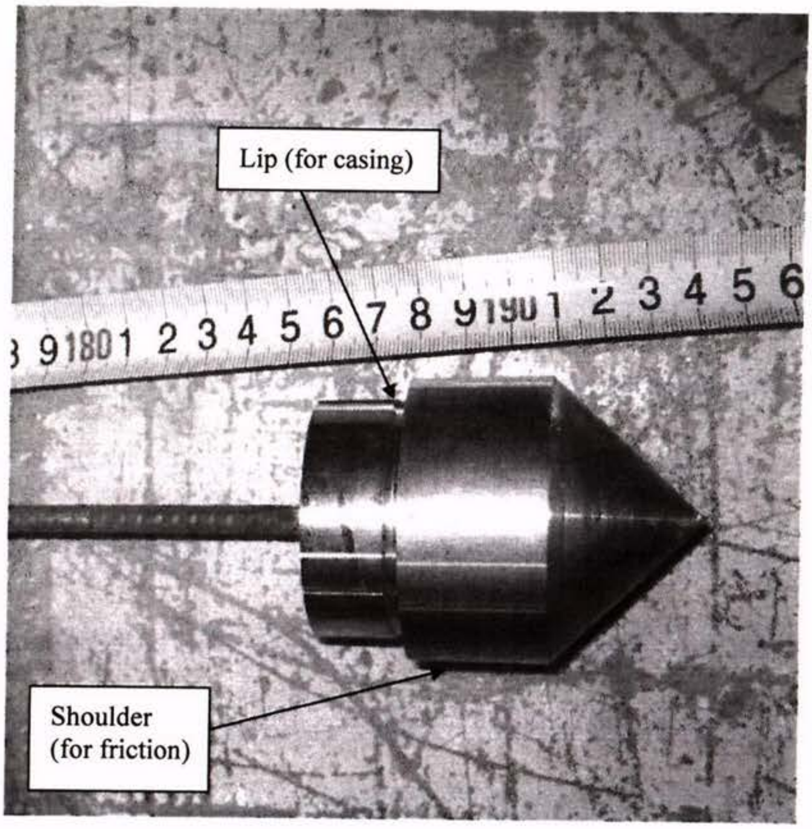

Figure 4.1. Detail of the pile tip

The grout used was the same mix used by Charton (2004) to ensure accurate comparisons. It was made with 50:50 (by mass) water and cement with 3 % of the cement mass of bentonite added. The bentonite was thoroughly mixed with the water before the cement as added. Compression testing of samples of grout was done, and the 28 day strength of the grout was 8 MPa. Observation of the grout in the micropiles upon demolition indicated that it was uniform and without cavities, showing that it was well mixed and sufficiently low viscosity to fill the casing entirely.

4.2 Installation

The micropiles were installed in the laminated tank once it had been filled with sand using the air pluviation method described previously. A frame was constructed to allow a hydraulic ram to push the pile tube into the sand, as shown in Figure 4.2. An I - beam fixed at 60^0 was used to guide the pile into the sand at the correct angle. The hydraulic ram pushing the pile was bolted to the I – beam. The availability of a reaction frame and the location of the supports for the frame limited the lateral positioning of the micropiles. The first two tests used micropiles installed at 500 mm spacings, then following major modifications to the pushing rig, the third test used equally spaced micropiles (400 mm).

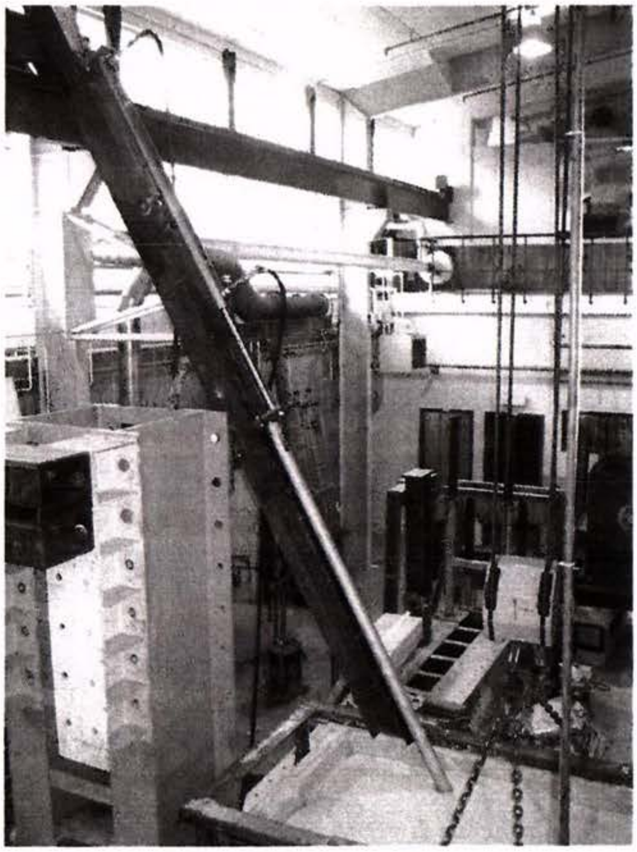

Figure 4.2. Micropile pushing apparatus

A plate with guide arms (Figure 4.3) was built to guide the end of the ram down the I beam to ensure the pile was inserted correctly. The cylinder welded to the guide plate fitted inside the micropile casing to provide a solid platform on which to push. The holes in the side of the cylinder line up with those in the casing and a bolt is pushed through the holes to enable the casing to be pulled out of the sand.

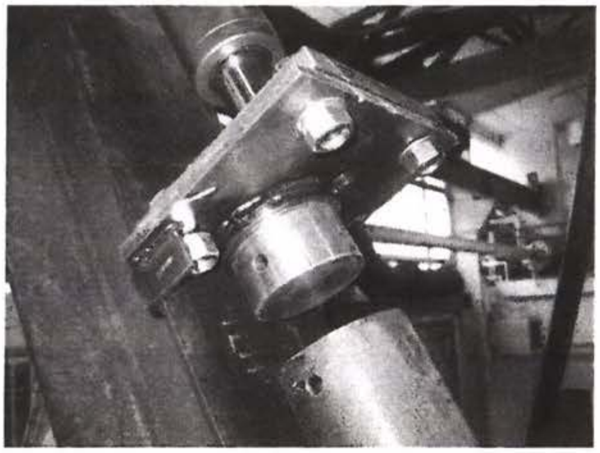

Figure 4.3. Guide plate and engagement cylinder

The hydraulic ram used had a stroke of 1.3 m, so it was necessary to fabricate a 1 m extension to allow the ram to push the pile full depth into the sand in two pushes without moving the ram. This was made from a section of the pile tubing with a coupling to attach it to the actual pile tube. Detail of the coupling is shown in Figure 4.4, and the pins used for pulling the pile tube out can clearly be seen. The coupling works in exactly the same way as the cylinder in Figure 4.3, fitting into both the extender and the casing. The anchor wire can also be seen through the window cut for pouring grout.

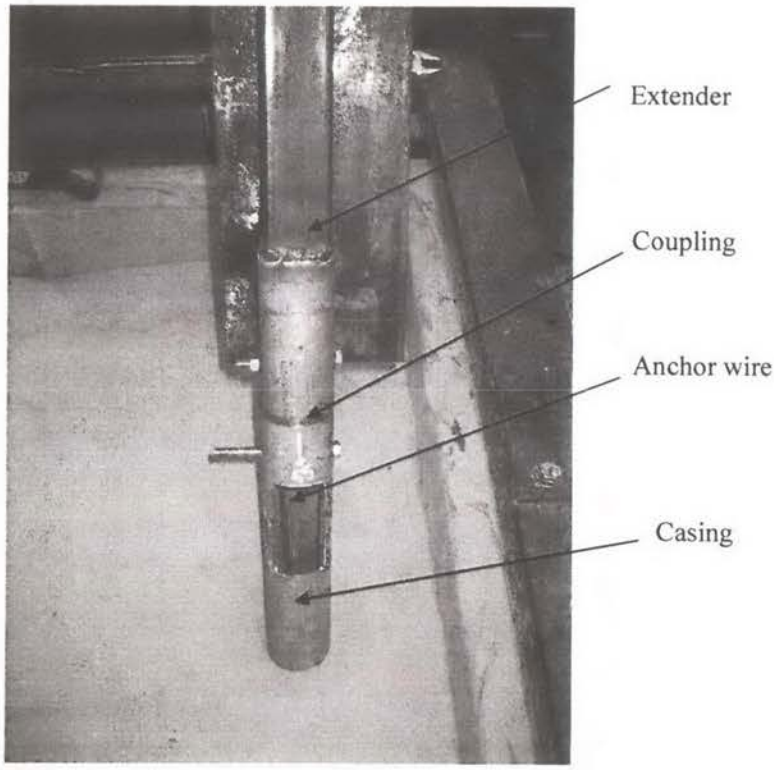

Figure 4.4. Detail of the coupling and grout slot

Once the pile was pushed to full depth in the soil, the grout (pre-mixed) was poured through the window cut in the top of the pile until the grout level was flush with the soil (see Figure 4.5).

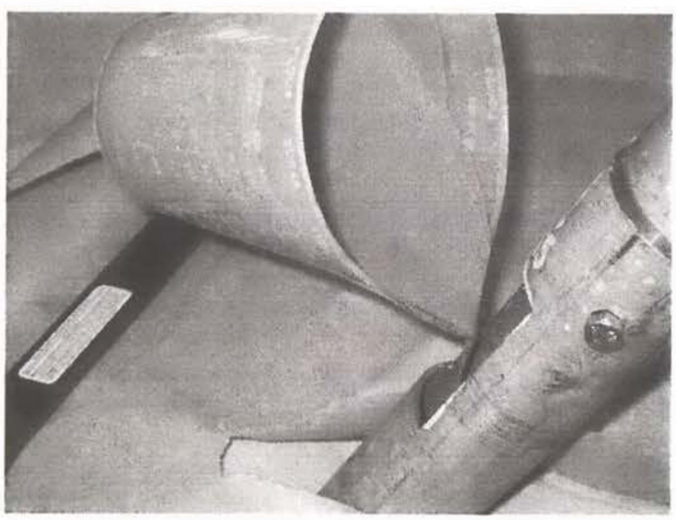

Figure 4.5. Detail of grout pour

The pile tubing was then pulled out, again in two stages, using the extender. When the extender was removed, more grout was poured down the pile tube to ensure a full pile was formed. It was vital to add this extra grout as the final pile diameter is slightly larger than the outside diameter of the tubing whereas the initial grout pour only filled the internal diameter of the pile. The reinforcing rod was centred using a wooden template while the grout cured for at least two days before testing. Figure 4.6 shows the completed micropiles in Test 2 with the templates in place to centre the steel rods.

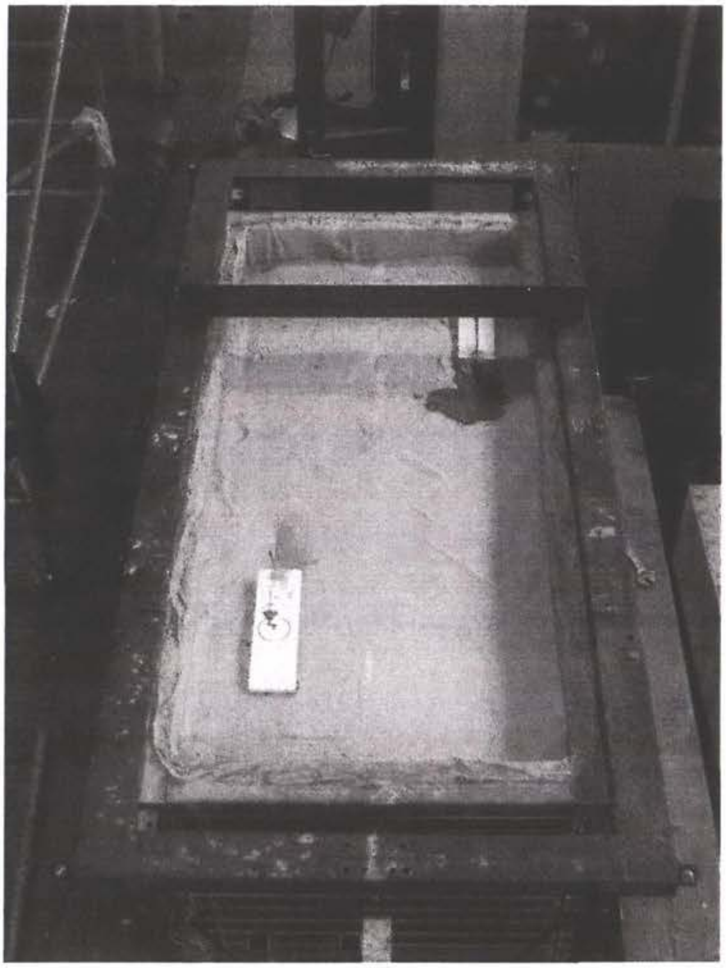

Figure 4.6. Completed micropiles in sand tank

4.3 Micropile Dimensions

Having tested the sand deposits reinforced with micropiles, the laminar tank was emptied and the micropiles removed. They were inspected and measured, and the dimensions are shown in Table 4.1. After Tests 2, 3 and 5 both of the piles were intact.

Following Test 4, the piles were extensively cracked, although they retained their shape and still had a thick layer of sand coating them.

After Test 2, both piles were shorter than the full depth of the hole. The lengths achieved were 1570 and 1600 mm, compared to the 1800 mm depth. This is a result of insufficient grout being poured into the hole during installation, and was remedied in future tests.

All of the piles had hollow sections at the top which were probably related to bleeding of the grout and associated loss of volume. These hollow sections did not adversely affect the performance of the piles because no failures were observed in this section of pile. There was a small nick point in every pile 1 m from the tip, which most likely represents some misalignment of the pile tube during the changeover from pulling with the extension bar to pulling the tube directly.

When the piles were exhumed, they had a thick coating of sand on them, giving the appearance of a pile some 20 mm larger in diameter than the grout. Once this sand was brushed off, the diameter of the pile was then measured at 10 equally spaced points. The fact that the sand was attached to the outside of the pile after the test shows that the full friction between the soil and the pile had been mobilised.

Table 4.1. Micropile Dimensions

Test Number	Nominal pile diameter (mm)	Mean pile diameter (mm)	Range of diameters
2	65 mm	66.6 mm	± 1.6 mm
		66.0 mm	± 1.7 mm
3	90 mm	89.9 mm	± 1.7 mm
		94.5 mm	± 1.3 mm
4	90 mm	Pile damaged by excess shaking	
5	90 mm	91.3 mm	± 1.1 mm
		89.5 mm	± 2.2 mm

The piles were highly uniform diameters, as seen from the range of sizes in Table 4.1 and Figures 4.7 and 4.8, which show the exhumed piles from Tests 2 and 3 respectively.

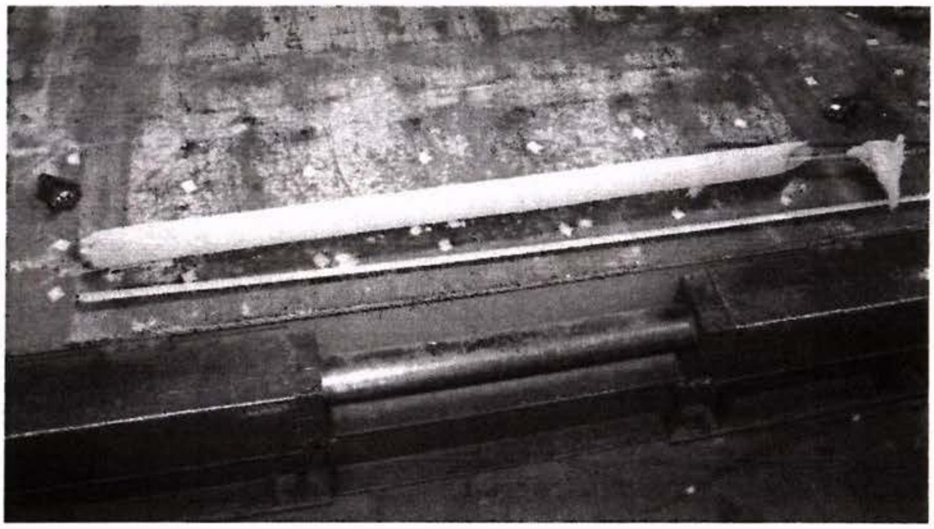

Figure 4.7. Exhumed pile from Test 2

Figure 4.8. Exhumed pile from Test 3

5 Results

5.1 Test 1: Unreinforced Soil

A loose sand with relative density $D_r = 0.05$ was subjected to 26 cycles of sine wave shaking with amplitude = 40 mm and frequency = 1 Hz. Differentiating this displacement twice yields a maximum acceleration of 0.16 g, as in McManus et al (2004). However, the shaking table is not able to precisely reproduce a sine wave, due to a lot of "jerkiness" in the motion. An enlargement of two cycles of the acceleration is shown in Figure 5.1, with the theoretical sine wave of the acceleration superimposed. The repeated peak acceleration for this test was 0.63 g.

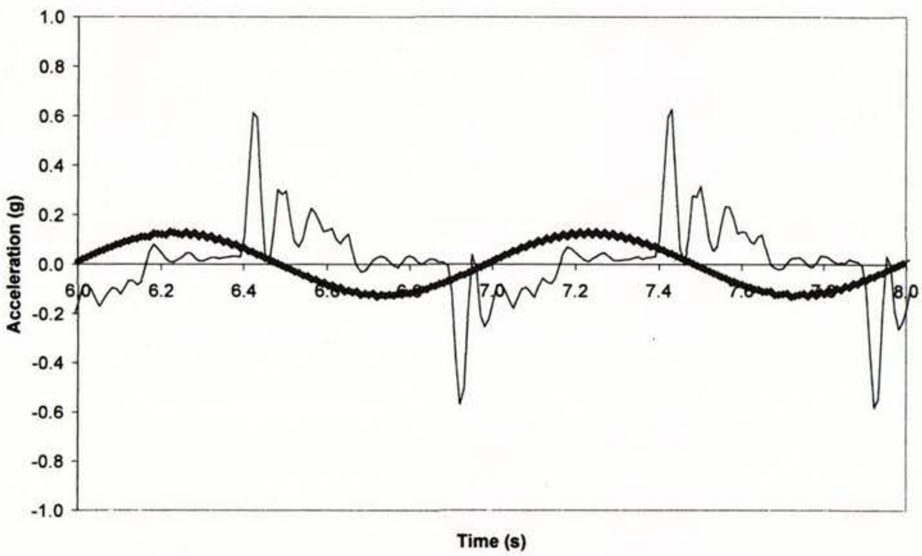

Figure 5.1. Two cycles of acceleration recorded on the table, ±40 mm

The sand densified significantly during shaking, with a change from a very loose, air pluviated sand ($D_r = 0.05$) to a denser $D_r = 0.29$. This large increase in density is similar to liquefaction because had the soil been saturated with water, excess pore pressures would have been generated, possibly leading to liquefaction. The rate of settlement versus time is shown in Figure 5.2, and was very rapid at first, but decayed exponentially as it increased in density. The total settlement was 80 mm, which represents a vertical strain of 4 %. The settlement measured by the settlement plate at mid-height in the deposit was 40 mm. This result is similar to that found by Charton.

Charton also carried out tests on similar deposits with 20 mm and 30 mm amplitude shaking, and found that very little settlement occurred in these.

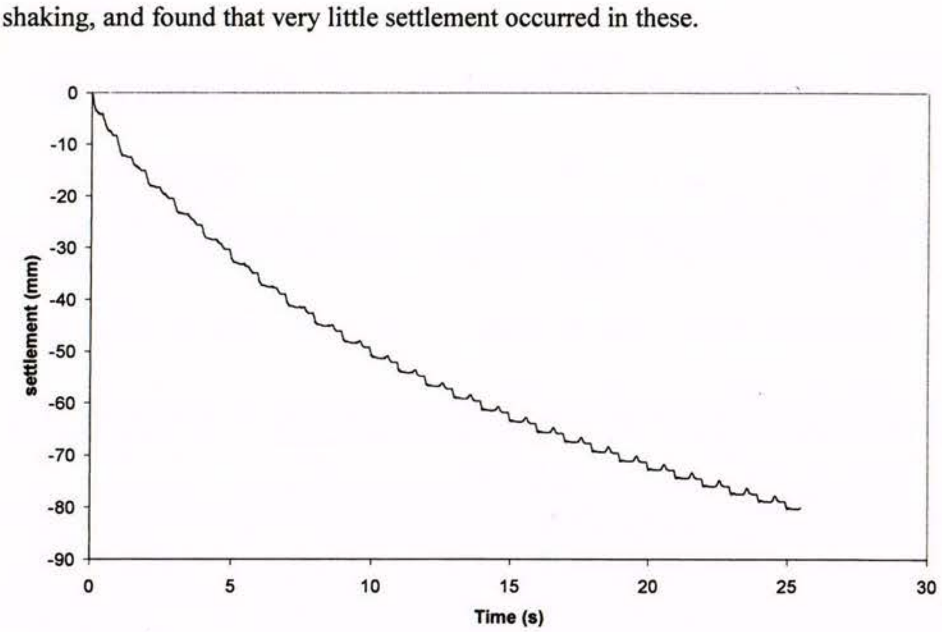

Figure 5.2. Settlement profile for unreinforced sand

The displacement profile recorded from the tank shows that the tank did not deform in pure shear. The displacement profile is non linear, with two distinct linear portions, that below 1500 mm height and that above 1500 mm height as shown in Figure 5.3. This is the same near surface non-linearity observed by Charton (2003).

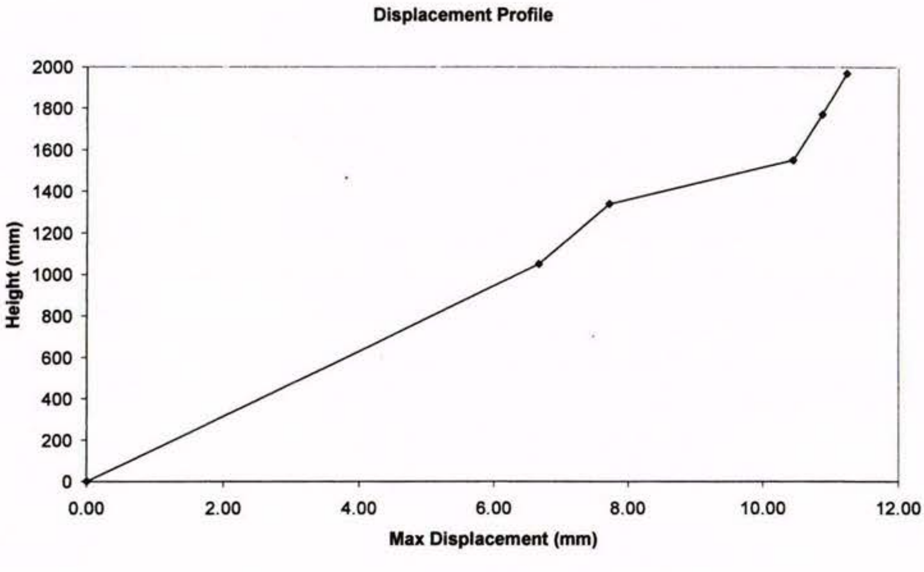

Figure 5.3. Maximum displacement profile for unreinforced soil

Plotting the full cyclic shear strain records from all potentiometers on the same graph shows that the tank deformed in a linear fashion with the peak shear strains at all levels occurring at the same time. All potentiometers took 6 cycles of shaking to reach their maximum displacement. Figure 5.4 shows the peak cyclic shear strain recorded at potentiometer 4 as this had the highest level of shearing. The peak cyclic shear strain per cycle reduces as the test progresses due to the densification and stiffening of the sand. Figures 5.3 and 5.4 show that the tank approximated pure shearing, but that some non linear behaviour occurred near the surface.

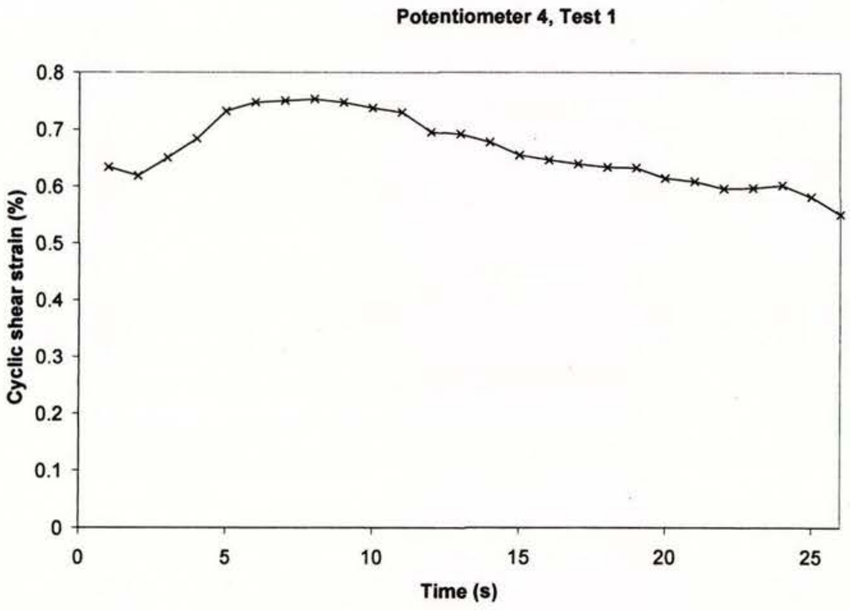

Figure 5.4. Peak Cyclic Shear Strain profile for Test 1

The results from this test show that the laminated tank is working as expected, and that the sand preparation is suitably similar to that done by Chambers and Charton to allow comparisons between the methods. It has established a baseline shaking response, to which subsequent results can be compared and therefore the effect of inserting the micropiles deduced. Test 2 will have the same shaking parameters, but micropiles will be installed in the sand tank prior to shaking. Any difference in the response of the sand can therefore be attributed to the micropiles.

5.2 Test 2: Reinforced Soil 1

This test was the first to be carried out using reinforcing elements. Two diagonally opposed micropiles were installed in the soil and left to cure for 4 days before testing. The tank was then subjected to exactly the same input motion as was applied in the baseline Test 1. This produced slightly different shaking to Test 1 due to the inaccuracies in the servo control system for the shake table. However, upon inspection, the acceleration graphs were similar enough to be assumed the same, and two cycles of the acceleration is shown in Figure 5.5.

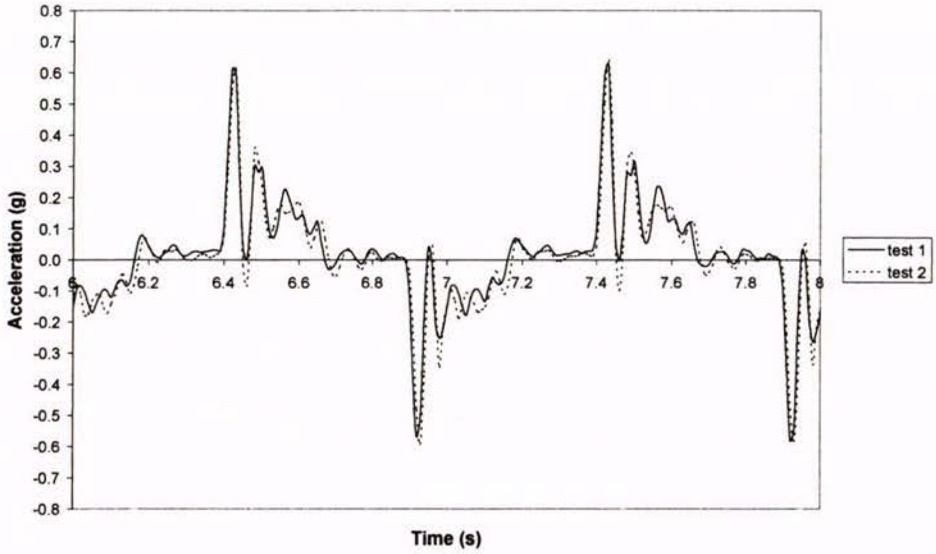

Figure 5.5. Graph showing two cycles of the acceleration in Tests 1 and 2

The settlement curve for Test 2 is very similar to that for Test 1, and both are shown together in Figure 5.6. For the first cycle of shaking, the micropile reduced settlement significantly, but the overall reduction in settlement due to the micropiles was only 2 mm. This is despite a lower initial relative density than in Test 1 ($D_r = 0.01$ compared to $D_r = 0.05$). From watching the test, it appeared that something in the system failed suddenly to allow a rapid increase in settlement. The relative density rose from $D_r = 0.01$ to $D_r = 0.26$ during the shaking.

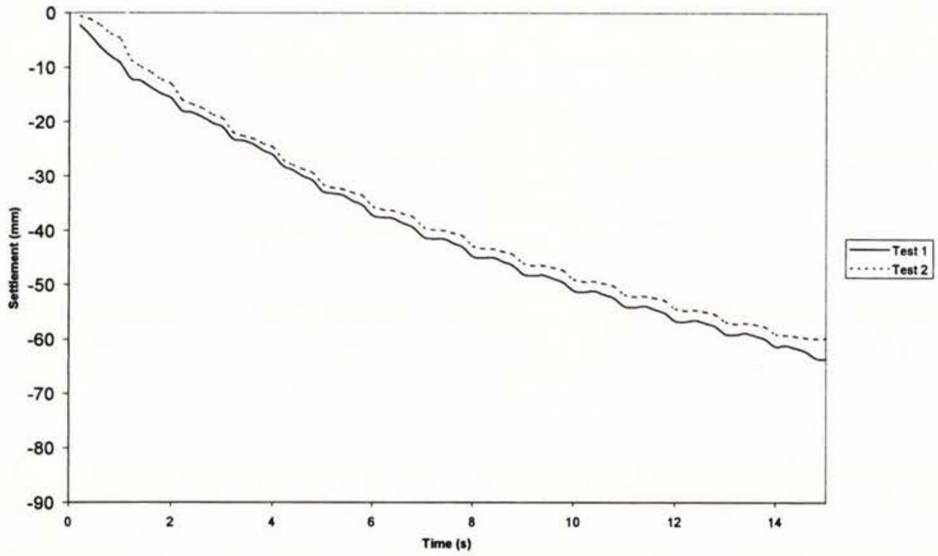

Figure 5.6. Settlement in Tests 1 and 2

The micropiles reduced the shear strain of the tank for the first cycle of shaking, but then reached a slightly higher value than in Test 1. This is likely to be a result of slightly higher intensity shaking, and can be seen in the plot of cyclic shear strain in Figure 5.7.

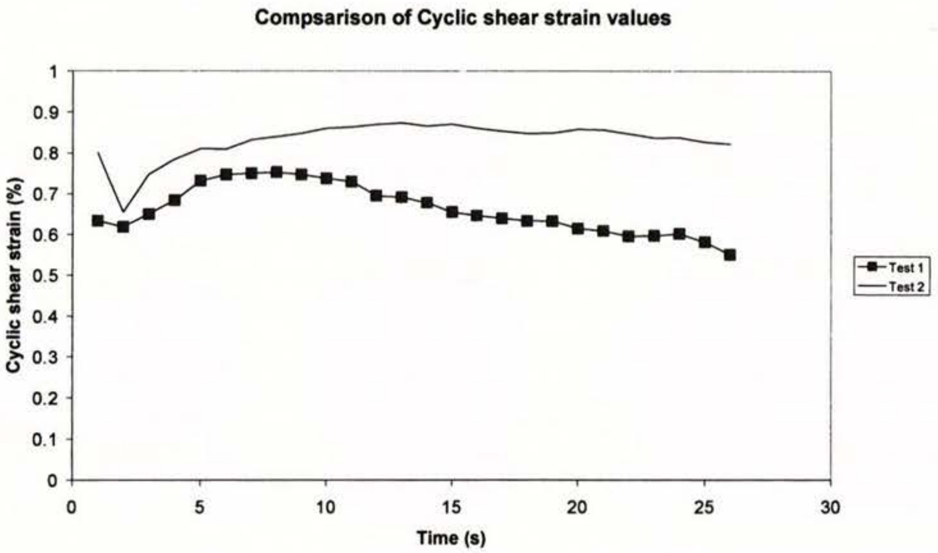

Figure 5.7. Peak Cyclic Shear Strain profile for Tests 1 and 2

5.3 Test 3: Reinforced Soil 2

Two larger diameter micropiles were installed in the sand tank in exactly the same location as those for Test 2. Once again, the piles were left for 4 days to cure before being shaken with the same motion as in Tests 1 and 2. The inaccuracy in the shaking table pump system was more noticeable in Test 3, with a significant difference between the acceleration records from Tests 1 and 3. The repeated peak acceleration in Test 3 was 0.71 g, over 10 % greater than in the previous tests. The accelerogram had a similar shape to those from previous tests, but appeared to have more of a jerk at the end of the displacement which resulted in the higher accelerations seen. Figure 5.8 shows a comparison of the accelerograms recorded during Tests 1 and 3, and that the accelerations are significantly different.

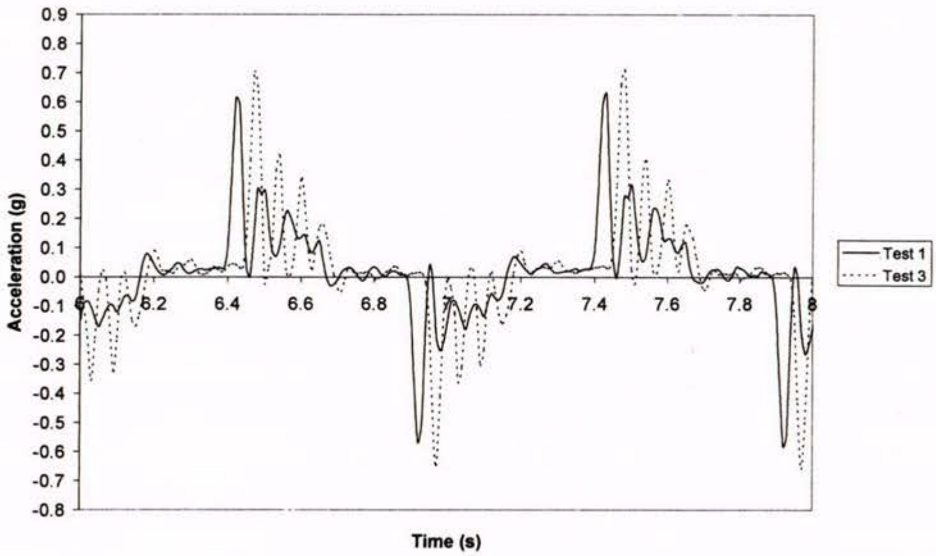

Figure 5.8. Graph showing the acceleration in Tests 1 and 3

Settlement was reduced significantly for the first cycles of shaking, but then a failure occurred and the settlement was the same as the unreinforced soil. Figure 5.9 shows the settlement profiles from Test 1 (unreinforced soil) and Test 3. In the first two cycles of shaking the settlement is reduced by 8 mm, at a time when the total settlement in the unreinforced soil was 16 mm. The initial relative densities in Tests 1 and 3 were exactly the same. The micropile then failed and the total settlement was similar to that of the unreinforced soil. The settlement recorded represents a change from relative density $D_r = 0.04$ to $D_r = 0.31$.

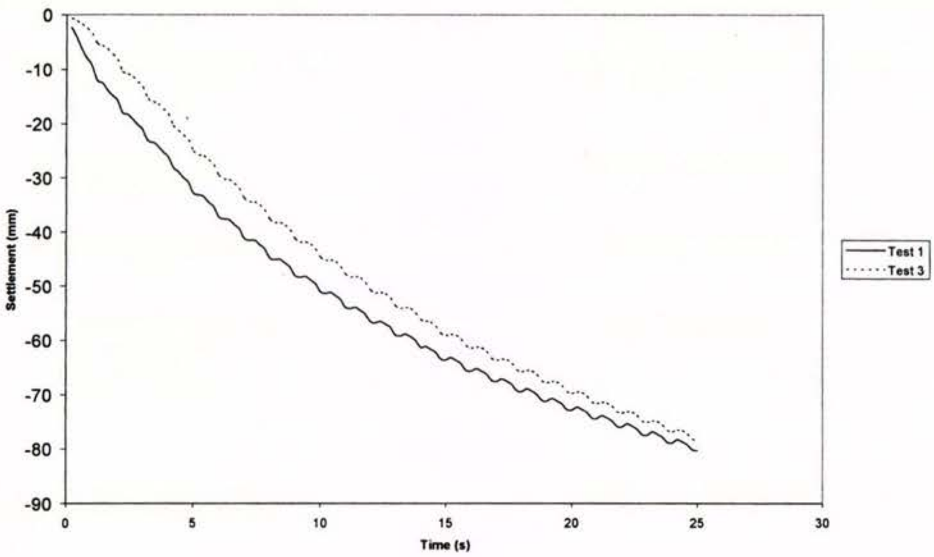

Figure 5.9. Settlement in Tests 1 and 3

Figure 5.10 shows the peak cyclic shear strain from Tests 1, 2 and 3, and that the peak shear is greater in Test 3 than Test 1. This is likely to have been caused by the increase in shaking intensity as previously discussed. From 10 s onwards, the cyclic strain in Test 3 was lower than that in Test 2, suggesting that the micropile did have an overall stiffening effect despite the higher acceleration.

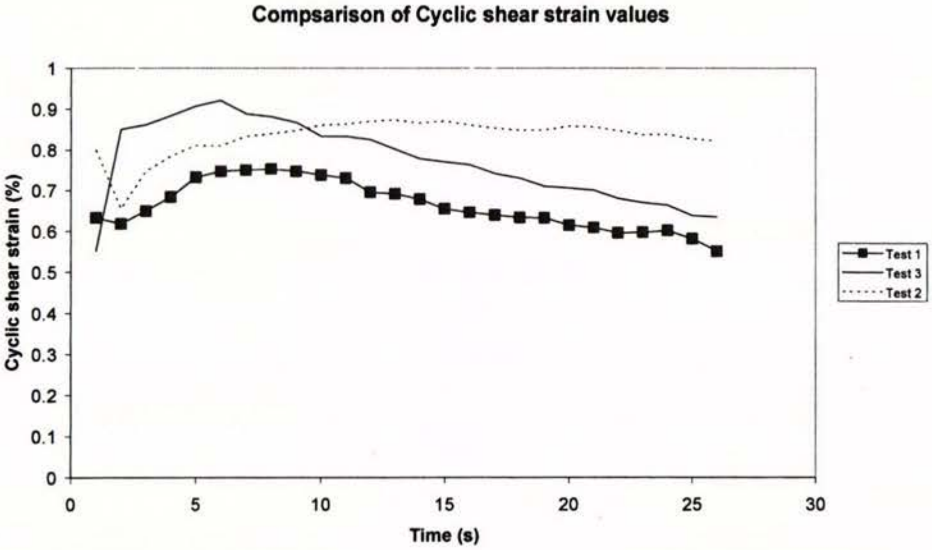

Figure 5.10. Peak Cyclic Shear Strain in Tests 1, 2 and 3

5.4 Test 5: Reinforced Soil 4

Prior to construction of the third reinforced soil deposit, the pushing rig was dismantled, modified and reassembled such that the micropiles were installed at one third and two thirds width in the tank. This represents a move towards the centre of the tank of 50 mm for each micropile. It was hoped that this would provide better reinforcing and avoid edge effects.

The shake table was tuned to provide a smoother sine wave. The acceleration values are still significantly different from the theoretical values, but are a significant improvement on those used for Tests 1-4. The new tuning was used for Tests 5/1 – 5/3, then the old tuning was reused to gain higher acceleration values. The peak acceleration value for each test using the new tuning was in the first cycle of negative acceleration. It is not known why this happened, nor was it possible to prevent it happening.

Test 5 was carried out on two 90 mm diameter micropiles installed in the centre of the tank. As with previous tests, the grout had been curing for 4 days.

There were five parts to Test 5, beginning with a small acceleration (0.2 g) and building to a large acceleration (0.9 g). Each test was carried out on the same deposit, so the relative densities at the start of each test got progressively higher.

5.4.1 Test 5/1

The repeated peak acceleration is Test 5/1 was 0.16 g, and two cycles of the accelerogram are shown in Figure 5.11. This is significantly smoother than those obtained during earlier tests, albeit far from a perfect sine wave.

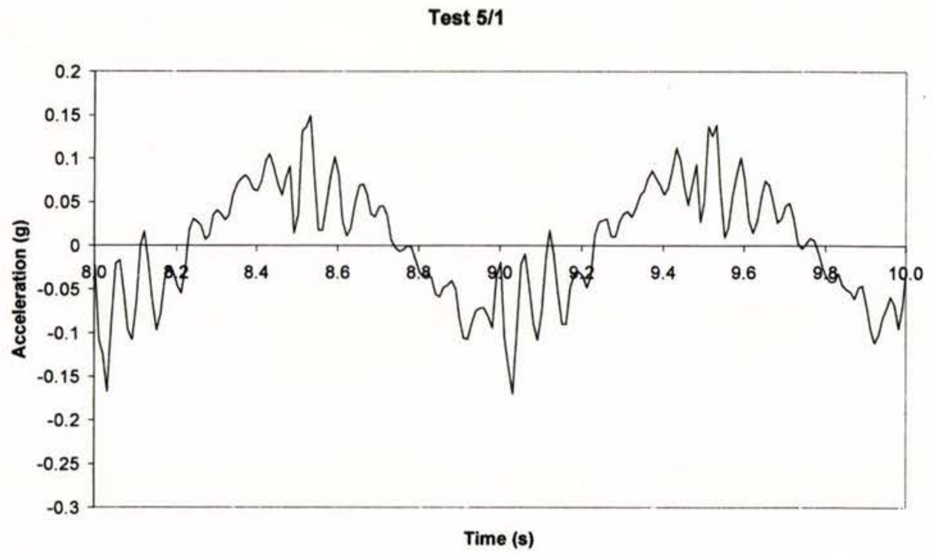

Figure 5.11. Two cycles of the accelerogram from Test 5/1

There was very little settlement recorded during Test 5/1, with a total of slightly greater than 2 mm, as shown in Figure 5.18. This settlement represents a change of less than 0.01 in relative density ($D_r = 0.116$ to $D_r = 0.122$).

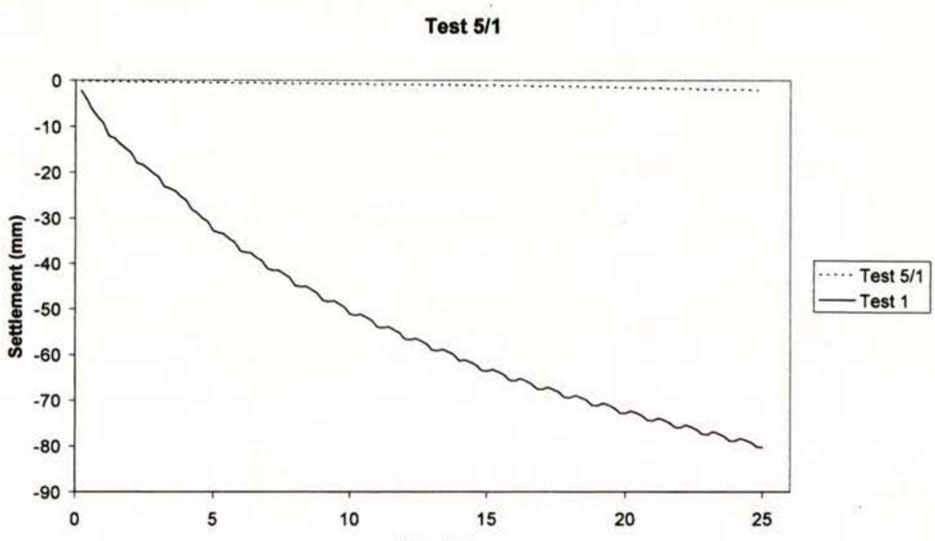

Figure 5.12. Settlement-time curve for Test 5/1

Figure 5.13 shows the cyclic strain profile for all potentiometers. It can be seen that the shear strain is significantly less than measured during any of the previous tests. A peak value of shear strain can be seen at 1 s which corresponds to the peak acceleration value for the test.

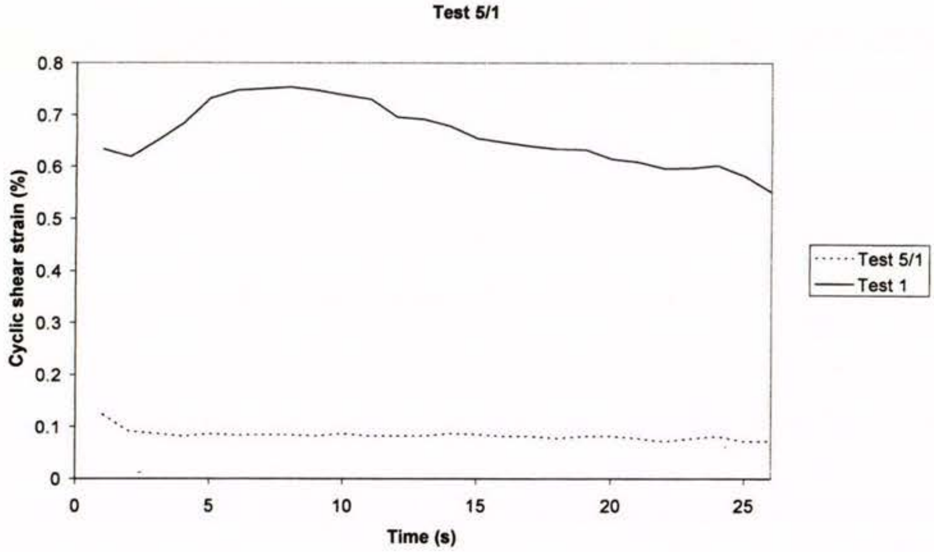

Figure 5.13. Peak Cyclic Shear Strain profile, Test 5/1

5.4.2 Test 5/2

The accelerogram for Test 5/2 is similar to that for Test 5/1. The initial high negative peak is present, followed by a stabilisation with subsequent peaks of approximately the same height (see Figure 5.14). The repeated peak acceleration is 0.25 g which is slightly greater than that in Test 5/1.

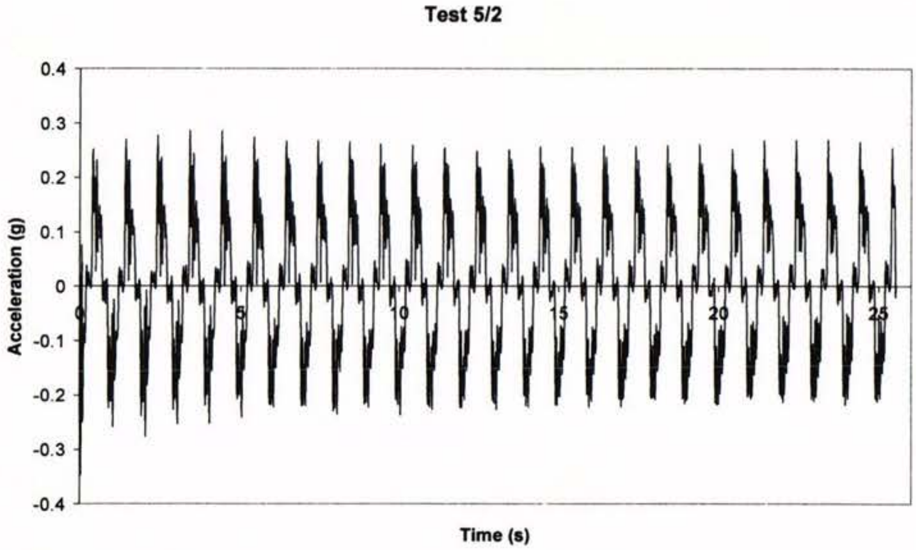

Figure 5.14. Accelerogram for Test 5/2

20 mm of settlement occurred during Test 5/2, with the same pattern as before of a reducing rate as the test progresses. The rate of settlement at the start of the test is significantly lower than was observed in Tests 1-3, and the settlement-time plot is shown in Figure 5.15. The relative density changed from $D_r = 0.12$ at the start of the test to $D_r = 0.22$ at the end of the shaking.

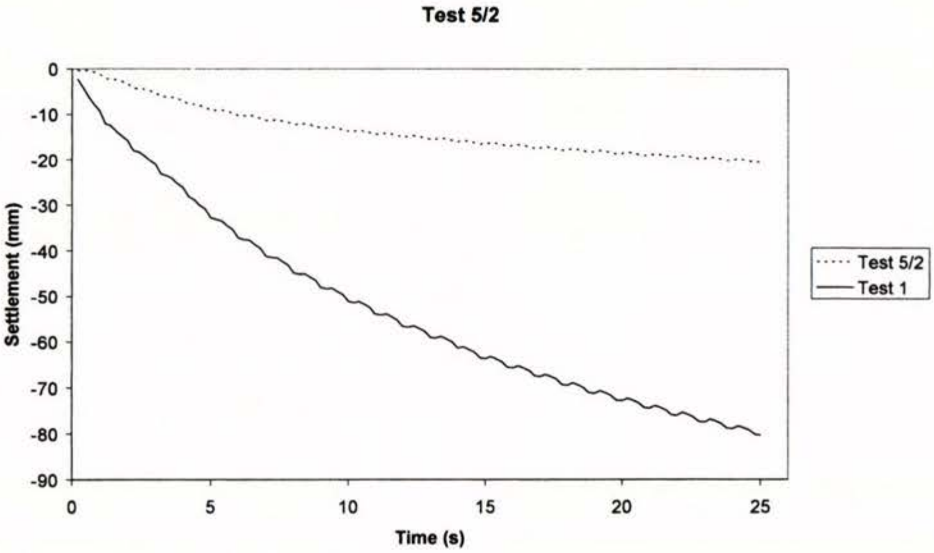

Figure 5.15. Settlement-time curve for Test 5/2

Figure 5.16 shows the cyclic shear strain profile recorded on all potentiometers in Test 5/2. As with Test 5/1 there is a strong correlation between the rate of settlement and the amount of shear strain at the beginning of the test. As the settlement rate reduces, so does the cyclic shear strain. However, towards the end of the test (beyond 15 s), the settlement rate reduces but the cyclic shear strain increases. The cyclic strain is significantly higher than in Test 5/1, but still significantly lower than in Tests 1-3, as a result of reduced acceleration.

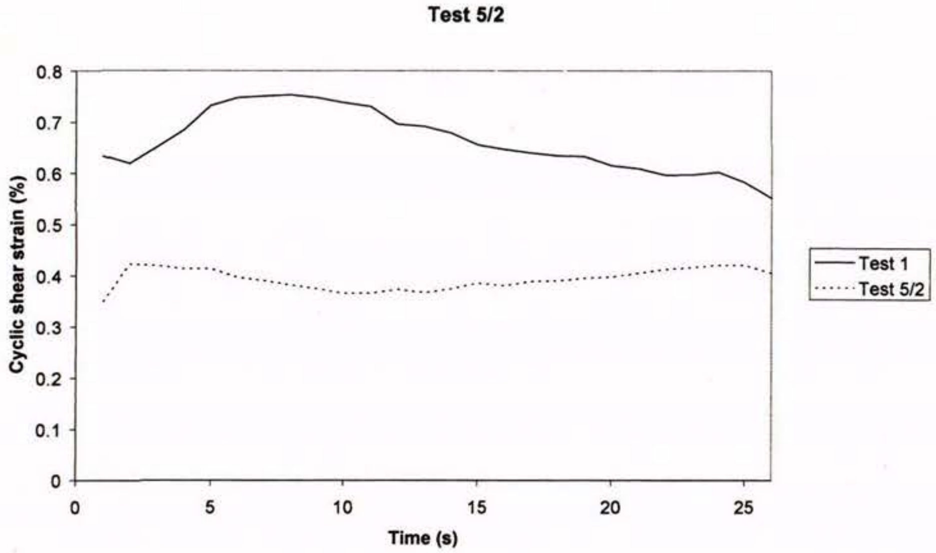

Figure 5.16. Peak Cyclic Shear Strain profile for Test 5/2

5.4.3 Test 5/3

Test 5/3 was run with a sine wave of 40 mm amplitude. The theoretical peak acceleration is 0.16 g, but in this test the maximum recorded was 0.40 g. The repeated peak acceleration of the test was 0.38 g, and the accelerogram is shown in Figure 5.17.

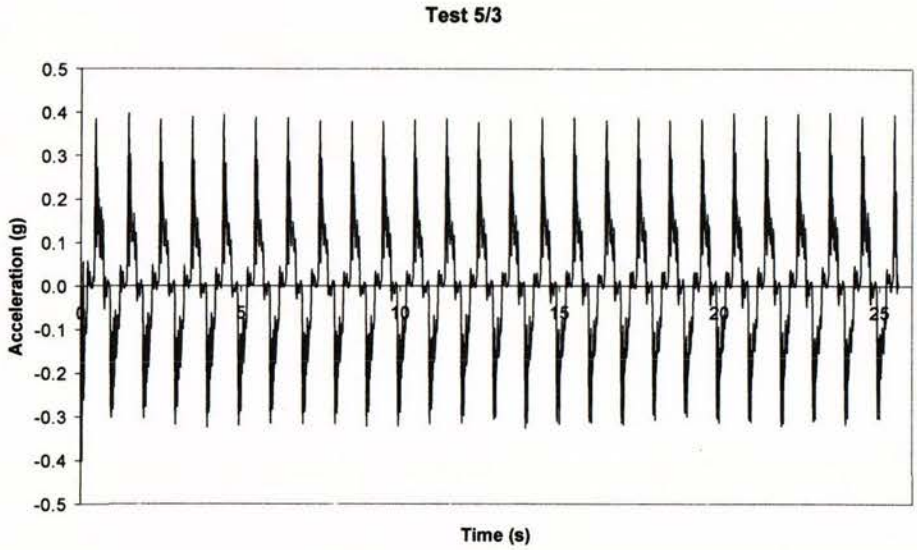

Figure 5.17. Accelerogram for Test 5/3

The settlement versus time curve for Test 5/3 is shown in Figure 5.18. It is significantly straighter than previous profiles, with only a slight reduction in settlement rate during the test. There was 24 mm of settlement, which is a change in relative density from $D_r = 0.22$ to $D_r = 0.31$.

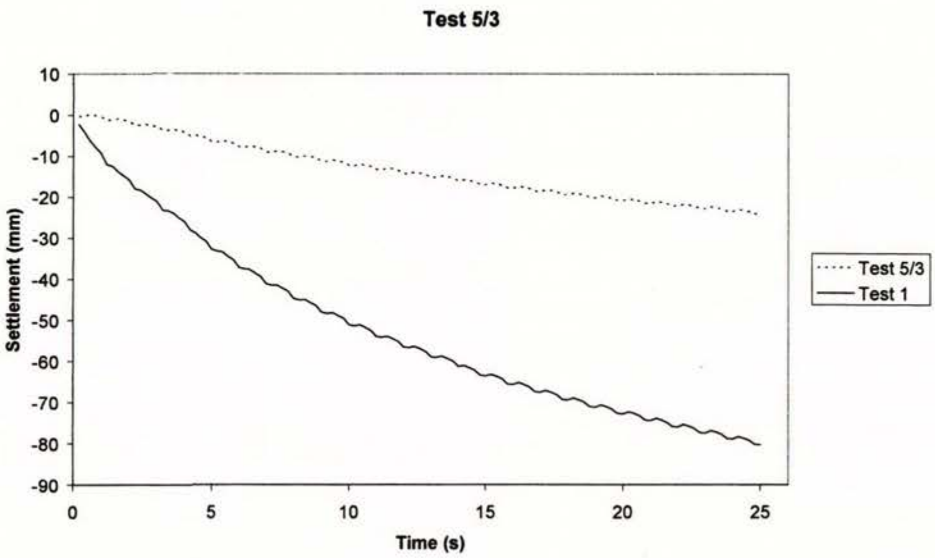

Figure 5.18. Settlement-time curve for Test 5/3

The slight time lag between the onset of shaking and the start of settlement as seen in Figure 5.18 can also be seen as a lag between the onset of shaking and the time to reach peak cyclic shear strain in the shear strain profile (Figure 5.19). Having reached the peak shear strain of approximately 0.45 % the shear strain reduces slightly, as would be expected from the settlement profile.

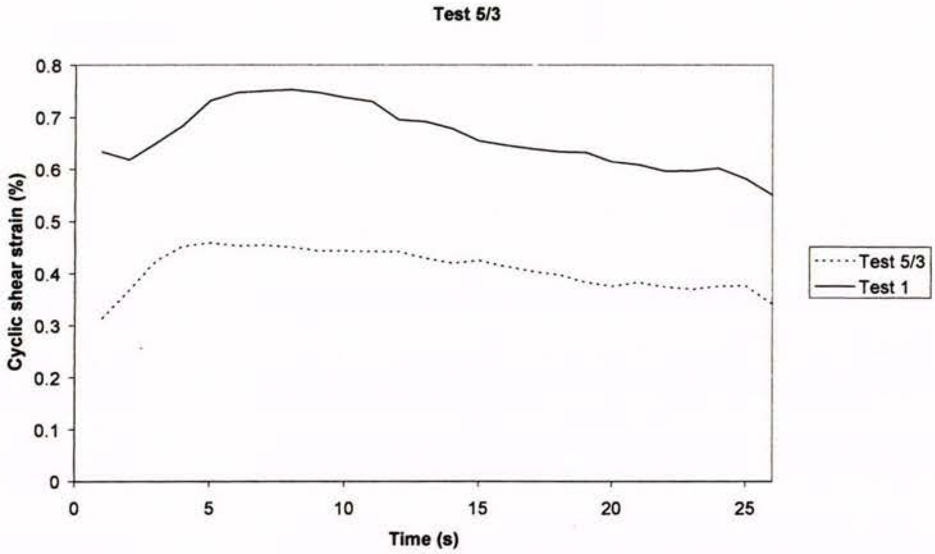

Figure 5.19. Peak Cyclic Shear Strain profile for Test 5/3

5.4.4 Test 5/4

Test 5/4 was the first in Test 5 to use the previous settings on the shake table. The effect of this was to make the motion rougher and consequently give a higher peak acceleration for the same motion. Figure 5.20 shows the acclerogram from this test, and it follows the same pattern as Tests 1-3, with even peaks in each cycle and no initial high peak. The repeated peak acceleration was 0.40 g.

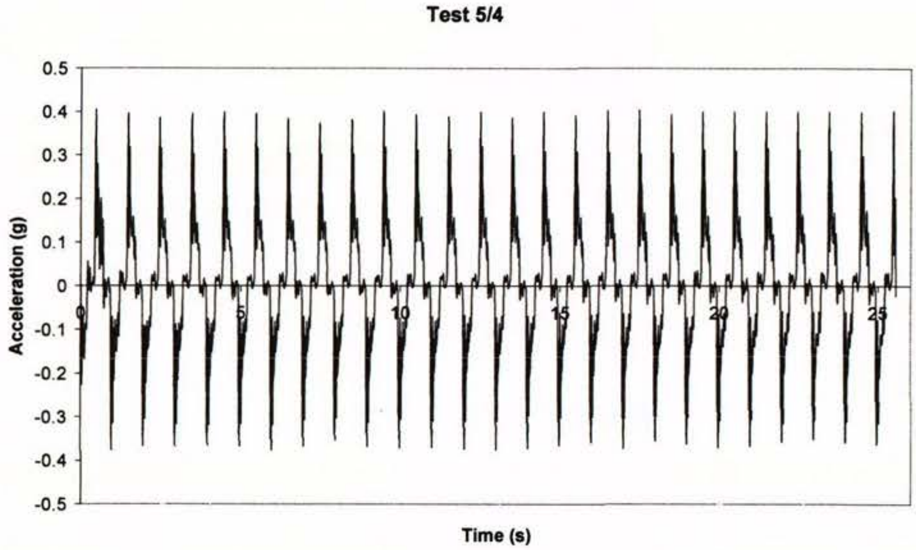

Figure 5.20. Acclerogram for Test 5/4

The settlement-time curve (Figure 5.21) was relatively linear for this test, contrary to previous observations. There was 15 mm total settlement, which represents a change in relative density from $D_r = 0.31$ to $D_r = 0.34$.

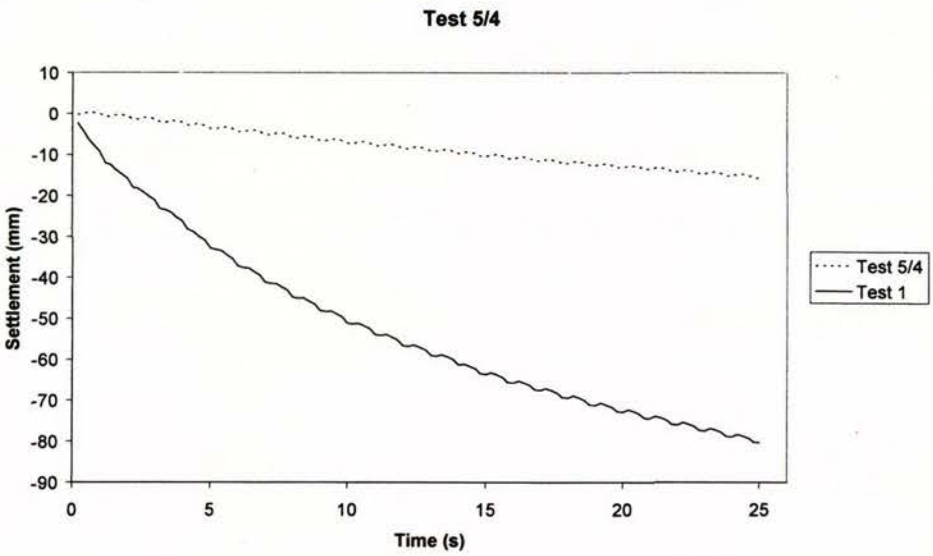

Figure 5.21. Settlement-time curve for Test 5/4

The peak cyclic shear strain profile from Test 5/4 is shown in Figure 5.22. The strain reaches a peak after four cycles of shaking and then is relatively uniform throughout the duration of the test, and is slightly greater than the strains recorded in previous parts of Test 5.

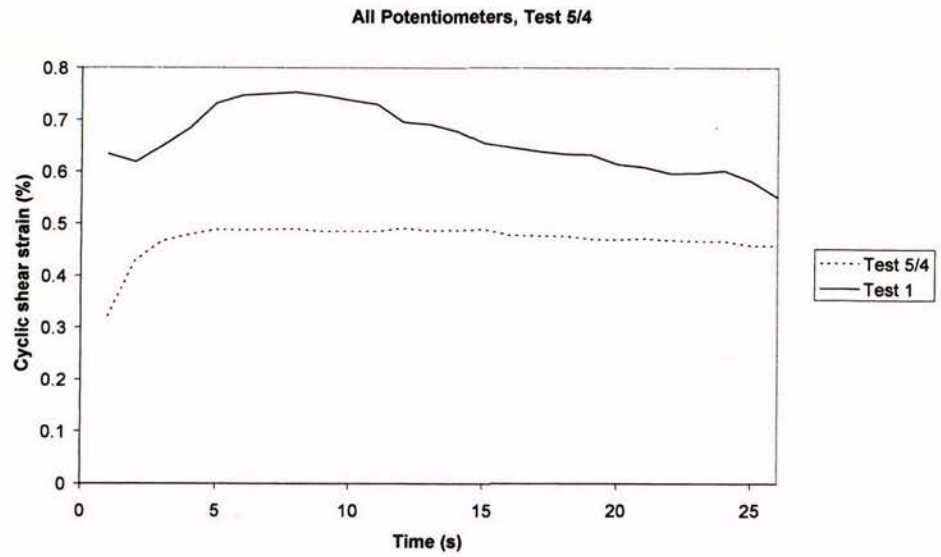

Figure 5.22. Peak Cyclic Shear Strain profile for Test 5/4

5.4.5 Test 5/5

Test 5/5 was the final test for the micropiles as the sand was densifying during all tests and was becoming stronger with each shake. The sand had a relative density of 34% at the start of the test, which is on the boundary between loose and medium-dense sand (McCarthy, 2002).

The accelerogram for Test 5/5 is shown in Figure 5.23, and it shows a repeated peak acceleration of 0.86 g. The accelerogram shows noise of less than 0.1 g during the centre of each cycle followed by two or three large peaks of approximately 0.85 g. This is a result of the shaking table moving rapidly between its lateral extents followed by a jerky transition to moving in the return direction.

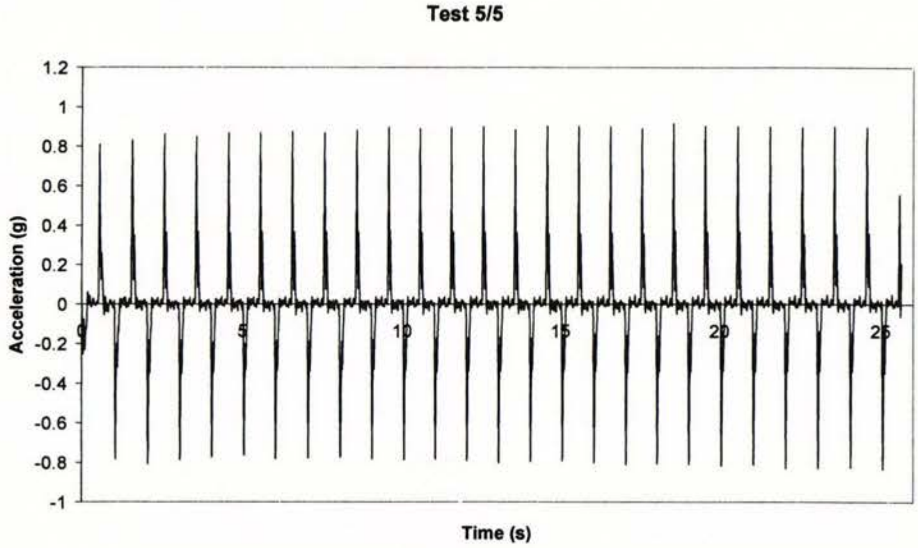

Figure 5.23. Accelerogram for Test 5/5

The settlement versus time graph (Figure 5.24) shows that the rate of settlement is very rapid, despite the higher relative density at the start of the test. Midway through the test, the potentiometer reached the end of its stroke, so stopped recording further settlement. The total settlement was measured as 51 mm, and corresponds to a final relative density of $D_r = 0.49$.

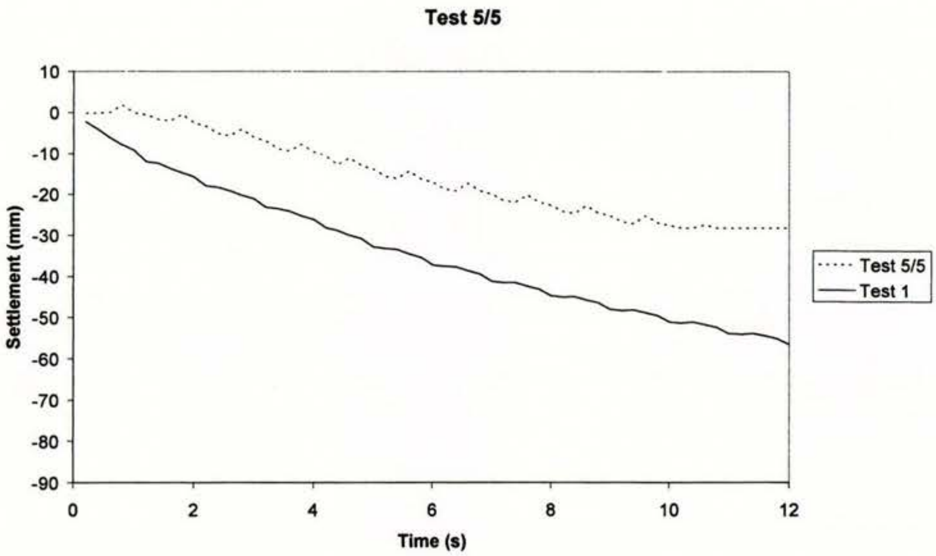

Figure 5.24. Settlement-time curve for Test 5/5

The cyclic shear strain profile (Figure 5.25) shows a large strain of approximately 1.1 % (20 mm) occurring consistently in each cycle of shaking. This was expected due to the high acceleration the deposit was subjected to. The high cyclic shear strain values start in the first cycle of displacement.

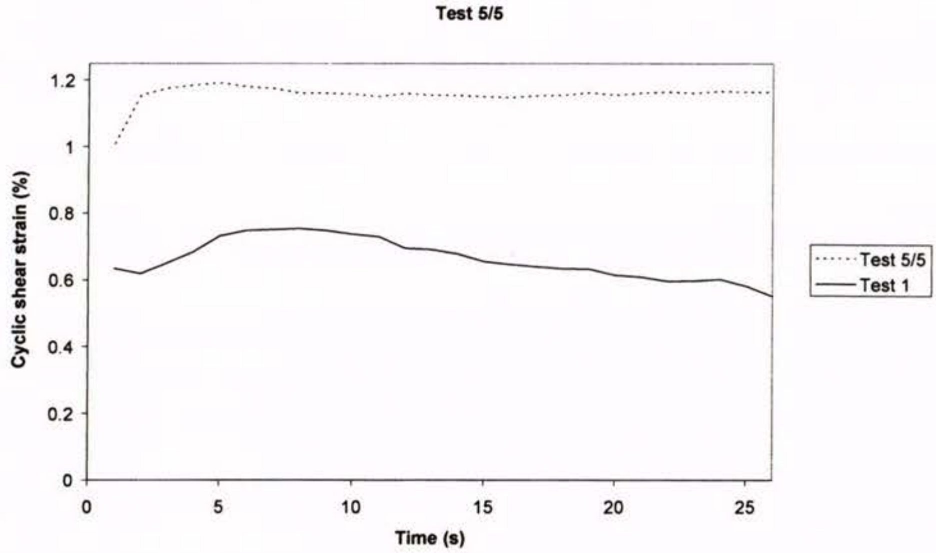

Figure 5.25. Peak Cyclic Shear Strain profile for Test 5/5

5.5 Summary of Charton's Results

Formatted: Bullets and Numbering

Charton's (2004) work included tests with three different shaking intensities on unreinforced and reinforced soil. He used the same apparatus to form the sand deposits, although the relative density of his deposits was higher than those tested in this work. His reinforced soil had a relative density D_r = 0.4. His work was also carried out on the University of Canterbury shaking table, and he defined the shaking using the theoretical peak accelerations rather than the actual peak ground accelerations. His work reported ±20 mm (0.08 g), ±30 mm (0.12 g) and ±40 mm (0.16 g) tests and he found that between 0.12 g and 0.16 g a threshold was crossed where settlement and strain increased markedly. Figure 5.26 shows the settlements he recorded in unreinforced soil, and the graph of horizontal strain follows a similar pattern.

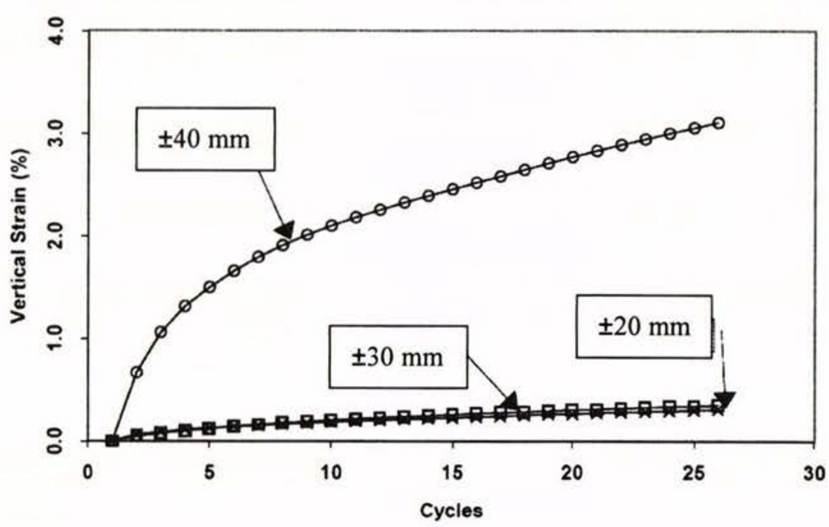

Figure 5.26. Charton's settlement results for unreinforced soil

The displacement curves obtained for unreinforced soil show some non-linearity in soil response near to the surface. Figure 5.27 shows the graph of displacement versus height, and upon close inspection a change of gradient can be seen at 1.5 m height.

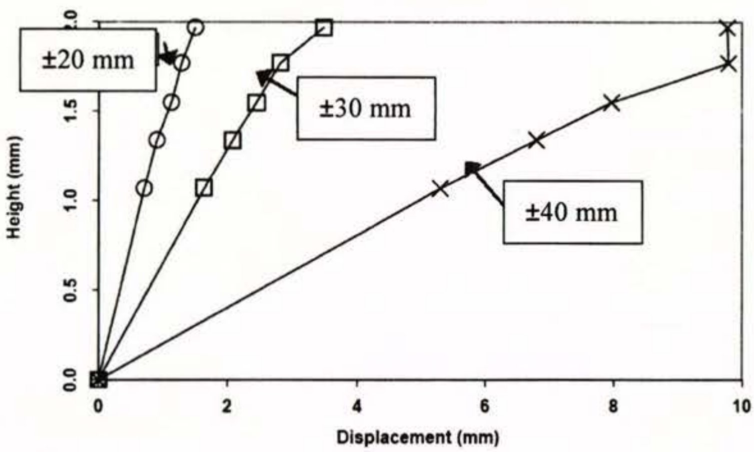

Figure 5.27. Charton's Displacement profiles

Having tested unreinforced soil to establish a baseline response, the soil was then reinforced using one and two micropiles, concentrating on the ±40 mm displacement.

Figure 5.28 shows the results of the tests on reinforced soil, using one and two micropiles and the unreinforced soil as a comparison.

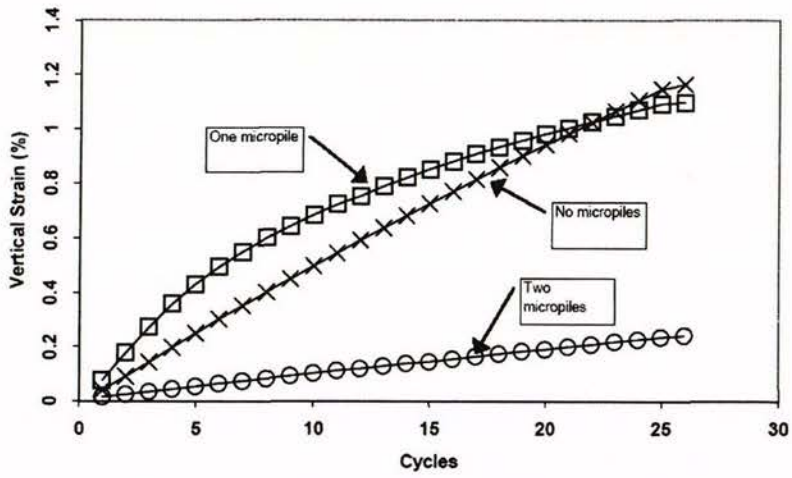

Figure 5.28. Charton's Final reinforcement results

It can be seen that the effect of one micropile was minimal, while the installation of two diagonally opposed micropiles reduced the settlement significantly.

5.6 Re-analysis of Charton's Acceleration levels

Following further study of Charton's raw data, the following accelerograms were graphed. They are all drawn from (Charton's) raw data obtained with the laminated tank on the shake table. Figures 5.29, 5.30 and 5.31 show accelerograms corresponding to his ±20 mm (0.08 g), ±30 mm (0.12 g) and ±40 mm (0.16 g) tests respectively.

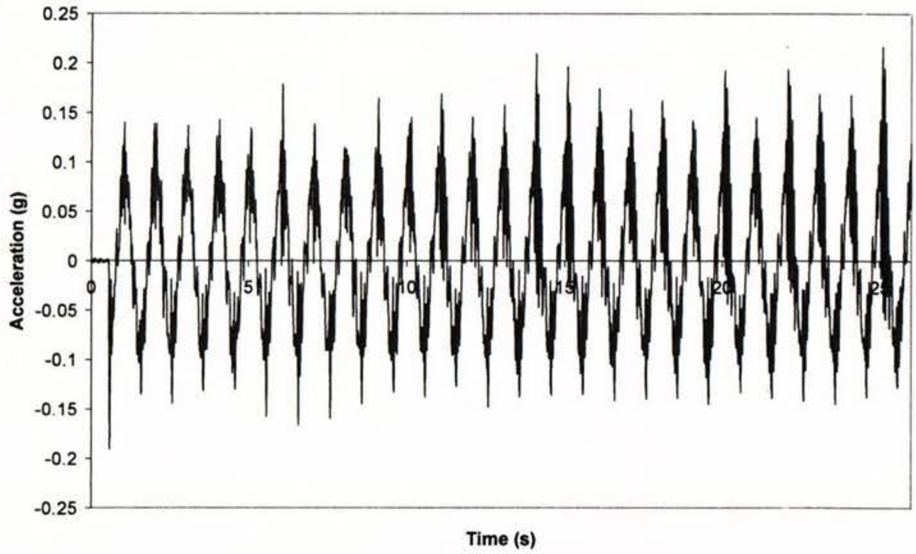

Figure 5.29. Accelerogram from ±20 mm record

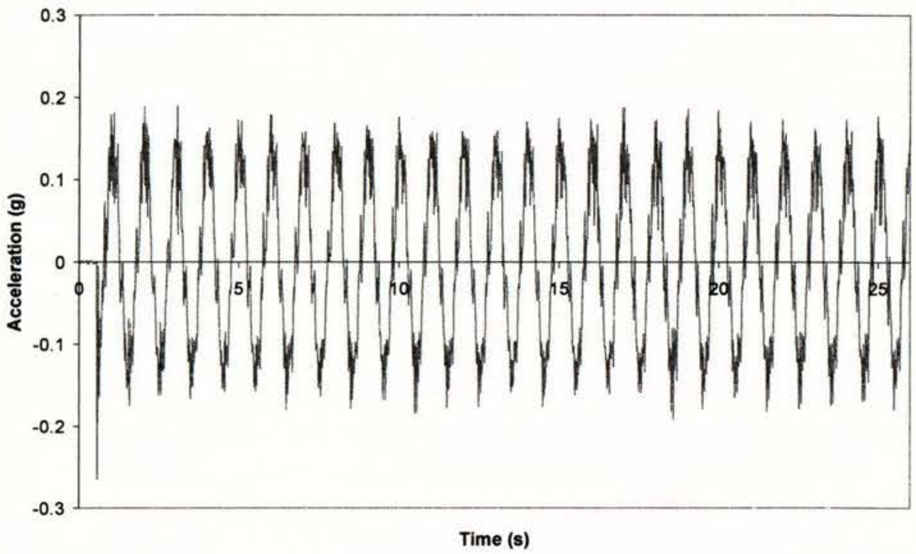

Figure 5.30. Accelerogram from ±30 mm record

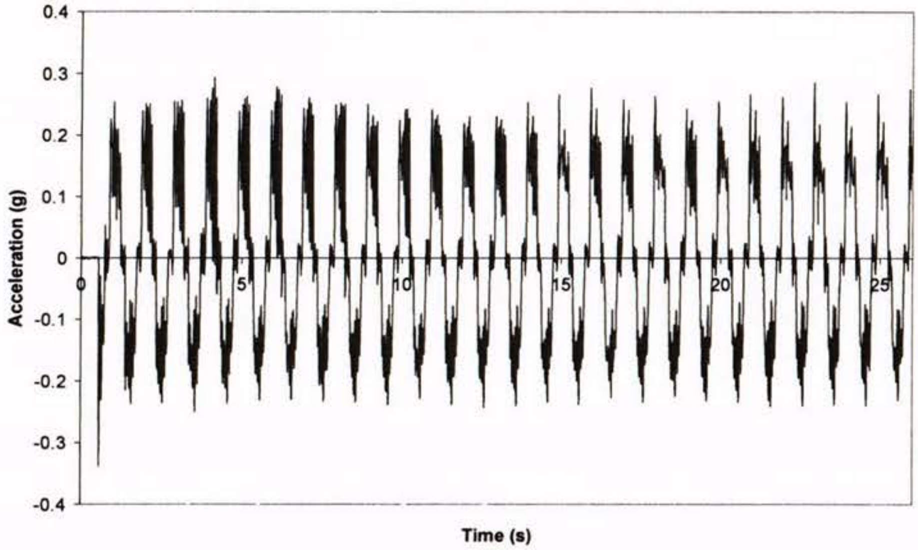

Figure 5.31. Accelerogram from ±40 mm record

It can be seen from Figures 5.29, 5.30 and 5.31 that the mean peak accelerations were greater than the smooth accelerations reported. It is suggested that the relevant peak acceleration is that which is repeated in over half of the cycles of shaking. This measure of acceleration shall be referred to as the repeated peak acceleration, and will be used to describe all the tests carried out in this report. Table 5.1 shows the theoretical and repeated peak accelerations for each displacement level.

Table 5.1. Theoretical and repeated peak accelerations for Charton's work

Displacement	Acceleration	
	Theoretical	Repeated Peak
±20 mm	0.08 g	0.15 g
±30 mm	0.12 g	0.18 g
±40 mm	0.16 g	0.26 g

6 Analysis

During the testing procedure the shake table was producing significantly rougher accelerations than the sine waves hoped for. This was probably due to worn bushings on the table. However, this roughness probably simulates a real earthquake more accurately than a smooth sine wave does. One consequence of the roughness is that the peak ground acceleration is not a suitable method of measuring and comparing each test. A repeat peak acceleration value is suggested, and this defined as the peak acceleration value that is repeated in at least half of the cycles of shaking. For example, in Test 5/1, the peak ground acceleration was 0.27 g in one spike, while the repeated peak was 0.16 g. Figure 6.1 shows a comparison between the repeated peak values and the peak values for all tests. It shows that there is a significant difference between the two values in most tests.

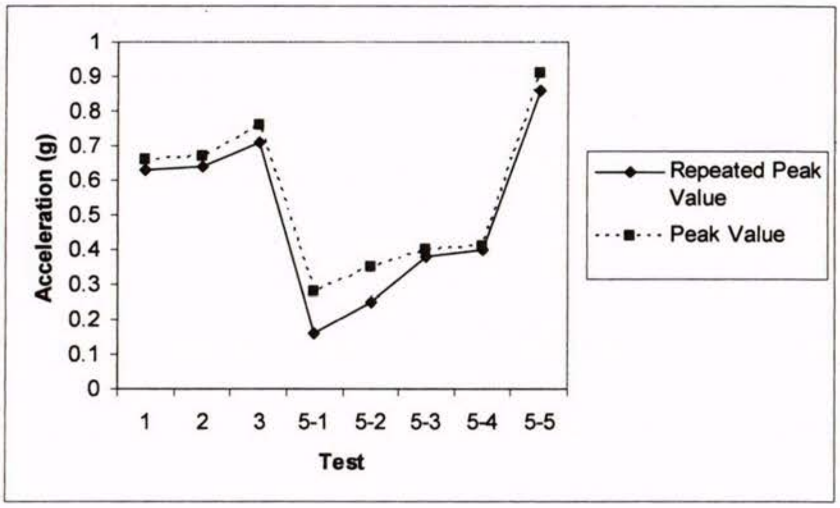

Figure 6.1. Repeated peak and peak acceleration for each test

In Section 2.5 the Seed and Idriss (1970) method for determining liquefaction susceptibility is presented. Their main formula (Equation 2.3, reproduced below) has a 0.65 multiplier to account for the fact that the average shear stress during an earthquake has been shown empirically to be 65% of the peak shear stress.

$$CSR = \frac{\tau}{\sigma'_{v0}} = 0.65 * \frac{a_{\max}}{g} * \frac{\sigma_{v0}}{\sigma'_{v0}} * \frac{r_D}{MSF} \qquad (2.3)$$

Figure 6.2 is taken from their paper and shows a real earthquake record annotated with τ_{max} and τ_{av}, the maximum and average shear stresses, respectively. By comparison, the average and maximum shear stresses will be equal for a true sine wave, so multiplying the maximum shear stress by 0.65 to yield an average value is inappropriate.

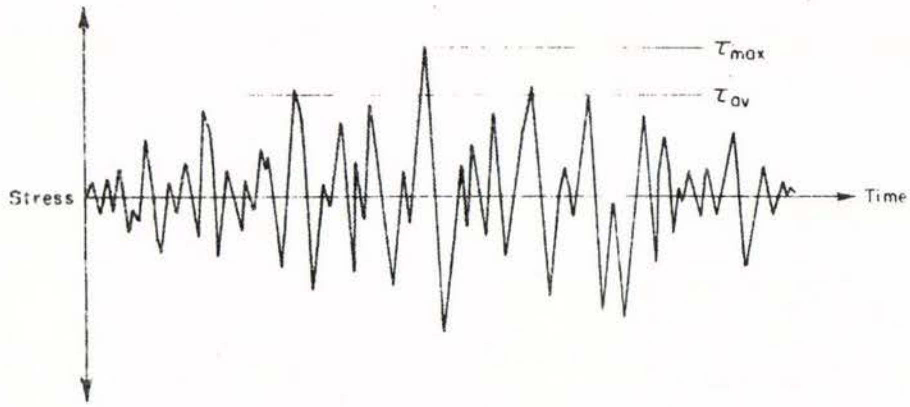

Figure 6.2. Time History of Shear Stress during an earthquake

For these reasons, it is suggested that when stating that the micropiles will resist shaking of a certain intensity that the lab intensities are divided by 0.65 to give a realistic field value. Thus, the repeated peak value of 0.4 g (in Test 5/4) becomes 0.62 g. These final values of acceleration will be referred to as equivalent field peak ground accelerations.

Table 6.1 summarises the results of all tests conducted. It also includes Chraton's results recalculated to the equivalent field peak ground acceleration level.

Table 6.1. Summary of test results

Test	Pile size	Repeat Peak acceleration	Equivalent field PGA	Relative density, D_r		Settlement	
				Start	End	mm	%
±20 mm	N/A	0.15 g	0.23 g	Acceleration from Charton's tests, recalculated to the new equivalent field PGA values.			
±30 mm	N/A	0.18 g	0.28 g				
±40 mm	N/A	0.26 g	0.40 g				
1	None	0.63 g	0.97 g	0.05	0.29	80	5.1
2	65 mm	0.64 g	0.98 g	0.01	0.26	77	4.2
3	90 mm	0.71 g	1.09 g	0.04	0.31	74	4.5
5/1	90 mm	0.16 g	0.25 g	0.12	0.12	2	0.1
5/2	90 mm	0.25 g	0.38 g	0.12	0.22	20	1.7
5/3	90 mm	0.38 g	0.58 g	0.22	0.31	24	1.4
5/4	90 mm	0.40 g	0.62 g	0.31	0.34	15	0.6
5/5	90 mm	0.86 g	1.32 g	0.34	0.49	51	2.7

It is apparent from Table 6.1 that large settlement occurred during Tests 1-3 and 5/5. This is not surprising given that the tests were equivalent to an earthquake with peak ground accelerations of almost 1 g. Tests 5/1 to 5/4 showed significantly lower settlements, and these suggest that the micropiles used were successful in reducing the risk of liquefaction. Settlement versus time curves for all tests are shown in Figure 6.3, and a significant reduction of settlement can be seen in Tests 5/1 to 5/4. This indicates that the micropiles successfully reduced settlement.

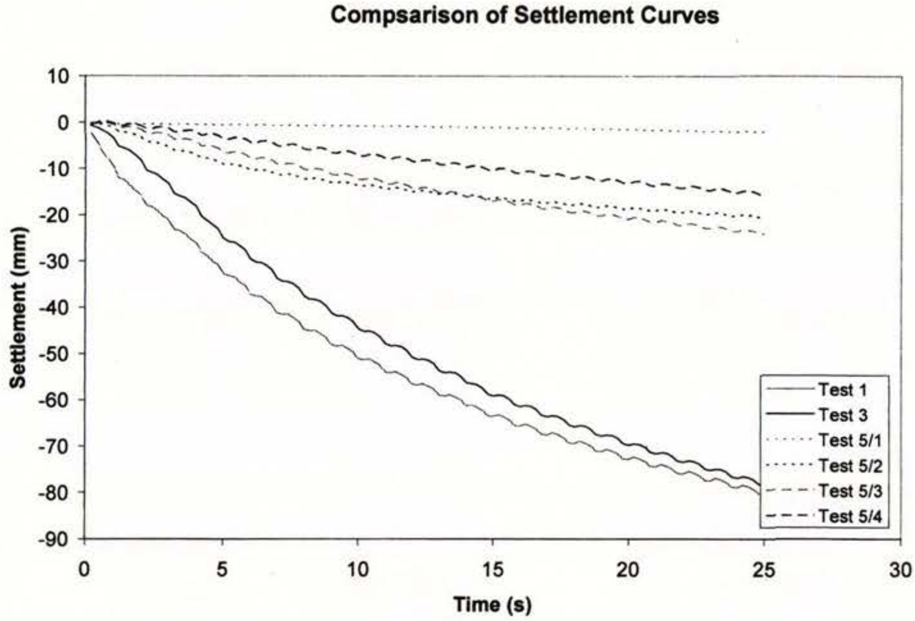

Figure 6.3. Comparison of settlement vs time for all tests

Figure 6.4 shows a graph of vertical vs horizontal strain, which clearly shows a relationship between settlement (vertical strain) and displacement (horizontal strain). The horizontal strain values are calculated using a repeated peak shear strain method the same as that used for accelerations. The trendline plotted has an R^2 value of 0.79, indicative of a good correlation. The graph shows that if the shear displacements can be reduced (i.e. the soil stiffened) then settlement (i.e. liquefaction) can be reduced.

It may be more appropriate to plot a series of trendlines with varying gradients around the existing line, each representing a value of relative density. As the relative density increases, the amount of vertical strain (settlement) for a given horizontal strain will decrease. Values of relative density from all tests have been added to the graph to show this is a feasible suggestion.

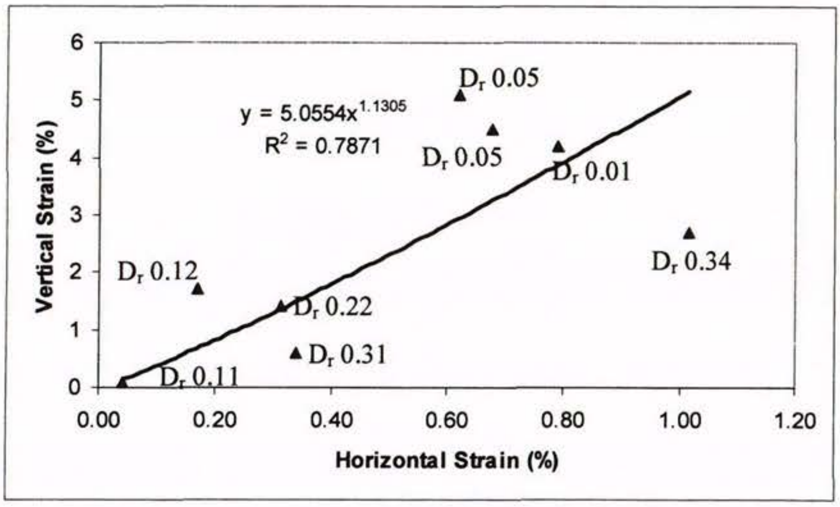

Figure 6.4. Vertical vs Horizontal shear strain for all tests

Figures 6.5 and 6.6 show graphs of the average peak shear strain (APSS) for tests 1-3 and 5/1 to 5/5 respectively. APSS is a parameter developed by Chambers (1999) to quantify the soils response to shaking. It takes into account the strains occurring in the soil at all depths and at all times during shaking. It is calculated using the following procedure:

- All displacement readings from the potentiometers are converted into shear strains;
- The average shear strain for each time interval is taken by averaging the readings from each potentiometer at each time interval;
- The peak average shear strain is found in each half cycle of shaking;
- The average of these values is then the APSS.

By taking the average shear strain over each potentiometer the variation in response with depth is accounted for. Averaging over time accounts for the variation as the soil stiffens during shaking.

Figure 6.5 shows that the micropiles in Tests 2 and 3 did reduce the shear strain despite the fact that significant settlement still occurred.

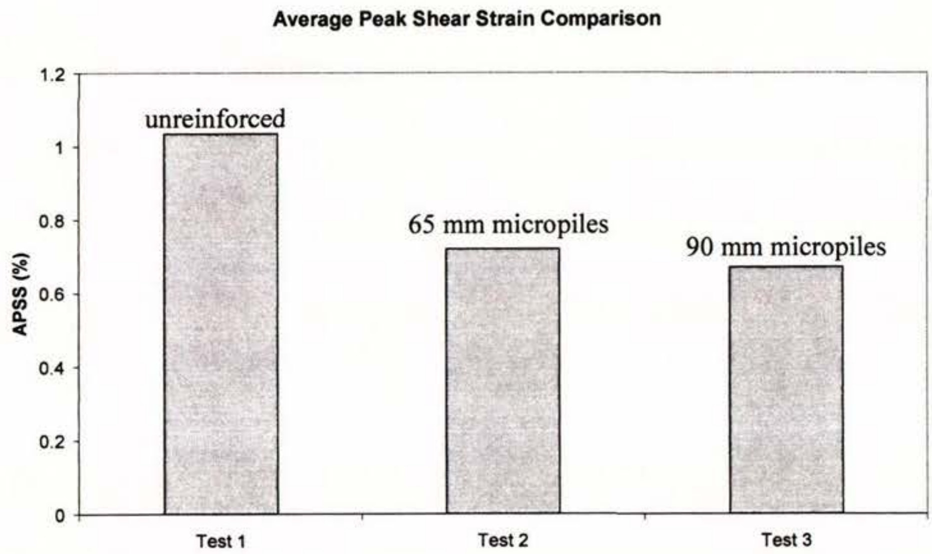

Figure 6.5. APSS values for Tests 1, 2 and 3.

Figure 6.6 shows that the micropiles in Tests 5/1 to 5/4 reduced strains greatly. Despite significant increases in acceleration between tests, the APSS values remained relatively constant. It appears that a threshold is crossed between Test 5/4 and Test 5/5 resulting in a significant increase in APSS. The APSS value for Test 5/5 is almost equal to that of Test 1 (unreinforced soil), despite the higher acceleration in Test 5/5 (1.32 g compared to 0.97 g). This shows that while settlement did occur, the response of the unreinforced soil to 0.97 g is similar to that of the reinforced soil to 1.32 g. This suggests that liquefaction will be reduced even when the capacity of the micropiles is exceeded.

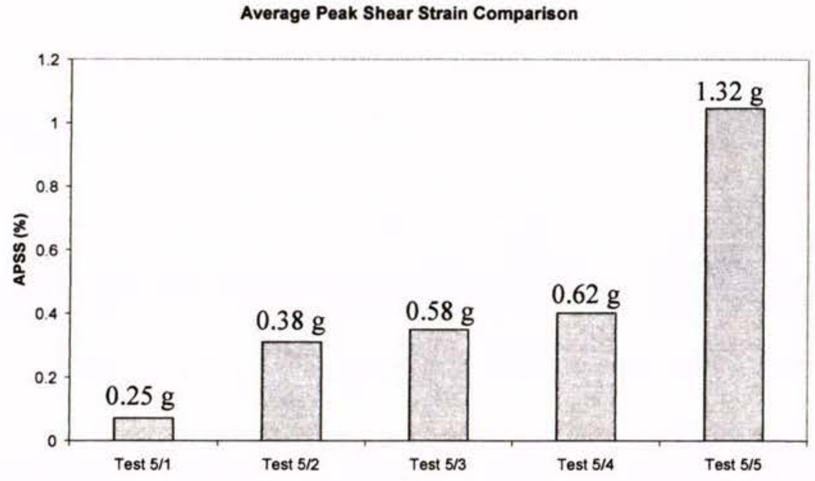

Figure 6.6. Comparison of APSS values for Test 5/1 to 5/5

Figure 6.7 shows a comparison of the cyclic shear strain values for those successful tests against the original unreinforced soil. It can be seen that all of those tests that reduced settlement also reduced the cyclic shear strain. The reduction is cyclic shear strain that may be expected as a result of stiffening as settlement occurs does not eventuate in these tests.

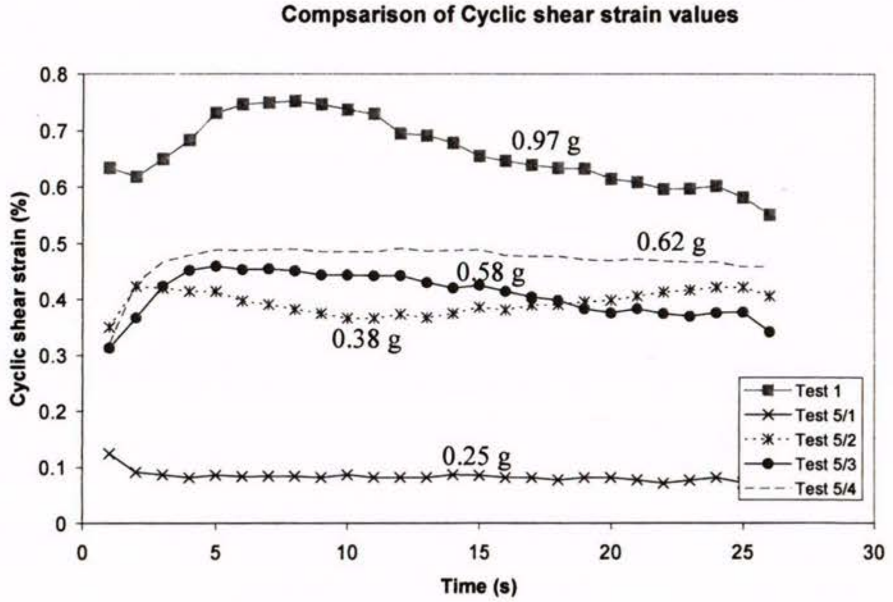

Figure 6.7. Comparison of cyclic shear strain values. Note that the acceleration values shown are the equivalent field PGAs.

Figure 6.8 plots the ratio of soil surface acceleration to base acceleration. If this value is greater than 1, the soil is stiffer and has amplified the shaking, while a value less than 1 indicates that energy has been absorbed by the soil. It is known that during liquefaction, soil surface accelerations are greatly reduced. Stiff soils have less damping of motion and energy absorption than a flexible soil, so the more successful the stiffening, the less damping and energy absorption occurs and consequently the acceleration of the soil will increase. Figure 6.8 shows that Tests 5/1 to 5/4 amplify the shaking while Tests 1-3 and 5/5 absorb energy, suggesting that the reinforcing was effective in Tests 5/1 to 5/4.

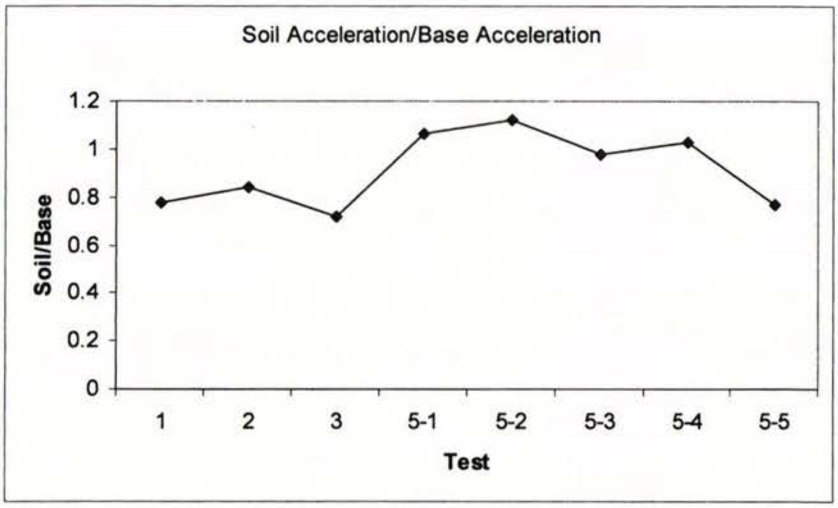

Figure 6.8. Soil Acceleration/Base Acceleration

Following the findings of McManus et al (2004), initial finite element modelling and observation of the tests carried out for this project, it appears that the friction between the piles and the soil is the limiting factor in the ability of these micropiles to stiffen the soil. McManus et al found that very little of the strength of the micropiles as tested by Charton (2003) was mobilised to stiffen the soil. Current experiments concur with that calculation, because even when the ability of the micropiles to stiffen the soil was exceeded, there was no damage to the piles. Observation of the testing showed that the piles appeared to fail in shear (by "popping out" of the ground) and thus allowed the soil to settle around them. Tests 2 and 3 showed this failure occurring, and it is suggested that the reduction in settlement and displacement for the first cycle of Test 2 (see Figures 5.6 and 5.7) and the first three cycles of Test 3 (see Figures 5.9 and 5.10) are indicative of the piles working. At this point during the test, they were observed to "pop out" of the ground, and it is suggested that this represents failure along the frictional interface between the soil and the pile.

Charton's findings (shown in Figure 5.28) were that for a soil with relative density $D_r = 0.4$ the use of two micropiles reduced settlement to 0.2 % when subjected to equivalent field PGA = 0.26 g (±40 mm). This shaking and density is approximated by Tests 5/2, 5/3 and 5/4. In Test 5/2 the shaking was similar, but the relative density less, while Tests 5/3 and 5/4 had greater shaking. The settlement in Tests 5/2, 5/3 and 5/4 vary between 0.6 and 1.7 %. This is a favourable comparison to Charton's results given that the relative densities of the sand are lower in the current work. This suggests that the new design of micropile is of equivalent performance to the significantly more expensive design used by Charton.

It should be remembered that these tests were all carried out in very loose sand and that the acceleration values are yet to be divided by 0.65 to take them to field values. Table 6.2 shows final field acceleration and settlement values. The success of the reinforcing in Tests 5/1 to 5/5 is based on judgement and comparisons with Charton's work, because there are no baseline tests applicable to these shaking levels.

Table 6.2. Final Results

Test	Field equivalent PGA	Peak cyclic shear strain	Settlement reduced successfully?
1	0.97 g	0.75 %	N/A
2	0.98 g	0.87 %	N
3	1.09 g	0.92 %	N
5/1	0.25 g	0.09 %	Y
5/2	0.39 g	0.42 %	Y
5/3	0.58 g	0.46 %	Y
5/4	0.62 g	0.48 %	Y
5/5	1.32 g	1.19 %	N

7 Local Seismology

The active seismicity in the Christchurch region is a result of motion along the plate boundary between the Australian and Pacific plates. The southern part of the boundary is the Alpine Fault while further north the boundary changes into the more complex Marlborough Fault Zone as shown in Figure 7.1 (from Toshinawa et al., 1997).

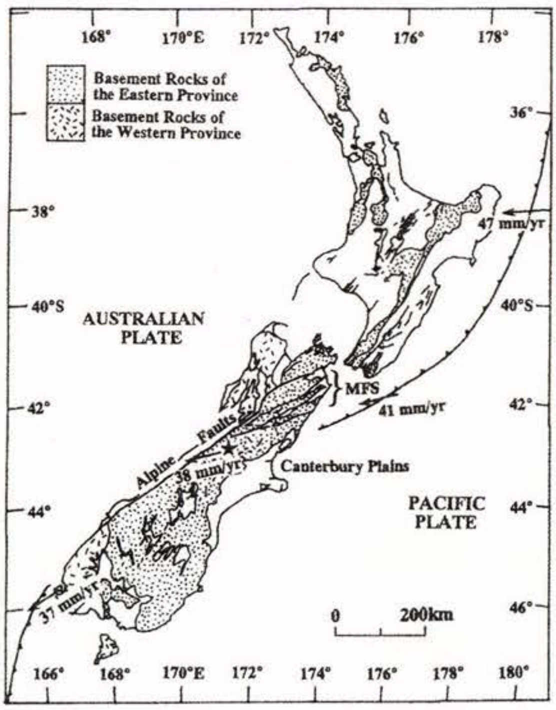

Figure 7.1. Pacific – Australian plate boundary and the main postglacial active faults in NZ

Figure 7.2 shows the peak ground accelerations expected to occur in Christchurch with a 10 % probability in a 50 year period (475 yr return interval). Much of the hazard is obtained from faults running along the western edge of the Canterbury Plains and from many hidden faults inferred to be running beneath the plains and Pegasus Bay (Stirling et al., 2000).

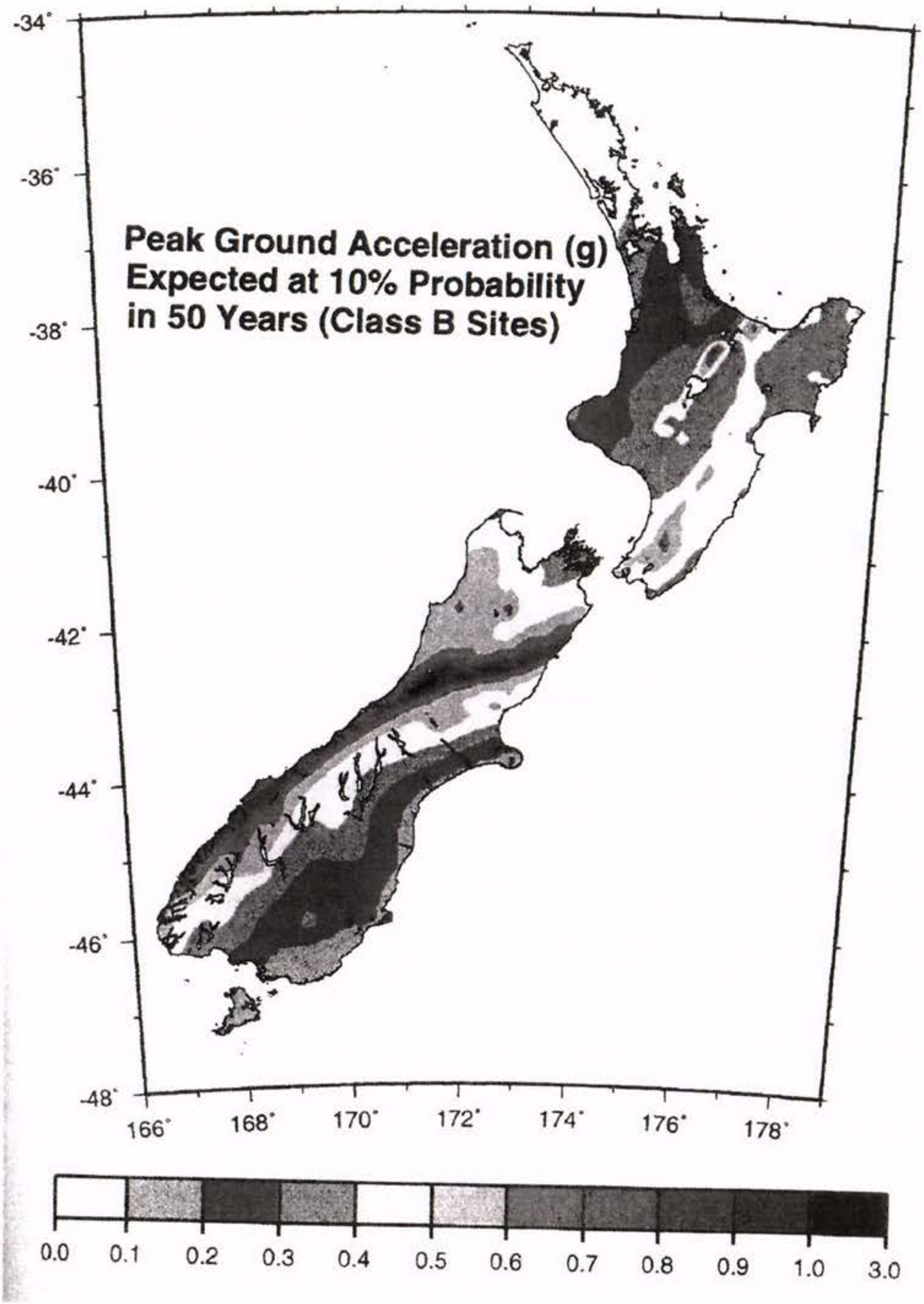

Figure 7.2. PGA expected at 475 yr interval map of New Zealand

Figure 7.2 (from Stirling et al., 2000) shows that the peak ground acceleration expected in Christchurch is less than 0.4 g, and possibly as low as 0.2 g depending upon the location in the city. There is significant lateral variation in the city in soil response spectra due to the complex sedimentation history as a result of changing sea levels and river courses (Toshinawa et al., 1997).

As discussed in section 6, the current design of micropiles significantly reduced settlement and therefore the likelihood of liquefaction at peak accelerations of up to 0.6 g. This shows that the micropile design and methodology presented in this project is suitable for application in the Christchurch region following successful field trials.

8 Plaxis Models

Plaxis 7.2 was used to model the performance of the laminated sand tank and micropiles using Finite Element Modelling. Models work on the assumption that they are representing an elastic continuum. The models are a complex interaction between cyclic loading of the soil and loading of the pile. During monotonic loading, a sand will dilate upon failure. However, during cyclic loading, loose sand will contract. Dilation causes an increase in soil strength upon failure, yet contraction will result in a significant decrease in soil strength. These tendencies are juxtaposed during the cyclic loading modelled here and result in a very complex scenario to model.

There is no method of specifying how loose the soil is. This means that the soil will be modelled correctly up to failure point, when the amount of settlement becomes critical. This means that the models would predict the failure time and failure strain, but not the amount of settlement expected. This information is useful as it allows an estimate of failure displacement to be made.

Models were devised that were simple approximations of the sand tank and the amount of strain was used as a comparison between models. The two diagonally opposed anchors would apparently cross over if represented in 2D, so the tank was simplified to a single anchor system. The shaking was then modelled as a static horizontal force applied against the side of the tank behind the anchor.

The micropiles are modelled as ground anchors. These are represented by a tie rod (the steel) surrounded by a geotextile (the grout) within the soil mass. Drained behaviour is used to simulate loose, highly permeable sand.

Figure 8.1 shows the results from one model run with the anchor. Hot colours represent areas of high strain, while cooler colours show less strain. The peak strain value was 4 % for unreinforced soil and 3 % for the reinforced soil. The intensity of shaking modelled had very little effect on peak strain values.

The models did not represent the actual tests well and despite many different model inputs, no success was achieved.

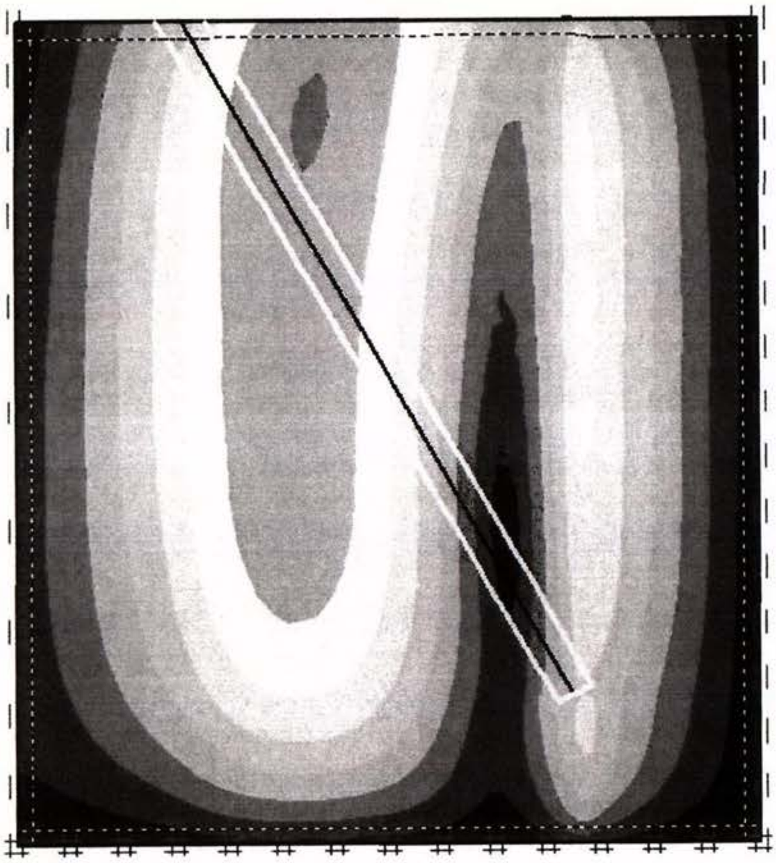

Figure 8.1. Results from Plaxis Modelling

9 Summary, Conclusions and Suggested Further Work

9.1 Summary

The objectives of this project as stated in Section 1 were

a) to reduce the cost of installation of micropiles by using a new construction method,

b) to compare the results of this method to those obtained by Charton (2004),

c) to determine the effectiveness of the micropiles in reducing settlement, and

d) to develop limits within which the micropiles could be relied upon to prevent liquefaction of the soil.

The new method of constructing the micropiles was a success. It was a relatively simple procedure to install micropiles in the sand deposit, and the micropiles used significantly less materials than those tested by Charton. A detailed cost analysis has not been carried out, but it is expected that a contractor would be able to install a number of these micropiles in less time than required for the Ischebeck product. This reduction in time and the reduction in raw materials suggests that they would be more economical than the Ischebeck units.

Direct comparisons between this method and that of Charton (2004) were very difficult to obtain. Differences in relative density and the "jerky" motion of the shake table meant that comparisons are of an indicative nature. Charton's micropiles were shown to reduce settlement at accelerations of up to 0.4 g. The new micropiles did not reduce settlement as effectively for the same acceleration but the sand had a significantly lower relative density. They also did not reduce settlement as effectively with a similar relative density but a higher acceleration (0.6 g). It is expected that if the relative densities and accelerations were equal then the reduction in settlement would be similar. This shows that the use of micropiles is an effective way of reducing settlement.

To develop limits on the acceleration and relative densities at which the micropiles work would require a lot more testing and a more reliable shake table. This has been suggested for further work.

9.2 Conclusions

This project has proved that a new method of constructing micropiles is a success in the lab. They have been tested at a range of acceleration and relative densities and compared favourably with previous work on the use of micropiles to resist shear strain and prevent liquefaction. The expected limits for the usage of these micropiles are within the expected PGA values for the city of Christchurch.

During this testing, the soil and reinforcement was pushed very hard as a result of inaccuracies in the shaking table. The testing may have proved more successful and more relevant to actual applications if "real" earthquake records were used. This would also remove any inaccuracies associated with converting laboratory sine wave accelerations to field PGA values with the Seed method.

Recommendations for using these micropiles in real situations to reduce earthquake induced liquefaction are a long way off. A number of issues have been identified that need attention during field trials.

This project has shown that there is significant potential in this method to provide an economical, non-intrusive method of reducing or preventing liquefaction.

9.3 Suggestions for Further Work

Further work is required to confirm the potential of these micropiles and to develop design guidelines governing the acceleration and relative densities at which liquefaction can be resisted. To do this will require testing in the laboratory at varying frequencies, suited to specific locations and the expected earthquake spectra at each locality. Surcharge loads on the ground surrounding the micropiles should also be considered. The effect of varying the spacing and orientation of the micropiles relative to three dimensional shaking should be considered.

Tests should also be carried out in saturated layered soil. Large bending moments develop at the interface between a liquefiable layer and a non liquefiable layer (as shown in Figure 2.7) and the effect of these on the micropiles is unknown. This testing could be carried out in the field at a utility site and monitored in the event of an earthquake. It is entirely possible that these micropiles may be significantly less effective in saturated soils due to the reduction in effective stress. It appears that the limiting factor on the performance of the micropiles is friction, which is proportional to effective stress. By saturating the soil, the effective stress is being reduced by approximately half.

Another issue that will need solving before large scale field trials are carried out is the effect of length on constructability. Currently the micropile reinforcing is a single piece, which works when the piles are less than 2 m long. It is envisaged that the micropiles used in the field will be up to 8 m long, and this will require a connection system for the reinforcing rod.

Field trials must also address the issue of settlement. By definition, consolidation settlement will not occur in the liquefiable layers but it may occur in interbedded or overlying layers. It is expected that large loads akin to negative skin friction will be imposed on the micropiles and that they may prove to be unsuitable in areas where this may occur.

10 References

Formatted: Bullets and Numbering

Bartlett, S.F., and Youd, T.L., 1992. Empirical analysis of horizontal ground displacement generated by liquefaction induced lateral spread. Technical Report NCEER-92-0021, National Centre for Earthquake Engineering Research, Buffalo, New York.

Bedenis, T.H.P, Thelen, M.J.P., and Maranowski, S., 2004. Micropiles to the rescue. In Civil Engineering Magazine, v74, 3, March 2004. Publ ASCE.

Bensilame, A., et al 1998. Seismic Retrofitting using micropile systems: centrifugal model studies. Proc. Fourth International Conference on Case Histories in Geotechnical Engineering.

Berrill, J.B., Christensen, S.A., Keenan, R.P., Okada, W. & Pettinga, J.R. (2001). Case study of lateral spreading forces on a piled foundation. Geotechnique 51, No. 6, pp. 501-517

Butterfield, K.J., Davis, R. O., Berrill, J. B., 2003. Seismic liquefaction trigger mechanisms. Research report (University of Canterbury. Dept. of Civil Engineering) ; 2003-06. Christchurch, N.Z. 106 p

Carr, K., 2004. Liquefaction case histories from the West Coast of the South Island, New Zealand. Unpublished Master of Engineering Thesis, held by the University of Canterbury.

Casagrande, A., 1936. Characteristics of cohesionless soils affecting the stability of slopes and earth fills. Journal of the Boston Society of Civil Engineers, reprinted in Contributions to Soil Mechanics, Boston Society of Civil Engineers, 1940, pp 257-276.

Chambers, A., 1999. The Seismic Response of Drilled Shaft Foundations. Unpublished PhD Thesis, University of Canterbury.

Charton, G., 2004. Prevention of Soil Liquefaction Using Micropiles. Unpublished Masters thesis, University of Canterbury.

Davis, R.O., and Berrill, J.B., 1982. Energy Dissipation and Seismic liquefaction in sands. Earthquake Engineering and Structural Dynamics, Vol. 10, No. 1, pp 59-68.

Dobry R., Ladd, R.S., Yokel, F.Y., Chung, R.M., and Powell, D., 1982. Prediction of pore water pressure build up and liquefaction of sands during earthquakes by cyclic strain method. NBS Building Science Series 138, National Bureau of Standards, Gaithersburg, Maryland, 150pp.

Hushmand, B., Scott, R.F. and Crouse, C.B., 1988. Centrifuge liquefaction tests in a laminar box. Geotechnique, Vol. 38, No.2, pp 253-262.

Jewell, R.A., 1980. Some effects of Reinforcement on the Mechanical Behaviour of soils. PhD Thesis, Cambridge University. Referenced in J Le Masurier (2000). An Investigation of soil nail interactions under direct shear. MPhil thesis, Cardiff University.

Kavvadas, M., and Gazetas, G., 1993. Kinematic seismic response and bending of free head piles in layered soil. Geotechnique, v43, 2, pp207-222.

Kishishita, T., Saito, E. and Miura, F., 2000. Dynamic-response characteristics of structures with micropile foundation system.

McCarthy, D.F., 2002. Essentials of Soil Mechanics and Foundations. Basic Geotechnics, 6th Edition. Prentice Hall, London.

McManus, K.J., Charton, G., and Turner, J.P., 2004. Effect of Micropiles on Seismic Shear Strain. In Proceedings of GeoSupport 2004: Drilled Shafts, Micropiling, Deep Mixing, Remedial Methods, and Specialty Foundation Systems, pp. 134-145. Publ. ASCE.

PHRI, 1997. Handbook on Liquefaction Remediation of reclaimed land. Japan Port and Harbour Research Institute. A.A. Balkema, Rotterdam.

Robertson, P.K. and Campanella, R.G., 1985. Liquefaction potential of sands using the CPT. Journal of Geotechnical Engineering, ASCE, vol. 111, No. 3, pp 384-403.

Seed, H.B., 1968. Landslides During Earthquakes due to Liquefaction. J Soil Mechanics and Foundations, Sep 1968, pp 1053-1122.

Seed, H.B., and Idriss, I.M., 1971. Simplified procedure for evaluating soil liquefaction potential. Journal of the Soil Mechanics and Foundation Division, ASCE, Vol. 107, No. SM9, pp 1249-1274.

Seed, H.B. and Idriss, I.M., 1982. Ground Motions and Soil Liquefaction during Earthquakes. Earthquake Engineering Research Institute Monograph Series.

Stirling, M., McVerry, G., Berryman, K., McGinty, P., Villamor, P., Van Dissen, R., Dowrick, D., Cousins, J., and Sutherland, R., 2000. Probabilistic Seismic Hazard Assessment of New Zealand: New Active Fault Data, Seismicity Data Attenuation Relationships and Methods. Unpublished report held by Institute of Geological and Nuclear Sciences, Lower Hutt, NZ.

Toshinawa, T, Taber, J.J., and Berrill, J.B., 1997. Distribution of Ground Motion Intensity Inferred from Questionnaire Survey, Earthquake recordings and Microtremor Measurements – A Case Study in Christchurch, New Zealand, during the 1994 Arthurs Pass Earthquake. Bulletin of the Seismological Society of America, vol. 87, No. 2, pp 356-369.

Yang, J., McManus, K.J., and Berrill, J.B., 2000. Kinematic Soil-Micropile Interaction. Paper 1501 in Vol 7 of Proc. 12th World Conference on Earthquake Engineering, Auckland, 2000. Publ. NZ Society for Earthquake Engineering, Upper Hutt, NZ.

Youd, T.L. and Idriss, I.M., 2001. Liquefaction Resistance of Soils: Summary Report from the 1996 NCEER and 1998 NCEER/NSF Workshops on Evaluation of Liquefaction Resistance of Soils Journal of Geotechnical and Geoenvironmental Engineering, Vol. 127, No. 4, April 2001, pp. 297-313